

Symplectic Contact Analysis of a Finite-sized Horizontally Graded Magneto-electro-elastic Plane

Lizichen Chen^a, Weiqiu Chen^{a,b,c,*}

^a*Key Laboratory of Soft Machines and Smart Devices of Zhejiang Province, Department of Engineering Mechanics, Soft Matter Research Center, Zhejiang University, Hangzhou 310027, P.R. China*

^b*Center for Soft Machines and Smart Devices, Huanjiang Laboratory, Zhuji 311816, P.R. China*

^c*Faculty of Mechanical Engineering and Mechanics, Ningbo University, Ningbo 315211, P.R. China*

Abstract

Material characterization using high-throughput testing (HTT) techniques have shown great promise in expediting the advancement of high-performance materials. A key step in HTT is the adoption of functionally graded specimen, whose material inhomogeneity however imposes a great challenge on analytically evaluating its responsive behavior under external loads. This work establishes the first symplectic framework for contact analysis of a finite-sized magneto-electro-elastic plane with an exponential material gradient along the horizontal direction. The governing equations are first represented in matrix form in a state space, with the full state vector defined and the operator matrix derived. The operator matrix is found to be distinct from the Hamiltonian operator matrix in the case of a homogeneous medium. With all the eigen-solutions obtained, the Hamiltonian mixed energy variational principle is then introduced to derive the coefficients in the symplectic expansion. The developed analytical solution not only exhibits asymmetry properties, but also converges rapidly. The analytical results are validated through comparison with the finite element simulations. The analytical platform established

* Corresponding author. Tel./Fax: 85-571-87951866; E-mail: chenwq@zju.edu.cn. (Weiqiu Chen)

This paper has been accepted by *Proceedings of the Royal Society A: Mathematical, Physical and Engineering Sciences*

here would work as an effective theoretical basis for subsequent development of quantitative HTT techniques.

Keywords: Symplectic framework; Contact analysis; Functionally graded material; Horizontal exponential gradient; Hamiltonian mixed energy variational principle

1. Introduction

Materials development has seen a significant boost through high-throughput testing (HTT), recognized as a pivotal aspect of the Materials Genome Initiative [1,2]. One standout advancement in HTT methods is the involvement of functionally graded materials (FGMs) for specimens [3]. The FGM specimens offer a highly time-efficient and space-compact approach to material characterization. However, a notable challenge follows, i.e., theoretical prediction of the response of a finite-sized functionally graded specimen under external load is extremely difficult. Hence, the current HTT methods are all qualitative, not quantitative. In particular, while the classical Hertzian contact theory has been popularly adopted in the characterization of homogeneous isotropic materials, the counterpart tailored for FGM specimens is still absent.

The complexity of developing theoretical models stems from the inherent material inhomogeneity [4]. Nonetheless, mechanics of FGMs has garnered substantial attention in solid mechanics since the 1980s due to their diverse applications [5]. Particularly, several experimental studies have highlighted the efficacy of FGMs in enhancing resistance to contact-related damage and cracks resulting from indentation and sliding [6-8]. In addition to the experimental investigations, researchers have thoroughly explored contact problems of FGMs using analytical and computational approaches, thereby enriching the contact theories and their

applications. Giannakopoulos and Suresh [9,10] investigated contact problems of functionally graded elastic half-spaces with the action of point forces and frictionless axisymmetric indenters. Choi and Paulino [11] introduced a novel approach based on singular integral equations, specifically addressing the influence of frictional heat on contact stress distribution in FGM coatings. Chen et al. [12] investigated the adhesive contact between a rigid sphere and a graded elastic half-space with Young's modulus varying with depth according to a power law, while Poisson's ratio remaining a constant. Jin et al. [13,14] established several models of adhesive contact between an axisymmetric rigid punch and a power-law graded elastic medium. Liu et al. [15] considered the axisymmetric double contact problems for an FGM layer indented simultaneously by a rigid cylindrical indenter and a rigid spherical indenter. Chidlow et al. [16] presented a semi-analytical algorithm for the determination of the contact half-width and surface pressure which results from both adhesive and non-adhesive contact problems of FGMs.

However, existing research primarily concentrates on vertically graded materials, with limited exploration into horizontally graded materials. Chen et al. [17] derived the surface Green's functions explicitly for a horizontally graded half-plane under the weak gradient assumption. Furthermore, almost all the previous works consider contact problems of a half-space (three-dimensional or 3D) or a half-plane (two-dimensional or 2D) rather than a domain of finite size, which obviously deviates from the physical reality. The symplectic framework for elasticity is a powerful but relatively new tool, leveraging the method of separation of variables significantly. The pioneering work of Zhong [18] for homogeneous materials has demonstrated remarkable efficacy in elucidating the physical essence of Saint-Venant solutions, and precisely forecasting local behaviors. Subsequently, Zhao and Chen [19,20] generalized the method to

investigate isotropic/transversely isotropic FGM beams characterized by exponentially varying material constants (e.g., Young's modulus) along the longitudinal axis.

This article attempts to establish the symplectic framework for a rigid punch with arbitrary profile acting but over a determined contact region of a finite-sized magneto-electro-elastic plane with an exponential material gradient in the horizontal direction. The state equations and the properties of operator matrix are first obtained for the contact problem in [Section 2.1](#), and the special and general eigenvalues together with the corresponding eigen-solutions are constructed analytically in [Sections 2.2](#) and [2.3](#), respectively, which facilitate the symplectic expansion for complete solutions in [Section 2.4](#). Finite element analyses for some examples are performed in [Section 3](#) to verify the correctness of the analytical solutions. The conclusions are given in [Section 4](#).

2. Contact of a horizontally graded magneto-electro-elastic plane

We first consider that a frictionless rigid punch of an arbitrary profile with determined contact region (i.e., $x \in [\tilde{a}, \tilde{b}]$) is applied on the surface of a functionally graded magneto-electro-elastic plane of finite size (i.e., a rectangle), as depicted in [figure 1](#). The material is transversely isotropic, with the poling direction along the z -axis. We denote c_{ij} , e_{ij} , q_{ij} , ε_{ij} , γ_{ij} , and d_{ij} as the elastic, piezoelectric, piezomagnetic, dielectric, magnetic and electromagnetic constants, respectively. All constants are assumed to vary exponentially along the x -direction in a unified manner:

$$c_{ij} = c_{ij}^0 e^{\beta x}, \quad e_{ij} = e_{ij}^0 e^{\beta x}, \quad q_{ij} = q_{ij}^0 e^{\beta x}, \quad \varepsilon_{ij} = \varepsilon_{ij}^0 e^{\beta x}, \quad \gamma_{ij} = \gamma_{ij}^0 e^{\beta x}, \quad d_{ij} = d_{ij}^0 e^{\beta x} \quad (2.1)$$

where β is the material gradient index. If $\beta > 0$, the material hardens along the x -direction,

while it softens for $\beta < 0$.

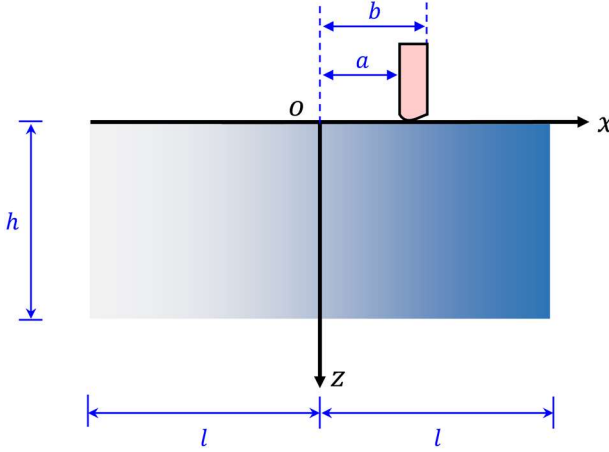


Figure 1. A frictionless rigid punch acting on the surface of a horizontally graded magneto-electro-elastic plane of finite size.

2.1. Basic formulations

Given the plane-strain assumption, the two-dimensional constitutive equations can be written as:

$$\begin{cases} \sigma_{xx} = c_{11} \frac{\partial u_x}{\partial x} + c_{13} \frac{\partial u_z}{\partial z} + e_{31} \frac{\partial \varphi}{\partial z} + q_{31} \frac{\partial \psi}{\partial z} \\ \sigma_{zz} = c_{13} \frac{\partial u_x}{\partial x} + c_{33} \frac{\partial u_z}{\partial z} + e_{33} \frac{\partial \varphi}{\partial z} + q_{33} \frac{\partial \psi}{\partial z} \\ \sigma_{xz} = c_{44} \left(\frac{\partial u_x}{\partial z} + \frac{\partial u_z}{\partial x} \right) + e_{15} \frac{\partial \varphi}{\partial x} + q_{15} \frac{\partial \psi}{\partial x} \\ D_x = e_{15} \left(\frac{\partial u_x}{\partial z} + \frac{\partial u_z}{\partial x} \right) - \varepsilon_{11} \frac{\partial \varphi}{\partial x} - d_{11} \frac{\partial \psi}{\partial x} \\ D_z = e_{31} \frac{\partial u_x}{\partial x} + e_{33} \frac{\partial u_z}{\partial z} - \varepsilon_{33} \frac{\partial \varphi}{\partial z} - d_{33} \frac{\partial \psi}{\partial z} \\ B_x = q_{15} \left(\frac{\partial u_x}{\partial z} + \frac{\partial u_z}{\partial x} \right) - d_{11} \frac{\partial \varphi}{\partial x} - \gamma_{11} \frac{\partial \psi}{\partial x} \\ B_z = q_{31} \frac{\partial u_x}{\partial x} + q_{33} \frac{\partial u_z}{\partial z} - d_{33} \frac{\partial \varphi}{\partial z} - \gamma_{33} \frac{\partial \psi}{\partial z} \end{cases} \quad (2.2)$$

where σ_{ij} are the stress components; u_x and u_z are the displacement components in the x - and z -directions, respectively; φ and ψ are the electric potential and magnetic potential, respectively; D_i and B_i are the components of the electric displacement and the magnetic induction, respectively. For the plane-stress situation, the constitutive equations look similar to

equation (2.2) but with different material coefficients.

By rearranging, we can write equation (2.2) and the equilibrium equations without body forces in the following form:

$$\left\{ \begin{array}{l} \frac{\partial u_x}{\partial z} = -\frac{\partial u_z}{\partial x} - \frac{e_{15}}{c_{44}} \frac{\partial \varphi}{\partial x} - \frac{q_{15}}{c_{44}} \frac{\partial \psi}{\partial x} + \frac{1}{c_{44}} \sigma_{xz} \\ \frac{\partial u_z}{\partial z} = -\frac{c_{13}}{c_{33}} \frac{\partial u_x}{\partial x} - \frac{e_{33}}{c_{33}} \frac{\partial \varphi}{\partial z} - \frac{q_{33}}{c_{33}} \frac{\partial \psi}{\partial z} + \frac{1}{c_{33}} \sigma_{zz} \\ \frac{\partial \varphi}{\partial z} = \frac{e_{31}}{\varepsilon_{33}} \frac{\partial u_x}{\partial x} + \frac{e_{33}}{\varepsilon_{33}} \frac{\partial u_z}{\partial z} - \frac{d_{33}}{\varepsilon_{33}} \frac{\partial \psi}{\partial z} - \frac{1}{\varepsilon_{33}} D_z \\ \frac{\partial \psi}{\partial z} = \frac{q_{31}}{\gamma_{33}} \frac{\partial u_x}{\partial x} + \frac{q_{33}}{\gamma_{33}} \frac{\partial u_z}{\partial z} - \frac{d_{33}}{\gamma_{33}} \frac{\partial \varphi}{\partial z} - \frac{1}{\gamma_{33}} B_z \\ \frac{\partial \sigma_{xz}}{\partial z} = -\frac{\partial \sigma_{xx}}{\partial x} \\ \frac{\partial \sigma_{zz}}{\partial z} = -\frac{\partial \sigma_{xz}}{\partial x} \\ \frac{\partial D_z}{\partial z} = -\frac{\partial D_x}{\partial x} \\ \frac{\partial B_z}{\partial z} = -\frac{\partial B_x}{\partial x} \end{array} \right. \quad (2.3)$$

On letting $\hat{\sigma}_{ji} = \sigma_{ji} e^{-\beta x}$, $\hat{D}_i = D_i e^{-\beta x}$, and $\hat{B}_i = B_i e^{-\beta x}$ ($i, j = z, x$), equation (2.3) can be further simplified to

$$\left\{ \begin{array}{l} \frac{\partial u_x}{\partial z} = -\frac{\partial u_z}{\partial x} - a_1 \frac{\partial \varphi}{\partial x} - a_2 \frac{\partial \psi}{\partial x} + a_3 \hat{\sigma}_{xz} \\ \frac{\partial u_z}{\partial z} = -a_4 \frac{\partial u_x}{\partial x} + a_5 \hat{\sigma}_{zz} + a_6 \hat{D}_z + a_7 \hat{B}_z \\ \frac{\partial \varphi}{\partial z} = a_8 \frac{\partial u_x}{\partial x} + a_6 \hat{\sigma}_{zz} - a_9 \hat{D}_z + a_{10} \hat{B}_z \\ \frac{\partial \psi}{\partial z} = a_{11} \frac{\partial u_x}{\partial x} + a_7 \hat{\sigma}_{zz} + a_{10} \hat{D}_z - a_{12} \hat{B}_z \\ \frac{\partial \hat{\sigma}_{xz}}{\partial z} = a_{13} \frac{\partial^2 u_x}{\partial x^2} - a_4 \frac{\partial \hat{\sigma}_{zz}}{\partial x} + a_8 \frac{\partial \hat{D}_z}{\partial x} + a_{11} \frac{\partial \hat{B}_z}{\partial x} + \beta \left(a_{13} \frac{\partial u_x}{\partial x} - a_4 \hat{\sigma}_{zz} + a_8 \hat{D}_z + a_{11} \hat{B}_z \right) \\ \frac{\partial \hat{\sigma}_{zz}}{\partial z} = -\frac{\partial \hat{\sigma}_{xz}}{\partial x} - \beta \hat{\sigma}_{xz} \\ \frac{\partial \hat{D}_z}{\partial z} = a_{14} \frac{\partial^2 \varphi}{\partial x^2} + a_{15} \frac{\partial^2 \psi}{\partial x^2} - a_1 \frac{\partial \hat{\sigma}_{xz}}{\partial x} + \beta \left(a_{14} \frac{\partial \varphi}{\partial x} + a_{15} \frac{\partial \psi}{\partial x} - a_1 \hat{\sigma}_{xz} \right) \\ \frac{\partial \hat{B}_z}{\partial z} = a_{15} \frac{\partial^2 \varphi}{\partial x^2} + a_{16} \frac{\partial^2 \psi}{\partial x^2} - a_2 \frac{\partial \hat{\sigma}_{xz}}{\partial x} + \beta \left(a_{15} \frac{\partial \varphi}{\partial x} + a_{16} \frac{\partial \psi}{\partial x} - a_2 \hat{\sigma}_{xz} \right) \end{array} \right. \quad (2.4)$$

Also, we can obtain the following supplementary equations

$$\begin{cases} \hat{\sigma}_{xx} = -a_{13} \frac{\partial u_x}{\partial x} + a_4 \hat{\sigma}_{zz} - a_8 \hat{D}_z - a_{11} \hat{B}_z \\ \hat{D}_x = -a_{14} \frac{\partial \varphi}{\partial x} - a_{15} \frac{\partial \psi}{\partial x} + a_1 \hat{\sigma}_{xz} \\ \hat{B}_x = -a_{15} \frac{\partial \varphi}{\partial x} - a_{16} \frac{\partial \psi}{\partial x} + a_2 \hat{\sigma}_{xz} \end{cases} \quad (2.5)$$

where a_i in [equations \(2.4\)](#) and [\(2.5\)](#) are given in [supplementary material A](#). With the full state vector \mathbf{f} defined as

$$\mathbf{f} = [\mathbf{q}, \mathbf{p}]^T = [u_x, u_z, \varphi, \psi, \hat{\sigma}_{xz}, \hat{\sigma}_{zz}, \hat{D}_z, \hat{B}_z]^T \quad (2.6)$$

one can rewrite [equation \(2.4\)](#) in matrix form:

$$\frac{\partial}{\partial z} \mathbf{I}_8 \mathbf{f} = \mathcal{H} \mathbf{f} \quad (2.7)$$

where \mathbf{I}_n is an n th-order identity matrix; \mathcal{H} is an operator matrix, as detailed in [supplementary material A](#).

To elucidate the properties of the operator matrix \mathcal{H} , we introduce the unit symplectic matrix:

$$\mathbf{J} = \begin{bmatrix} 0 & \mathbf{I}_4 \\ -\mathbf{I}_4 & 0 \end{bmatrix} \quad (2.8)$$

and denote the symplectic inner product as

$$\begin{aligned} \langle \mathbf{f}_1, \mathbf{f}_2 \rangle &= \int_{-l}^l \mathbf{f}_1^T \mathbf{J} \mathbf{f}_2 dx \\ &= \int_{-l}^l (u_{x1} \hat{\sigma}_{xz2} + u_{z1} \hat{\sigma}_{zz2} + \varphi_1 \hat{D}_{z2} + \psi_1 \hat{B}_{z2} - \hat{\sigma}_{xz1} u_{x2} - \hat{\sigma}_{zz1} u_{z2} - \hat{D}_{z1} \varphi_2 - \hat{B}_{z1} \psi_2) dx \end{aligned} \quad (2.9)$$

where the subscript 1 or 2 denotes a specified state vector. It is worth noting that [equation \(2.9\)](#) satisfies the four conditions of symplectic inner product [\[21\]](#). Hence, the space expanded by all the state vectors is a symplectic space. Through integration by parts, and making use of the homogeneous boundary conditions at $x = \pm l$,

$$\begin{cases} -a_{13}\frac{\partial u_x}{\partial x} + a_4\hat{\sigma}_{zz} - a_8\hat{D}_z - a_{11}\hat{B}_z = 0 \\ \hat{\sigma}_{xz} = 0 \\ -a_{14}\frac{\partial \varphi}{\partial x} - a_{15}\frac{\partial \psi}{\partial x} + a_1\hat{\sigma}_{xz} = 0 \\ -a_{15}\frac{\partial \varphi}{\partial x} - a_{16}\frac{\partial \psi}{\partial x} + a_2\hat{\sigma}_{xz} = 0 \end{cases} \quad (2.10)$$

we can prove that

$$\langle \mathbf{f}_1, \mathcal{H}\mathbf{f}_2 \rangle = \langle \mathbf{f}_2, \mathcal{H}\mathbf{f}_1 \rangle - \beta \langle \mathbf{f}_1^*, \mathbf{f}_2^* \rangle \quad (2.11)$$

where $\mathbf{f}^* = [u_x, u_z, \varphi, \psi, \hat{\sigma}_{xx}, \hat{\sigma}_{xz}, \hat{D}_x, \hat{B}_x]^T$ is a dual full state vector. Therefore, \mathcal{H} is a quasi-Hamiltonian operator matrix, the eigenvectors of which are not mutually adjoint symplectic orthogonal for the stress-free case.

Without loss of generality, the solution is assumed as

$$\mathbf{f}(x, z) = \boldsymbol{\Phi}(x)\xi(z) = [u(x), w(x), \phi(x), \psi(x), \tau(x), \sigma(x), D(x), B(x)]^T \xi(z) \quad (2.12)$$

Substituting [equation \(2.12\)](#) into [equation \(2.7\)](#) for separation of variables, we find

$$\frac{\frac{\partial}{\partial z} \xi(z)}{\xi(z)} = [\mathcal{H}\boldsymbol{\Phi}(x)]\boldsymbol{\Phi}^{-1}(x) \quad (2.13)$$

from which we derive

$$\xi(z) = e^{\mu z} \quad (2.14)$$

together with the following eigen equation

$$\mathcal{H}\boldsymbol{\Phi}(x) = \mu\boldsymbol{\Phi}(x) \quad (2.15)$$

where μ is the eigenvalue, and $\boldsymbol{\Phi}(x)$ is the eigenvector which satisfies the homogeneous boundary conditions. The eigen analysis of [equation \(2.15\)](#) in the following is very similar to the standard symplectic analysis pioneered by Wanxie Zhong for elasticity, see Yao et al. [\[21\]](#) for example.

2.2. Eigen-solutions of special eigenvalues

The zero and $-\beta$ eigenvalues, if exist, are special eigenvalues, since the corresponding displacement and stress components do not decay exponentially in the z -direction, respectively. To derive the eigen-solutions for zero-eigenvalue, we commence by establishing the following equations:

$$\left\{ \begin{array}{l} -\frac{\partial w}{\partial x} - a_1 \frac{\partial \phi}{\partial x} - a_2 \frac{\partial \psi}{\partial x} + a_3 \tau = 0 \\ -a_4 \frac{\partial u}{\partial x} + a_5 \sigma + a_6 D + a_7 B = 0 \\ a_8 \frac{\partial u}{\partial x} + a_6 \sigma - a_9 D + a_{10} B = 0 \\ a_{11} \frac{\partial u}{\partial x} + a_7 \sigma + a_{10} D - a_{12} B = 0 \\ a_{13} \frac{\partial^2 u}{\partial x^2} - a_4 \frac{\partial \sigma}{\partial x} + a_8 \frac{\partial D}{\partial x} + a_{11} \frac{\partial B}{\partial x} + \beta \left(a_{13} \frac{\partial u}{\partial x} - a_4 \sigma + a_8 D + a_{11} B \right) = 0 \\ -\frac{\partial \tau}{\partial x} - \beta \tau = 0 \\ a_{14} \frac{\partial^2 \phi}{\partial x^2} + a_{15} \frac{\partial^2 \psi}{\partial x^2} - a_1 \frac{\partial \tau}{\partial x} + \beta \left(a_{14} \frac{\partial \phi}{\partial x} + a_{15} \frac{\partial \psi}{\partial x} - a_1 \tau \right) = 0 \\ a_{15} \frac{\partial^2 \phi}{\partial x^2} + a_{16} \frac{\partial^2 \psi}{\partial x^2} - a_2 \frac{\partial \tau}{\partial x} + \beta \left(a_{15} \frac{\partial \phi}{\partial x} + a_{16} \frac{\partial \psi}{\partial x} - a_2 \tau \right) = 0 \end{array} \right. \quad (2.16)$$

The eigenvectors of equation (2.16) with the homogeneous boundary conditions are

$$\begin{aligned} \mathbf{f}_{0,1}^{(0)} &= \boldsymbol{\Phi}_{0,1}^{(0)} = [1, 0, 0, 0, 0, 0, 0, 0]^T, & \mathbf{f}_{0,2}^{(0)} &= \boldsymbol{\Phi}_{0,2}^{(0)} = [0, 1, 0, 0, 0, 0, 0, 0]^T \\ \mathbf{f}_{0,3}^{(0)} &= \boldsymbol{\Phi}_{0,3}^{(0)} = [0, 0, 1, 0, 0, 0, 0, 0]^T, & \mathbf{f}_{0,4}^{(0)} &= \boldsymbol{\Phi}_{0,4}^{(0)} = [0, 0, 0, 1, 0, 0, 0, 0]^T \end{aligned} \quad (2.17)$$

where the superscript stands for the order of Jordan form; the subscript $0,s$ ($s=1,\dots,4$) represents the s -th Jordan chain for zero eigenvalue. It is important to note that the eigen-solutions remain the same as the eigenvectors respectively in the zero-eigenvalue case.

Similarly, the first-order Jordan form eigen-solutions of zero eigenvalue are derived via

$$\mathcal{H} \boldsymbol{\Phi}_{0,s}^{(1)} = \boldsymbol{\Phi}_{0,s}^{(0)} \quad (s=1,\dots,4) \quad (2.18)$$

from which we arrive at

$$\begin{aligned} \boldsymbol{\Phi}_{0,1}^{(1)} &= [0, -x, 0, 0, 0, 0, 0, 0]^T, & \boldsymbol{\Phi}_{0,2}^{(1)} &= [-a_{17}x, 0, 0, 0, 0, k_1, k_2, k_3]^T \\ \boldsymbol{\Phi}_{0,3}^{(1)} &= [-a_{18}x, 0, 0, 0, 0, k_4, k_5, k_6]^T, & \boldsymbol{\Phi}_{0,4}^{(1)} &= [-a_{19}x, 0, 0, 0, 0, k_7, k_8, k_9]^T \end{aligned} \quad (2.19)$$

where k_i are constants, as detailed in [supplementary material A](#). Notwithstanding the first-order Jordan form eigenvectors in [equation \(2.19\)](#) are no longer the solution of [equation \(2.16\)](#) with the homogeneous boundary conditions, the eigen-solutions are rewritten as

$$\mathbf{f}_{0,s}^{(1)} = \boldsymbol{\Phi}_{0,s}^{(1)} + z\boldsymbol{\Phi}_{0,s}^{(0)} \quad (s=1,\dots,4) \quad (2.20)$$

Following the same procedure as for [equation \(2.18\)](#), we can also consider the second-order Jordan form eigenvectors with

$$\mathcal{H}\boldsymbol{\Phi}_{0,s}^{(2)} = \boldsymbol{\Phi}_{0,s}^{(1)} \quad (s=1,\dots,4) \quad (2.21)$$

No practical solution satisfies the last three equations in [equation \(2.21\)](#) (i.e., $s = 2,3,4$), and the chain of Jordan form eigen-solutions is terminated. Nevertheless, the eigenvector for the first equation of [equation \(2.21\)](#) is

$$\boldsymbol{\Phi}_{0,1}^{(2)} = \left[\frac{a_{17}}{2}x^2, 0, 0, 0, 0, -k_1x, -k_2x, -k_3x \right]^T \quad (2.22)$$

and the respective eigen-solution is given by

$$\mathbf{f}_{0,1}^{(2)} = \boldsymbol{\Phi}_{0,1}^{(2)} + z\boldsymbol{\Phi}_{0,1}^{(1)} + \frac{z^2}{2}\boldsymbol{\Phi}_{0,1}^{(0)} \quad (2.23)$$

To avoid the absence of practical solution to the eigen equation, we may set the second-order Jordan form eigenvector in the form of

$$\boldsymbol{\Phi}_0^{(2)} = \boldsymbol{\Phi}_{0,1}^{(2)} + \zeta_1\boldsymbol{\Phi}_{0,2}^{(1)} + \zeta_2\boldsymbol{\Phi}_{0,3}^{(1)} + \zeta_3\boldsymbol{\Phi}_{0,4}^{(1)} \quad (2.24)$$

where ζ_1, ζ_2 , and ζ_3 are the constants to be determined. Hence, the eigen equation is expressed as

$$\mathcal{H}\boldsymbol{\Phi}_0^{(3)} = \boldsymbol{\Phi}_0^{(2)} \quad (2.25)$$

which reads

$$\left\{
\begin{aligned}
& -\frac{\partial w^{(3)}}{\partial x} - a_1 \frac{\partial \phi^{(3)}}{\partial x} - a_2 \frac{\partial \psi^{(3)}}{\partial x} + a_3 \tau^{(3)} = \frac{a_{17}}{2} x^2 - \zeta_1 a_{17} x - \zeta_2 a_{18} x - \zeta_3 a_{19} x \\
& -a_4 \frac{\partial u^{(3)}}{\partial x} + a_5 \sigma^{(3)} + a_6 D^{(3)} + a_7 B^{(3)} = 0 \\
& a_8 \frac{\partial u^{(3)}}{\partial x} + a_6 \sigma^{(3)} - a_9 D^{(3)} + a_{10} B^{(3)} = 0 \\
& a_{11} \frac{\partial u^{(3)}}{\partial x} + a_7 \sigma^{(3)} + a_{10} D^{(3)} - a_{12} B^{(3)} = 0 \\
& a_{13} \frac{\partial^2 u^{(3)}}{\partial x^2} - a_4 \frac{\partial \sigma^{(3)}}{\partial x} + a_8 \frac{\partial D^{(3)}}{\partial x} + a_{11} \frac{\partial B^{(3)}}{\partial x} + \beta \left(a_{13} \frac{\partial u^{(3)}}{\partial x} - a_4 \sigma^{(3)} + a_8 D^{(3)} + a_{11} B^{(3)} \right) = 0 \\
& -\frac{\partial \tau^{(3)}}{\partial x} - \beta \tau^{(3)} = -k_1 x + \zeta_1 k_1 + \zeta_2 k_4 + \zeta_3 k_7 \\
& a_{14} \frac{\partial^2 \phi^{(3)}}{\partial x^2} + a_{15} \frac{\partial^2 \psi^{(3)}}{\partial x^2} - a_1 \frac{\partial \tau^{(3)}}{\partial x} + \beta \left(a_{14} \frac{\partial \phi^{(3)}}{\partial x} + a_{15} \frac{\partial \psi^{(3)}}{\partial x} - a_1 \tau^{(3)} \right) = -k_2 x + \zeta_1 k_2 + \zeta_2 k_5 + \zeta_3 k_8 \\
& a_{15} \frac{\partial^2 \phi^{(3)}}{\partial x^2} + a_{16} \frac{\partial^2 \psi^{(3)}}{\partial x^2} - a_2 \frac{\partial \tau^{(3)}}{\partial x} + \beta \left(a_{15} \frac{\partial \phi^{(3)}}{\partial x} + a_{16} \frac{\partial \psi^{(3)}}{\partial x} - a_2 \tau^{(3)} \right) = -k_3 x + \zeta_1 k_3 + \zeta_2 k_6 + \zeta_3 k_9
\end{aligned}
\right. \tag{2.26}$$

(2.26)

Substitution of the boundary conditions at $x = \pm l$ to the last four equations of [equation \(2.26\)](#)

yields

$$\left\{
\begin{aligned}
& a_{13} \frac{\partial u^{(3)}}{\partial x} - a_4 \sigma^{(3)} + a_8 D^{(3)} + a_{11} B^{(3)} = 0 \\
& -\tau^{(3)} = C_1 e^{-\beta x} + \frac{1}{\beta^2} [(\zeta_1 k_1 + \zeta_2 k_4 + \zeta_3 k_7) \beta + k_1 - \beta k_1 x] \\
& a_{14} \frac{\partial \phi^{(3)}}{\partial x} + a_{15} \frac{\partial \psi^{(3)}}{\partial x} - a_1 \tau^{(3)} = C_2 e^{-\beta x} + \frac{1}{\beta^2} [(\zeta_1 k_2 + \zeta_2 k_5 + \zeta_3 k_8) \beta + k_2 - \beta k_2 x] \\
& a_{15} \frac{\partial \phi^{(3)}}{\partial x} + a_{16} \frac{\partial \psi^{(3)}}{\partial x} - a_2 \tau^{(3)} = C_3 e^{-\beta x} + \frac{1}{\beta^2} [(\zeta_1 k_3 + \zeta_2 k_6 + \zeta_3 k_9) \beta + k_3 - \beta k_3 x]
\end{aligned}
\right. \tag{2.27}$$

where

$$\left\{
\begin{aligned}
C_i &= -k_i \frac{l \operatorname{csch}(\beta l)}{\beta} \quad (i=1,2,3) \\
\zeta_1 &= l \coth(\beta l) - \frac{1}{\beta}, \quad \zeta_2 = 0, \quad \zeta_3 = 0
\end{aligned}
\right. \tag{2.28}$$

Meanwhile, the first four equations of [equation \(2.26\)](#) together with the first equation of [equation \(2.27\)](#) lead to the derivation of the remaining variables, which results in

$$\boldsymbol{\Phi}_0^{(3)} = [0, \frac{k_{10}}{\beta} \varsigma(x) - a_{17} (\frac{x^3}{6} - \frac{\beta l \coth(\beta l) - 1}{2\beta} x^2), \frac{k_{11}}{\beta} \varsigma(x), \frac{k_{12}}{\beta} \varsigma(x), \frac{k_1}{\beta} \frac{d\varsigma}{dx}, 0, 0, 0]^T \tag{2.29}$$

where

$$\varsigma(x) = \frac{x^2}{2} - l \coth(\beta l)x - \frac{l \operatorname{csch}(\beta l)}{\beta} e^{-\beta x} \quad (2.30)$$

The correctness of [equation \(2.29\)](#) may be verified by the Maclaurin series with respect to β .

When the gradient index β is small, higher order terms in the Maclaurin series are neglectable,

therefore $\Phi_0^{(3)}$ is simplified as

$$\Phi_0^{(3)} = \begin{Bmatrix} 0 \\ -\frac{k_{10}}{\beta^3} + \frac{k_{10}l^2}{6\beta} - \frac{k_{10}l^2}{2}x + \frac{k_{10}-a_{17}}{6}x^3 \\ -\frac{k_{11}}{\beta^3} + \frac{k_{11}l^2}{6\beta} - \frac{k_{11}l^2}{2}x + \frac{k_{11}}{6}x^3 \\ -\frac{k_{12}}{\beta^3} + \frac{k_{12}l^2}{6\beta} - \frac{k_{12}l^2}{2}x + \frac{k_{12}}{6}x^3 \\ \frac{k_1}{2}(x^2 - l^2) \\ 0 \\ 0 \\ 0 \end{Bmatrix} \quad (2.31)$$

As can be seen, if the rigid body displacements and the constants are removed, [equation \(2.31\)](#)

is in accordance with the third-order Jordan form eigenvector in the homogeneous case [22].

Now, we eventually arrive at the eigen-solution:

$$\mathbf{f}_0^{(3)} = \Phi_0^{(3)} + z\Phi_{0,1}^{(2)} + \frac{z^2}{2!}\Phi_{0,1}^{(1)} + \frac{z^3}{3!}\Phi_{0,1}^{(0)} + \zeta_1(z\Phi_{0,2}^{(1)} + \frac{z^2}{2!}\Phi_{0,2}^{(0)}) \quad (2.32)$$

The correctness of the above eigen-solution can also be verified through the limits $\beta \rightarrow 0$,

$\zeta_1 \rightarrow 0$, which corresponds to the one in the homogeneous case as well [22].

It can be found that no feasible solution satisfies the eigen equation corresponding to $-\beta$, which indicates that $-\beta$ is not the eigenvalue. Thus, we have derived all the Saint-Venant solutions via the method of separation of variables. For clarity, the Saint-Venant solutions are eigen-solutions of special eigenvalues, through which the influence of the non-equilibrated external loads propagates to the farther area. The Saint-Venant solutions serve as a criterion for the Saint-Venant principle, i.e., the behaviors of the components in the full state vector are

local or not.

2.3. Eigen-solutions of general eigenvalues

The general eigenvalues play a pivotal role in satisfying the mixed boundary-value conditions, particularly in cases where abrupt variations in external loads and displacements occur within the region. The eigen equation is formulated as [equation \(2.15\)](#) with μ being nonzero eigenvalues. Assuming that the eigenvalue in the x -direction is η , we obtain

$$\det \begin{bmatrix} -\mu & -\eta & -a_1\eta & -a_2\eta & a_3 & 0 & 0 & 0 \\ -a_4\eta & -\mu & 0 & 0 & 0 & a_5 & a_6 & a_7 \\ a_8\eta & 0 & -\mu & 0 & 0 & a_6 & -a_9 & a_{10} \\ a_{11}\eta & 0 & 0 & -\mu & 0 & a_7 & a_{10} & -a_{12} \\ a_{13}(\eta^2 + \beta\eta) & 0 & 0 & 0 & -\mu & -a_4(\eta + \beta) & a_8(\eta + \beta) & a_{11}(\eta + \beta) \\ 0 & 0 & 0 & 0 & -(\eta + \beta) & -\mu & 0 & 0 \\ 0 & 0 & a_{14}(\eta^2 + \beta\eta) & a_{15}(\eta^2 + \beta\eta) & -a_1(\eta + \beta) & 0 & -\mu & 0 \\ 0 & 0 & a_{15}(\eta^2 + \beta\eta) & a_{16}(\eta^2 + \beta\eta) & -a_2(\eta + \beta) & 0 & 0 & -\mu \end{bmatrix} = 0 \quad (2.33)$$

which reads:

$$\theta_8\eta^8 + \theta_7\eta^7 + \theta_6\eta^6 + \theta_5\eta^5 + \theta_4\eta^4 + \theta_3\eta^3 + \theta_2\eta^2 + \theta_1\eta + \theta_0 = 0 \quad (2.34)$$

where θ_i ($i=0,\dots,8$) are parameters that consist of a_i, μ , and β , see [supplementary material](#)

[B.](#)

Although no general analytical formula is available for the solutions of the eight-degree algebraic equation, [equation \(2.34\)](#), it can be transformed to a four-degree one by replacing η with $\sqrt{\lambda} - \beta/2$ as

$$\begin{aligned} A_0\lambda^4 + (\mu^2 A_1 + \beta^2 A_2)\lambda^3 + (\mu^4 A_3 + \mu^2\beta^2 A_4 + \beta^4 A_5)\lambda^2 \\ + (\mu^6 A_6 + \mu^4\beta^2 A_7 + \mu^2\beta^4 A_8 + \beta^6 A_9)\lambda \\ + (\mu^8 A_{10} + \mu^6\beta^2 A_{11} + \mu^4\beta^4 A_{12} + \mu^2\beta^6 A_{13} + \beta^8 A_{14}) = 0 \end{aligned} \quad (2.35)$$

where A_k ($k = 0, \dots, 14$) are shown in [supplementary material B](#). Thus, the four roots of [equation \(2.35\)](#) are deduced analytically as λ_i ($i = 1, \dots, 4$), which can be rewritten as the eight roots η_t ($t = 1, \dots, 8$) of [equation \(2.34\)](#). Then, for general eigenvalues, the eigenvectors may be expressed as

$$\boldsymbol{\Phi} = \sum_{t=1}^8 e^{\eta_t x} [\tilde{A}_t, \tilde{B}_t, \tilde{C}_t, \tilde{D}_t, \tilde{E}_t, \tilde{F}_t, \tilde{G}_t, \tilde{H}_t]^T \quad (2.36)$$

where $\tilde{A}_t, \tilde{B}_t, \tilde{C}_t, \tilde{D}_t, \tilde{E}_t, \tilde{F}_t, \tilde{G}_t$, and \tilde{H}_t are constants, the relations of which can be derived after substituting [equation \(2.36\)](#) into the eigen equation. The constants can be represented in terms of \tilde{E}_t as

$$\begin{bmatrix} \tilde{A}_t \\ \tilde{B}_t \\ \tilde{C}_t \\ \tilde{D}_t \\ \tilde{F}_t \\ \tilde{G}_t \\ \tilde{H}_t \end{bmatrix} = \begin{bmatrix} -\mu & -\eta_t & -a_1\eta_t & -a_2\eta_t & 0 & 0 & 0 \\ -a_4\eta_t & -\mu & 0 & 0 & a_5 & a_6 & a_7 \\ a_8\eta_t & 0 & -\mu & 0 & a_6 & -a_9 & a_{10} \\ a_{11}\eta_t & 0 & 0 & -\mu & a_7 & a_{10} & -a_{12} \\ 0 & 0 & 0 & 0 & -\mu & 0 & 0 \\ 0 & 0 & a_{14}(\eta_t^2 + \beta\eta_t) & a_{15}(\eta_t^2 + \beta\eta_t) & 0 & -\mu & 0 \\ 0 & 0 & a_{15}(\eta_t^2 + \beta\eta_t) & a_{16}(\eta_t^2 + \beta\eta_t) & 0 & 0 & -\mu \end{bmatrix}^{-1} \begin{bmatrix} -a_3 \\ 0 \\ 0 \\ 0 \\ (\eta_t + \beta) \\ a_1(\eta_t + \beta) \\ a_2(\eta_t + \beta) \end{bmatrix} \tilde{E}_t \quad (2.37)$$

$$\equiv [\chi_{1t}, \chi_{2t}, \chi_{3t}, \chi_{4t}, \chi_{5t}, \chi_{6t}, \chi_{7t}]^T \tilde{E}_t$$

where χ_{jt} ($j = 1, \dots, 7; t = 1, \dots, 8$) are given in [supplementary material B](#).

Subsequently, by replacing $\tilde{A}_t, \tilde{B}_t, \tilde{C}_t, \tilde{D}_t, \tilde{F}_t, \tilde{G}_t$, and \tilde{H}_t in the homogeneous boundary conditions at $x = \pm l$ with \tilde{E}_t , we have:

$$\begin{cases} -a_{13} \frac{\partial u}{\partial x} + a_4 \sigma - a_8 D - a_{11} B = \sum_{t=1}^8 \varpi_{1t} \tilde{E}_t e^{\pm l\eta_t} = 0 \\ \tau = \sum_{t=1}^8 \varpi_{2t} \tilde{E}_t e^{\pm l\eta_t} = 0 \\ -a_{14} \frac{\partial \phi}{\partial x} - a_{15} \frac{\partial \psi}{\partial x} + a_1 \tau = \sum_{t=1}^8 \varpi_{3t} \tilde{E}_t e^{\pm l\eta_t} = 0 \\ -a_{15} \frac{\partial \phi}{\partial x} - a_{16} \frac{\partial \psi}{\partial x} + a_2 \tau = \sum_{t=1}^8 \varpi_{4t} \tilde{E}_t e^{\pm l\eta_t} = 0 \end{cases} \quad (2.38)$$

where

$$\begin{cases} \varpi_{1t} = -a_{13}\chi_{1t}\eta_t + a_4\chi_{5t} - a_8\chi_{6t} - a_{11}\chi_{7t} \\ \varpi_{2t} = 1 \\ \varpi_{3t} = -a_{14}\chi_{3t}\eta_t - a_{15}\chi_{4t}\eta_t + a_1 \\ \varpi_{4t} = -a_{15}\chi_{3t}\eta_t - a_{16}\chi_{4t}\eta_t + a_2 \end{cases} \quad (2.39)$$

If nontrivial solutions to [equation \(2.38\)](#) exist, the determinant of coefficient matrix should vanish:

$$\det \left[\varpi_{\lceil \frac{i}{2} \rceil j} e^{(-1)^{i+1} \eta_j l} \right] = 0 \quad (i=1, \dots, 8; j=1, \dots, 8) \quad (2.40)$$

where the subscript $\lceil \frac{i}{2} \rceil$ represents the ceiling function, which maps $\frac{i}{2}$ to the smallest integer greater than or equal to $\frac{i}{2}$. Then, the characteristic equation is derived through [equation \(2.40\)](#), which determines the eigenvalues μ_i . The parameters of nontrivial solutions are deduced as

$$\tilde{E}_{1i} = \mu_i, \quad \tilde{E}_{(t+1)i} = \Omega_{ti} \tilde{E}_{1i} \quad (t=1, \dots, 7) \quad (2.41)$$

where the subscript of μ_i represents the i -th root of the characteristic equation, and Ω_{ti} are given in [supplementary material B](#). We eventually arrive at the eigen-solutions for general eigenvalues as

$$\mathbf{f}_{\mu,i} = e^{\mu_i z} \Phi_i \quad (2.42)$$

2.4. Complete solution

According to symplectic expansion, the complete solution of [equation \(2.7\)](#) is

$$\tilde{\mathbf{f}} = \sum_{i=1}^{10} m_{0,i} \tilde{\mathbf{f}}_{0,i} + \sum_{i=1}^{\infty} \left[(m_{\mu,i}^{\text{Re}} \text{Re} \tilde{\mathbf{f}}_{\mu,i} + m_{\mu,i}^{\text{Im}} \text{Im} \tilde{\mathbf{f}}_{\mu,i}) + (m_{-\mu,i}^{\text{Re}} \text{Re} \tilde{\mathbf{f}}_{-\mu,i} + m_{-\mu,i}^{\text{Im}} \text{Im} \tilde{\mathbf{f}}_{-\mu,i}) \right] \equiv \sum_{i=1}^{\infty} m_i \tilde{\mathbf{f}}_i \quad (2.43)$$

where $\mathbf{f}_{0,i}$ ($i=1, 2, \dots, 10$) represent the eigen-solutions of zero eigenvalue, $\mathbf{f}_{\mu,i}$ and $\mathbf{f}_{-\mu,i}$ are the eigen-solutions of general eigenvalues μ_i and $-\mu_i$, respectively; $m_{0,i}$, $m_{\mu,i}^{\text{Re}}$, $m_{\mu,i}^{\text{Im}}$, $m_{-\mu,i}^{\text{Re}}$, and $m_{-\mu,i}^{\text{Im}}$ are the expansion coefficients to be determined for a particular problem; $\text{Re} \mathbf{f}$ and $\text{Im} \mathbf{f}$ represent the real part and imaginary part of the state vector \mathbf{f} , respectively, which build a bridge between real full state vectors and complex eigen-solutions, since the

characteristic equation may lead to complex eigenvalues. It is noted that, the eigen-solutions are distinct from the full state vectors $\tilde{\mathbf{f}}$ such that

$$\tilde{\mathbf{f}} = \mathcal{M}\mathbf{f} \quad (2.44)$$

where $\mathcal{M} = \text{diag}[1, 1, 1, 1, e^{\beta x}, e^{\beta x}, e^{\beta x}, e^{\beta x}]$.

To obtain the expansion coefficients, we first clarify the boundary conditions at $z = h$ and $z = 0$. The plane rectangle is fixed at $z = h$, and the electric and magnetic potential are also set as zero there:

$$u = 0, \quad w = 0, \quad \phi = 0, \quad \psi = 0 \quad (2.45)$$

If the indenter is frictionless and perfectly insulated, the mixed boundary-value conditions at $z = 0$ are

$$\begin{cases} w = d - \kappa(x) & x \in [\tilde{a}, \tilde{b}] \\ \sigma = 0 & x \in [-l, \tilde{a}] \cup [\tilde{b}, l] \end{cases}, \quad \tau = 0, \quad D = 0, \quad B = 0 \quad (2.46)$$

While, for a conducting indenter, we have

$$\begin{cases} w = d - \kappa(x) & x \in [\tilde{a}, \tilde{b}] \\ \sigma = 0 & x \in [-l, \tilde{a}] \cup [\tilde{b}, l] \end{cases}, \quad \tau = 0, \quad \begin{cases} \phi = \phi_0 & x \in [\tilde{a}, \tilde{b}] \\ D = 0 & x \in [-l, \tilde{a}] \cup [\tilde{b}, l] \end{cases}, \quad B = 0 \quad (2.47)$$

where d represents the maximum indentation depth, $\kappa(x)$ is the function that reflects the indenter shape, ϕ_0 is the electric potential of the indenter, and $x \in [\tilde{a}, \tilde{b}]$ is the region within contact.

The Hamiltonian mixed energy variational principle [23] for the mixed boundary-value problems is expressed as

$$\delta \left\{ \int_0^h \int_{-l}^l \left[\mathbf{p}^T \frac{\partial \mathbf{q}}{\partial z} - H(\mathbf{q}, \mathbf{p}) \right] dx dz - \int_{\Gamma_{q_h}} [\mathbf{p}^T (\mathbf{q} - \bar{\mathbf{q}}_h)] dx - \int_{\Gamma_{p_h}} [\bar{\mathbf{p}}_h^T \mathbf{q}] dx + \int_{\Gamma_{q_0}} [\mathbf{p}^T (\mathbf{q} - \bar{\mathbf{q}}_0)] dx + \int_{\Gamma_{p_0}} [\bar{\mathbf{p}}_0^T \mathbf{q}] dx \right\} = 0 \quad (2.48)$$

Since the adjoint vectors fulfill the canonical equation within the domain, [equation \(2.48\)](#) is

further simplified to:

$$\begin{aligned} & \int_{\Gamma_{p_h}} [(\delta \mathbf{q})^T (\mathbf{p} - \bar{\mathbf{p}}_h)] dx - \int_{\Gamma_{q_h}} [(\delta \mathbf{p})^T (\mathbf{q} - \bar{\mathbf{q}}_h)] dx \\ & + \int_{\Gamma_{q_0}} [(\delta \mathbf{p})^T (\mathbf{q} - \bar{\mathbf{q}}_0)] dx - \int_{\Gamma_{p_0}} [(\delta \mathbf{q})^T (\mathbf{p} - \bar{\mathbf{p}}_0)] dx = 0 \end{aligned} \quad (2.49)$$

Substituting [equation \(2.43\)](#) into [equation \(2.49\)](#), we have

$$\begin{aligned} & \int_{\Gamma_{p_h}} \left[\left(\sum_{i=1}^{\infty} \delta m_i \mathbf{q}_i \right)^T \left(\sum_{j=1}^{\infty} m_j \mathbf{p}_j - \bar{\mathbf{p}}_h \right) \right] dx - \int_{\Gamma_{q_h}} \left[\left(\sum_{i=1}^{\infty} \delta m_i \mathbf{p}_i \right)^T \left(\sum_{j=1}^{\infty} m_j \mathbf{q}_j - \bar{\mathbf{q}}_h \right) \right] dx \\ & + \int_{\Gamma_{q_0}} \left[\left(\sum_{i=1}^{\infty} \delta m_i \mathbf{p}_i \right)^T \left(\sum_{j=1}^{\infty} m_j \mathbf{q}_j - \bar{\mathbf{q}}_0 \right) \right] dx - \int_{\Gamma_{p_0}} \left[\left(\sum_{i=1}^{\infty} \delta m_i \mathbf{q}_i \right)^T \left(\sum_{j=1}^{\infty} m_j \mathbf{p}_j - \bar{\mathbf{p}}_0 \right) \right] dx = 0 \end{aligned} \quad (2.50)$$

Setting

$$\begin{aligned} \mathcal{A}_{ij} &= \int_{\Gamma_{p_h}} [(\mathbf{q}_i)^T \mathbf{p}_j] dx - \int_{\Gamma_{q_h}} [(\mathbf{p}_i)^T \mathbf{q}_j] dx + \int_{\Gamma_{q_0}} [(\mathbf{p}_i)^T \mathbf{q}_j] dx - \int_{\Gamma_{p_0}} [(\mathbf{q}_i)^T \mathbf{p}_j] dx \\ \mathcal{H}_i &= \int_{\Gamma_{p_h}} [(\mathbf{q}_i)^T \bar{\mathbf{p}}_h] dx - \int_{\Gamma_{q_h}} [(\mathbf{p}_i)^T \bar{\mathbf{q}}_h] dx + \int_{\Gamma_{q_0}} [(\mathbf{p}_i)^T \bar{\mathbf{q}}_0] dx - \int_{\Gamma_{p_0}} [(\mathbf{q}_i)^T \bar{\mathbf{p}}_0] dx \end{aligned} \quad (2.51)$$

leads to

$$\mathcal{A}_{ij} m_j = \mathcal{H}_i \quad (2.52)$$

According to the Kronecker-Capelli theorem [\[24\]](#), if [equation \(2.52\)](#) is compatible, the solution to the system is

$$m_k = \frac{\det \mathcal{A}_{ij;k}}{\det \mathcal{A}_{ij}} \quad (2.53)$$

where $\mathcal{A}_{ij;k}$ is the matrix formed by replacing the k -th column of \mathcal{A}_{ij} by the column vector \mathcal{H}_i . Now, we have accomplished the symplectic theory for the contact analysis of a finite-sized functionally graded plane with multi-field coupling.

3. Numerical results and discussions

3.1. Scenario 1

We first consider a relatively simple example, i.e., a rigid flat punch acting on the surface

of a finite horizontally graded isotropic elastic plane with the length of $2l = 20(\text{m})$ and width of $h = 10(\text{m})$, as depicted in [figure 2](#). The Young's modulus $E(x) = E_0 e^{\beta x}$ varies exponentially along the x -axis with $E_0 = 1(\text{Pa})$ and a constant Poisson's ratio $\nu_0 = 0.25$. The gradient index is taken as $\beta = 0.1 (\text{m}^{-1})$, and the contact region is assumed to be $x \in [-0.5, 0.5] (\text{m})$ with the maximum indentation depth $d = 0.02(\text{m})$.

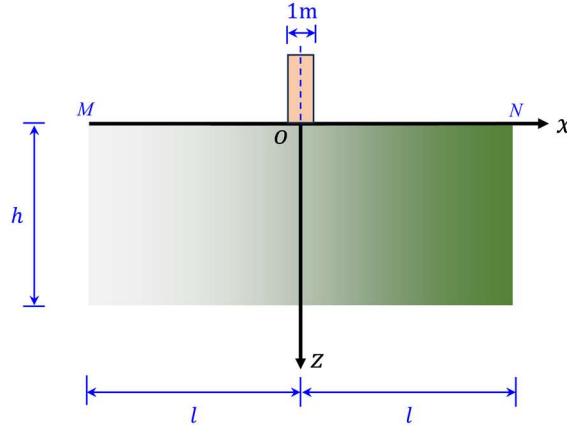


Figure 2. A rigid flat punch applied at the center on the surface of a finite horizontally graded isotropic plane.

The governing equations in matrix form are

$$\frac{\partial}{\partial z} \begin{bmatrix} u_z \\ u_x \\ \hat{\sigma}_{zz} \\ \hat{\tau}_{xz} \end{bmatrix} = \begin{bmatrix} 0 & -\nu_0 \frac{\partial}{\partial x} & \frac{1-\nu_0^2}{E_0} & 0 \\ -\frac{\partial}{\partial x} & 0 & 0 & \frac{2(1+\nu_0)}{E_0} \\ 0 & 0 & 0 & -\beta - \frac{\partial}{\partial x} \\ 0 & -E_0 \frac{\partial^2}{\partial x^2} - E_0 \beta \frac{\partial}{\partial x} & -\nu_0 \frac{\partial}{\partial x} - \nu_0 \beta & 0 \end{bmatrix} \begin{bmatrix} u_z \\ u_x \\ \hat{\sigma}_{zz} \\ \hat{\tau}_{xz} \end{bmatrix} \quad (3.1)$$

The homogeneous boundary conditions at $x = \pm l$ may be expressed as

$$E_0 \frac{\partial u_x}{\partial x} + \nu_0 \hat{\sigma}_{zz} = 0, \quad \hat{\tau}_{xz} = 0 \quad (3.2)$$

where σ_{ij} are the stress components; u_x and u_z are the displacement components in the x - and z -directions, respectively; $\hat{\sigma}_{xx} = \sigma_{xx} e^{-\beta x}$, $\hat{\sigma}_{zz} = \sigma_{zz} e^{-\beta x}$, and $\hat{\tau}_{xz} = \sigma_{xz} e^{-\beta x}$. The boundary conditions at the other two sides are:

$$z=h, \quad \begin{cases} u_z=0 \\ u_x=0 \end{cases} \quad z=0, \quad \begin{cases} \hat{\tau}_{xz}=0 & x \in [-l, l] \\ u_z=d & x \in [a, b] \\ \hat{\sigma}_{zz}=0 & x \in [-l, a] \cup [b, l] \end{cases} \quad (3.3)$$

Through the method of separation of variables, the eigen-solutions for zero eigenvalue are

obtained as

$$\begin{aligned} \mathbf{f}_{0,1}^{(0)} &= \boldsymbol{\Phi}_{0,1}^{(0)} = [1, 0, 0, 0]^T, & \mathbf{f}_{0,2}^{(0)} &= \boldsymbol{\Phi}_{0,2}^{(0)} = [0, 1, 0, 0]^T \\ \mathbf{f}_{0,1}^{(1)} &= \boldsymbol{\Phi}_{0,1}^{(1)} + z\boldsymbol{\Phi}_{0,1}^{(0)} = [z, -\nu_0 x, E_0, 0]^T, & \mathbf{f}_{0,2}^{(1)} &= \boldsymbol{\Phi}_{0,2}^{(1)} + z\boldsymbol{\Phi}_{0,2}^{(0)} = [-x, z, 0, 0]^T \\ \mathbf{f}_{0,2}^{(2)} &= \boldsymbol{\Phi}_{0,2}^{(2)} + z\boldsymbol{\Phi}_{0,2}^{(1)} + \frac{z^2}{2}\boldsymbol{\Phi}_{0,2}^{(0)} = [-xz, \frac{1}{2}(\nu_0 x^2 + z^2), -E_0 x, 0]^T \\ \mathbf{f}_0^{(3)} &= \boldsymbol{\Phi}_0^{(3)} + z\boldsymbol{\Phi}_{0,2}^{(2)} + \frac{z^2}{2!}\boldsymbol{\Phi}_{0,2}^{(1)} + \frac{z^3}{3!}\boldsymbol{\Phi}_{0,2}^{(0)} + \zeta_0(z\boldsymbol{\Phi}_{0,1}^{(1)} + \frac{z^2}{2!}\boldsymbol{\Phi}_{0,1}^{(0)}) \end{aligned} \quad (3.4)$$

where

$$\boldsymbol{\Phi}_0^{(3)} = \left\{ \begin{array}{c} \frac{2(1+\nu_0)}{E_0} \left[-\frac{E_0 l}{\beta^2 \sinh(\beta l)} e^{-\beta x} + \frac{E_0}{\beta} \frac{x^2}{2} - \left(\frac{\zeta_0 E_0}{\beta} + \frac{E_0}{\beta^2} \right) x \right] - \frac{1}{6} \nu_0 x^3 + \frac{1}{2} \zeta_0 \nu_0 x^2 \\ 0 \\ 0 \\ \frac{E_0 l}{\beta \sinh(\beta l)} e^{-\beta x} + \frac{E_0}{\beta} x - \left(\frac{\zeta_0 E_0}{\beta} + \frac{E_0}{\beta^2} \right) \end{array} \right\} \quad (3.5)$$

and

$$\zeta_0 = \frac{l \cosh(\beta l)}{\sinh(\beta l)} - \frac{1}{\beta} \quad (3.6)$$

While for general eigenvalues, the eigen-solutions may be expressed as

$$\mathbf{f}_{\mu,n} = e^{\mu_n z} \boldsymbol{\Phi}_n = e^{\mu_n z} \sum_{i=1}^4 \left(e^{\eta_m x} [\mathcal{A}_m, \mathcal{B}_m, \mathcal{C}_m, \mathcal{D}_m]^T \right) \quad (3.7)$$

where \mathcal{A}_m , \mathcal{B}_m , \mathcal{C}_m , and \mathcal{D}_m are constants, the relations of which are clarified in [supplementary material C](#).

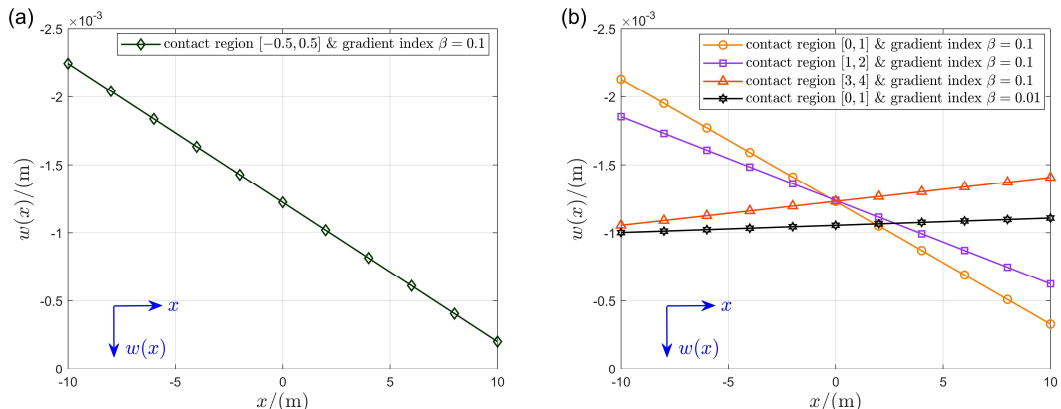


Figure 3. Saint-Venant solutions for $w(x)$. (a) Vertical displacement with contact region $x \in [-0.5, 0.5]$ and gradient index 0.1. (b) Comparison among Saint-Venant solutions in different cases.

The Saint-Venant solutions for zero eigenvalue will be calculated first. The distribution of the vertical displacement along the x -axis is illustrated in [figure 3\(a\)](#). It is interesting to find that the Saint-Venant displacement displays an upward phenomenon though the indenter acts downward on the surface vertically. This peculiar phenomenon is due to the fact that the Saint-Venant solution only corresponds to the non-exponential decay part. As a solution that reflects the behavior over the entire domain, it usually exhibits itself in regions distant from the contact surface, for its magnitude is less significant in comparison to the exponentially decaying terms in regions closer to the indenter.

[Figure 3\(b\)](#) demonstrates the comparison among the Saint-Venant solutions for different cases of material inhomogeneity and contact region. When the indenter is symmetrically pressed (with respect to the z -axis), the surface at the softer side rises higher. As the indenter moves along the x -direction, the degree of asymmetry of the vertical displacement due to the change of the contact region gradually outweighs that due to the material inhomogeneity. In addition, the displacement component at the coordinate origin keeps approximately unchanged with varying contact region under the action of a flat punch for the same material inhomogeneity, since the terms containing the parameters of contact region a and b will vanish at $x = 0$. If the gradient index is reduced to 0.01, the asymmetry of the contact region is a large factor compared to the material inhomogeneity. Moreover, the horizontal displacement remains constant along the x -axis at the same depth, and the stress components are all zero. This indicates the normal and tangential stresses only contain the decaying terms, coinciding with

the deficiency of the eigenvalue $-\beta$.

For the eigen-solutions of general eigenvalues, the characteristic equation is.

$$\begin{aligned} & (\eta_1 - \eta_2)(\eta_3 - \eta_4) + (\eta_1 - \eta_4)(\eta_2 - \eta_3) \cosh[(\eta_1 - \eta_2 - \eta_3 + \eta_4)l] \\ & + (\eta_1 - \eta_3)(\eta_4 - \eta_2) \cosh[(\eta_1 - \eta_2 + \eta_3 - \eta_4)l] = 0 \end{aligned} \quad (3.8)$$

where

$$\begin{aligned} \eta_1 &= -\frac{1}{2}\beta + \frac{1}{2}\sqrt{\beta^2 - 4\mu^2 - 4\mu\beta\sqrt{\nu_0}} & \eta_2 &= -\frac{1}{2}\beta - \frac{1}{2}\sqrt{\beta^2 - 4\mu^2 - 4\mu\beta\sqrt{\nu_0}} \\ \eta_3 &= -\frac{1}{2}\beta + \frac{1}{2}\sqrt{\beta^2 - 4\mu^2 + 4\mu\beta\sqrt{\nu_0}} & \eta_4 &= -\frac{1}{2}\beta - \frac{1}{2}\sqrt{\beta^2 - 4\mu^2 + 4\mu\beta\sqrt{\nu_0}} \end{aligned} \quad (3.9)$$

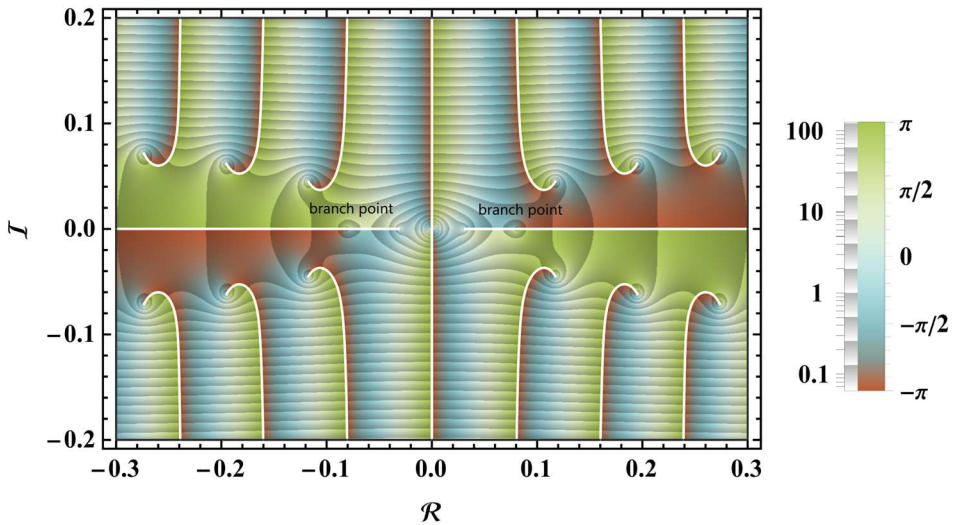


Figure 4. The characteristic equation on the complex plane of eigenvalue μ (real axis $\Re(\mu) \in [-0.3, 0.3]$ and imaginary axis $\Im(\mu) \in [-0.2, 0.2]$). The absolute value of the equation is represented with contours, and the argument is colored. Branch points and zeros are illustrated with circles, where the branch points are located on the real axis (except for $(0,0)$), and the rest are the zeros.

Figure 4 displays the left-hand side of equation (3.8) on the complex plane of μ , with all the zeros and branch points clearly indicated by circles. Obviously, the roots are symmetric about the real and imaginary axes. Without loss of generality, we may classify the roots into two sets: $\tilde{\alpha}$ -set: μ_n and μ_n^\dagger ; $\tilde{\beta}$ -set: $-\mu_n$ and $-\mu_n^\dagger$, where μ^\dagger represents the complex conjugation of μ . It warrants noting that the real parts of the roots are periodically distributed, and the period may be deduced from the characteristic equation as $\pi/20$.

We then substitute the roots of equation (3.8) into the eigen-solutions, and the results are

depicted in figure 5. Additionally, the results from finite element analysis (FEA) are also presented therein for comparison. To illustrate, equation (2.43) has been transformed into a real canonical one by reassembling the eigenvalues in the $\tilde{\alpha}$ -set and $\tilde{\beta}$ -set to avoid the presence of complex operation as follows

$$\begin{aligned} w_n &= \sum_{i=1}^4 \left\{ \mathcal{A}_{1in} e^{(\operatorname{Re} \eta_{in})x} \cos[(\operatorname{Im} \eta_{in})x + (\operatorname{Im} \mu_n)z] + \mathcal{A}_{2in} e^{(\operatorname{Re} \eta_{in})x} \sin[(\operatorname{Im} \eta_{in})x + (\operatorname{Im} \mu_n)z] \right\} \\ u_n &= \sum_{i=1}^4 \left\{ \mathcal{B}_{1in} e^{(\operatorname{Re} \eta_{in})x} \cos[(\operatorname{Im} \eta_{in})x + (\operatorname{Im} \mu_n)z] + \mathcal{B}_{2in} e^{(\operatorname{Re} \eta_{in})x} \sin[(\operatorname{Im} \eta_{in})x + (\operatorname{Im} \mu_n)z] \right\} \\ \sigma_n &= \sum_{i=1}^4 \left\{ \mathcal{C}_{1in} e^{(\operatorname{Re} \eta_{in})x} \cos[(\operatorname{Im} \eta_{in})x + (\operatorname{Im} \mu_n)z] + \mathcal{C}_{2in} e^{(\operatorname{Re} \eta_{in})x} \sin[(\operatorname{Im} \eta_{in})x + (\operatorname{Im} \mu_n)z] \right\} \\ \tau_n &= \sum_{i=1}^4 \left\{ \mathcal{D}_{1in} e^{(\operatorname{Re} \eta_{in})x} \cos[(\operatorname{Im} \eta_{in})x + (\operatorname{Im} \mu_n)z] + \mathcal{D}_{2in} e^{(\operatorname{Re} \eta_{in})x} \sin[(\operatorname{Im} \eta_{in})x + (\operatorname{Im} \mu_n)z] \right\} \end{aligned} \quad (3.10)$$

where $\mathcal{A}_{kin}, \mathcal{B}_{kin}, \mathcal{C}_{kin}$, and \mathcal{D}_{kin} ($k=1,2; i=1,2,3,4$) are constants.

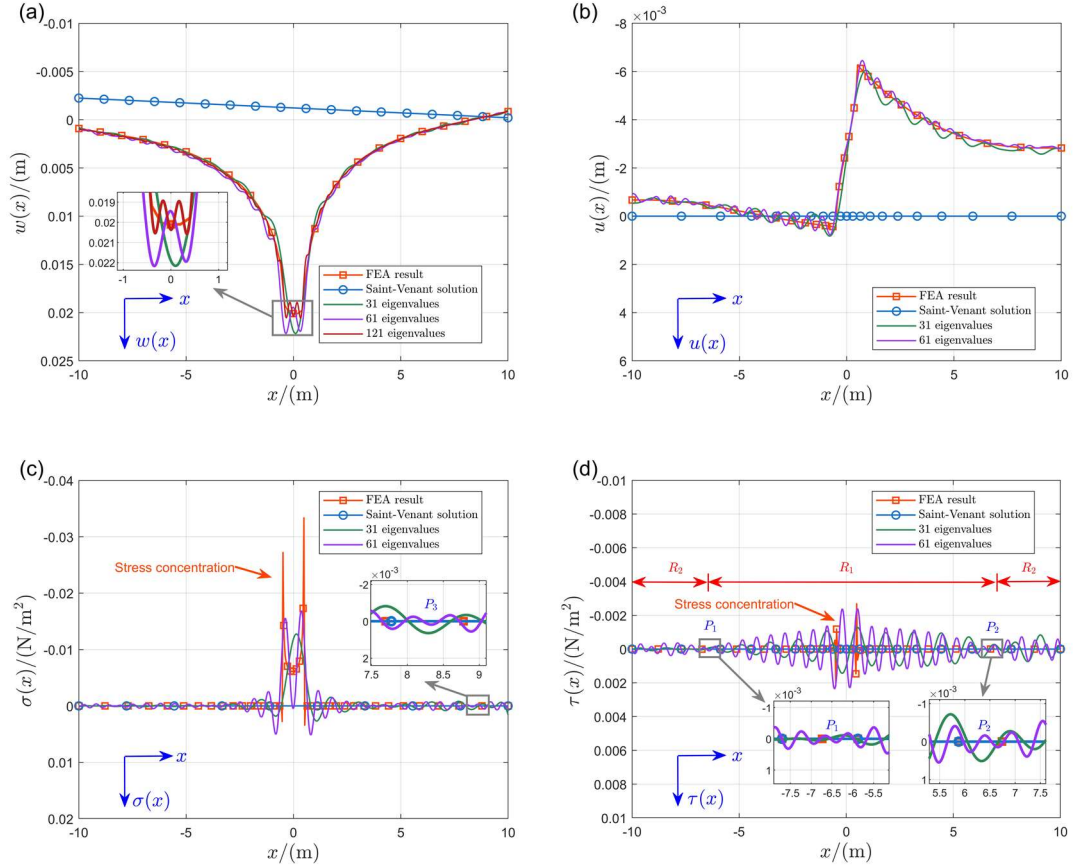


Figure 5. Comparison between FEA results and analytical solutions of complete solutions on the surface along the x -axis. (a) Vertical displacement. (b) Horizontal displacement. (c) Normal stress. (d) Shear stress. To display the relations among the curves, (a), (c) and (d) are locally enlarged. The Saint-Venant solutions are also displayed, respectively.

The symplectic solutions are applicable to the whole plane (of finite size), while we only take the case with $z = 0$ for discussion. As shown in [figure 5](#), the more eigenvalues are involved, the more accurate the results are. For instance, with 61 eigenvalues, the absolute error of the numerical result for vertical displacement is less than 10^{-3} , which achieves a higher accuracy compared to the result obtained with 31 eigenvalues. Interestingly, a common feature is observed that all the symplectic solutions are oscillating. Take the case with 61 eigenvalues displayed in [figure 5\(d\)](#) for example. The region with oscillation can be divided into R_1 and R_2 based on the cut-off points P_1 and P_2 (P_3 in [figure 5\(c\)](#) is also a cut-off point). Theoretically, the conditions near the lateral boundary (i.e., over the region R_2) should be satisfied precisely, whereas minor oscillation happens. The existence of geometric singularities at the corner points $M(-l, 0)$ and $N(l, 0)$ of the plane, as exhibited in [figure 2](#), leads to the singularities in the analytical solutions, which contributes to the occurrence of oscillation. Furthermore, relatively large oscillation also appears, as illustrated in the region R_1 , which requires a large enough number of eigenvalues for an accurate description of contact interaction. Fortunately, the oscillating phenomenon over the whole region will be diminished after employing a considerable number of eigen-solutions for superposition, leading to the convergent consequences. Additionally, the eigen-solutions with general eigenvalues outweigh the Saint-Venant solutions, as compared in [figure 5\(a\)](#), from which we can observe that the upward and downward parts are contrary near the lateral boundaries.

It is important to emphasize that the flat punch is one of the indenters that are difficult to analyze in comparison with the spherical or other indenters with a smooth shape function.

This is because the flat punch contains two cusps, leading to the Gibbs phenomenon, which is a source of error. To clarify, the Gibbs phenomenon refers to the oscillatory behavior observed in the series of a piecewise continuously differentiable function near a discontinuity. Moreover, the oscillations in the FEA result and analytical solution are caused by stress concentration and Gibbs phenomenon, respectively, as demonstrated in [figure 5\(c\)](#).

The FEA results are displayed in [figure 6](#), the parameters of which remain the same as those in the analytical solutions. It is seen that the left half of the plane is with large deformation and small stresses in contrast to the other half at the same depth, which reveals the asymmetry with respect to the z -axis. In addition, the stress contours are more densely distributed than the displacement contours, which coincides with the fact that the non-exponential decay terms are absent in the symplectic solutions. Furthermore, the vertical displacement reflected by contours at the bottom of the plane is with minor negative value in [figure 6\(a\)](#), as predicted to be the Saint-Venant solutions.

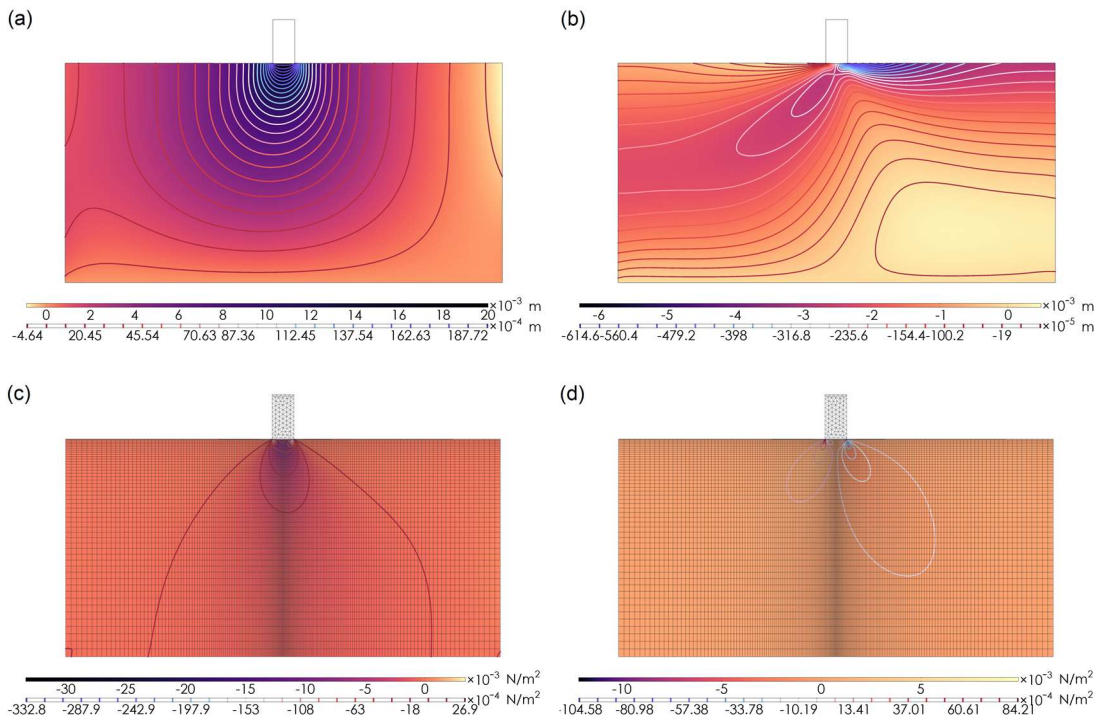


Figure 6. FEA results for deformation and stress distributions when a rigid flat punch acts on the surface of a horizontally graded plane **(a)** Vertical displacement. **(b)** Horizontal displacement. **(c)** Normal stress. **(d)** Shear stress. 10331 nodes are refined on the surface, especially within the contact region, as shown in the figures (c) and (d). The mesh for displacement remains the same, which is omitted in the figures (a) and (b). The augmented Lagrangian method (ALM) is used to solve the contact problem, which is a combination of both the penalty and the Lagrange multiplier techniques [25-26].

To facilitate engineering applications, we may rewrite the relationship between the indentation depth and the normal force in a compact form as:

$$P = \int_a^b \tilde{\sigma} \Big|_{z=0} dx = \sum_{k=1}^{\infty} m_k \int_a^b \tilde{f}_{k|3} \Big|_{z=0} dx \quad (3.11)$$

where $\tilde{f}_{k|3}$ represents the third element in the full state vector, and \tilde{f}_k is defined in [equation \(2.43\)](#). Considering the fact that $\mathcal{H}_i \propto d$, $f_{0,1|3}^{(1)} \propto E_0$, $f_{0,2|3}^{(2)} \propto E_0$, and $C_m \propto E_0$, which leads to $m_k \propto d$ and $\tilde{f}_{k|3} \propto E_0$, [equation \(3.11\)](#) is further simplified as

$$\begin{aligned} P &= \left[\sum_{k=1}^{\infty} \left(\frac{\det \mathcal{A}'_{ij;k}}{\det \mathcal{A}_{ij}} \int_a^b \tilde{f}'_{k|3} \Big|_{z=0} dx \right) \right] E_0 d \\ &\approx \left[\sum_{k=1}^N \left(\frac{\det \mathcal{A}'_{ij;k}}{\det \mathcal{A}_{ij}} \int_a^b \tilde{f}'_{k|3} \Big|_{z=0} dx \right) \right] E_0 d \\ &\equiv \mathcal{G}(\mu_n, \beta, \nu_0, a, b) E_0 d \end{aligned} \quad (3.12)$$

where $\mathcal{A}'_{ij;k}$ is a matrix constructed by replacing the k -th column of \mathcal{A}_{ij} by the vector $\mathcal{H}'_i = \int_a^b \tilde{f}_{i|3} \Big|_{z=0} dx$, and $\tilde{f}'_{k|3} = \tilde{f}_{k|3} / E_0$. The approximate equality holds if and only if N is sufficient to fulfill the convergence of the symplectic expansion. For example, we find that if we take $N=126$, the relative error is about 1.8%. It is noted that, $\mathcal{G}(\mu_n, \beta, \nu_0, a, b)$ defined by

$$\mathcal{G} = \sum_{k=1}^N \left(\frac{\det \mathcal{A}'_{ij;k}}{\det \mathcal{A}_{ij}} \int_a^b \tilde{f}'_{k|3} \Big|_{z=0} dx \right) \quad (3.13)$$

is a constant when the five parameters listed in the brackets are specified. For materials of unknown properties, we can ascertain the equivalent material parameter, i.e., the slope of $P-d$ curve in [figure 7](#), through the indentation technique.

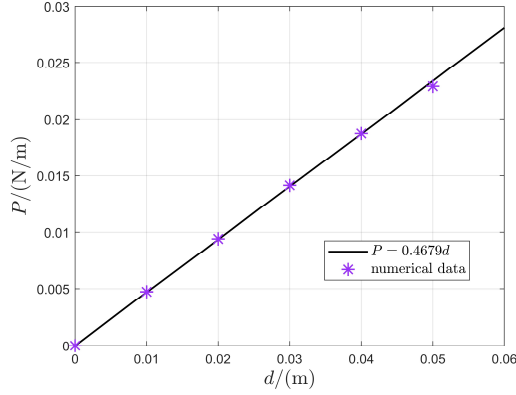


Figure 7. Relationship between the indentation depth and the normal force. Numerical data are generated from FEA with all parameters the same as those for [figure 6](#).

3.2. Scenario 2

Given that a perfectly insulated flat punch is applied on the surface of a horizontally graded magneto-electro-elastic plane with the length of $2l = 20(\text{m})$ and width of $h = 10(\text{m})$. The elastic, piezoelectric, piezomagnetic, dielectric, magnetic and electromagnetic constants are assumed to vary exponentially along the x -axis in a unified manner as [equation \(2.1\)](#), with their values being

$$\begin{aligned} c_{11}^0 &= 2.26 \times 10^{11} (\text{N/m}^2) & e_{31}^0 &= -2.20 (\text{C/m}^2) & e_{33}^0 &= 9.30 (\text{C/m}^2) & e_{15}^0 &= 5.80 (\text{C/m}^2) \\ c_{13}^0 &= 1.24 \times 10^{11} (\text{N/m}^2) & q_{31}^0 &= 2.90 \times 10^2 (\text{N/Am}) & q_{33}^0 &= 3.50 \times 10^2 (\text{N/Am}) & q_{15}^0 &= 2.75 \times 10^2 (\text{N/Am}) \\ c_{33}^0 &= 2.16 \times 10^{11} (\text{N/m}^2) & \varepsilon_{11}^0 &= 5.64 \times 10^{-9} (\text{C}^2/\text{Nm}^2) & \gamma_{11}^0 &= 2.97 \times 10^{-4} (\text{Ns}^2/\text{C}^2) & d_{11}^0 &= 0.00 (\text{Ns/VC}) \\ c_{44}^0 &= 4.4 \times 10^{10} (\text{N/m}^2) & \varepsilon_{33}^0 &= 6.35 \times 10^{-9} (\text{C}^2/\text{Nm}^2) & \gamma_{33}^0 &= 8.35 \times 10^{-5} (\text{Ns}^2/\text{C}^2) & d_{33}^0 &= 0.00 (\text{Ns/VC}) \end{aligned}$$

at the coordinate origin, respectively. The gradient index is taken as $\beta = 0.1(\text{m}^{-1})$, and the contact region is assumed to be $x \in [-0.5, 0.5] (\text{m})$ with the maximum indentation depth $d = 0.02(\text{m})$. We therefore obtain the numerical results for Saint-Venant solutions in [figure 8](#).

The vertical displacement also exhibits the peculiar phenomenon mentioned earlier, and the rest elements in the state vector \mathbf{q} remain constants, respectively. In addition, all the elements in the state vector \mathbf{p} keeps zero similarly, which indicates all the solutions will decay exponentially along the z -direction.

The boundary conditions in the z -direction are set as

$$z = h, \quad \begin{cases} u = 0 \\ w = 0 \\ \phi = 0 \\ \psi = 0 \end{cases} \quad z = 0, \quad \begin{cases} \tau = 0 & x \in [-l, l] \\ w = d & x \in [a, b] \\ \sigma = 0 & x \in [-l, a] \cup [b, l] \\ D = 0 & x \in [-l, l] \\ B = 0 & x \in [-l, l] \end{cases}$$

To clarify the coefficients in the symplectic expansion, [equation \(2.51\)](#) is detailed as

$$\begin{aligned} \mathcal{A}_{ij} &= -\int_{-l}^l [(\tau)_i(u)_j + (\sigma)_i(w)_j + (D)_i(\phi)_j + (B)_i(\psi)_j] \Big|_{z=h} dx + \int_a^b [(\sigma)_i(w)_j] \Big|_{z=0} dx \\ &\quad - (\int_{-l}^a + \int_b^l) [(w)_i(\sigma)] \Big|_{z=0} dx - \int_{-l}^l [(u)_i(\tau)_j + (\phi)_i(D)_j + (\psi)_i(B)_j] \Big|_{z=0} dx \quad (3.14) \\ \mathcal{H}_i &= \int_a^b d \cdot (\sigma)_i \Big|_{z=0} dx \end{aligned}$$

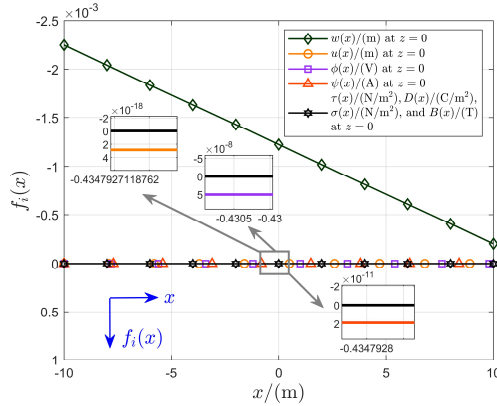


Figure 8. Saint-Venant solutions at $z = 0$ for the case of a perfectly insulated flat punch applied on the surface of a horizontally graded magneto-electro-elastic plane. To illustrate the relations among the curves, the figure is locally enlarged.

4. Conclusions

To conclude, the symplectic framework for contact analysis of a magneto-electro-elastic plane with a specific horizontal material gradient has been established. The operator matrix of the governing equations exhibits distinct properties compared with the Hamiltonian operator matrix for a homogeneous medium, resulting in the introduction of Hamiltonian mixed energy variational principle rather than adjoint symplectic orthogonality to deduce the coefficients in the symplectic expansion. The eigenvectors and the corresponding eigen-solutions of zero

eigenvalue are derived analytically for the four Jordan chains, leading to the Saint-Venant solutions. It is important to highlight that the third-order Jordan form eigenvector is constructed subtly to get the Jordan chain elongated, arriving at the tenth eigenvector for zero eigenvalue. However, the absence of $-\beta$ in the special eigenvalue case indicates the occurrence of exponential decay in the stress distributions. As for the general eigenvectors, the eight-degree algebraic equation is transformed to a four-degree equation, which gives a feasible way to derive the eigen-solutions. This significantly contributes to our analytical establishment of the symplectic framework, together with the quantitative characterization of deformation and stress distributions in contact analysis. In addition, the symplectic expansion is transformed into a real expression by reassembling the eigenvalues in the $\tilde{\alpha}$ -set and $\tilde{\beta}$ -set to avoid the presence of complex operation in the mixed boundary value problem. It is worth noting that the contact analysis is conducted in a finite plane with the homogeneous lateral boundary conditions, which is closer to physical reality than the existing researches for an infinite half-plane. Furthermore, using the technique of separating the variables, the theory is applicable for the indenters with arbitrary profiles, if the contact region is determined.

In numerical examples, we observed a peculiar phenomenon in the Saint-Venant solutions, which is understandable by analogizing the deformation of a water surface. Furthermore, the material inhomogeneity and the contact region act as a competing pair, which lead to the upper right or bottom left tendency of the curve in the vertical displacements. Moreover, the existence of the fixed point is also elucidated in the Saint-Venant solutions, which may serve as a criterion for distinguishing different material gradient indexes. With sufficient eigen-solutions for superposition, the analytical solutions converge with high precision in comparison with the FEA

results. To illustrate, the Gibbs phenomenon and oscillations are clarified mechanistically with the action of flat punch on the surface. The oscillations may be diminished by involving ample eigen-solutions, while the Gibbs phenomenon still presents.

The symplectic theory can also be applied to the cases with the non-homogeneous lateral boundary conditions, if the particular solutions are constructed to homogenize the lateral boundaries. Overall, the symplectic approach demonstrates effectiveness on tackling certain unsolved problems related to contact analysis, paving the way for subsequent development of quantitative HTT techniques using functionally graded material specimens.

Authors' contributions

Lizichen Chen: writing – original draft, Validation, Methodology, Investigation, Conceptualization; **Weiqiu Chen:** Writing – review and editing, Supervision, Funding acquisition.

Funding

The work was supported by the National Natural Science Foundation of China (Nos. 12192211 and 12192210), the Natural Science Foundation of Zhejiang Province (No. LD21A020001), and the 111 Project, PR China (No. B21034). This work was also partly supported by the specialized research projects of Huanjiang Laboratory, Zhuji, Zhejiang Province.

References

- [1] Y. Lan *et al.*, “Materials genomics methods for high-throughput construction of COFs and targeted synthesis,” *Nature Communication*, vol. 9, no. 1, p. 5274, Dec. 2018, doi: 10.1038/s41467-018-07720-x.
- [2] A. Ludwig, “Discovery of new materials using combinatorial synthesis and high-throughput characterization of thin-film materials libraries combined with computational methods,” *npj Computational Materials*, vol. 5, no. 1, p. 70, Jul. 2019, doi: 10.1038/s41524-019-0205-0.
- [3] A. J. Ruys, E. B. Popov, D. Sun, J. J. Russell, and C. C. J. Murray, “Functionally graded electrical/thermal ceramic systems,” *Journal of the European Ceramic Society*, vol. 21, no. 10–11, pp. 2025–2029, Jan. 2001, doi: 10.1016/S0955-2219(01)00165-0.
- [4] Z. Zhong, L. Wu, and W. Chen, “Progress in the study of mechanics problems of functionally graded materials and structures,” *Advances in Mechanics*, vol. 40, no. 5, pp. 528–541, 2010, doi: 10.3788/gzxb20103908.1438. (in Chinese)
- [5] C. F. Lü, W. Q. Chen, and C. W. Lim, “Elastic mechanical behavior of nano-scaled FGM films incorporating surface energies,” *Composites Science and Technology*, vol. 69, no. 7–8, pp. 1124–1130, Jun. 2009, doi: 10.1016/j.compscitech.2009.02.005.
- [6] S. Suresh, “Graded Materials for Resistance to Contact Deformation and Damage,” *Science, New Series*, vol. 292, no. 5526, pp. 2447–2451, 2001, doi: 10.1126/science.1059716.
- [7] T. M. Yue and T. Li, “Laser cladding of Ni/Cu/Al functionally graded coating on

- magnesium substrate,” *Surface and Coatings Technology*, vol. 202, no. 13, pp. 3043–3049, Mar. 2008, doi: 10.1016/j.surfcoat.2007.11.007.
- [8] M. R. Marulli, J. Bonari, J. Reinoso, and M. Paggi, “A coupled approach to predict cone-cracks in spherical indentation tests with smooth or rough indenters,” *Journal of the Mechanics and Physics of Solids*, vol. 178, p. 105345, Sep. 2023, doi: 10.1016/j.jmps.2023.105345.
- [9] A. E. Giannakopoulos and S. Suresh, “Indentation of solids with gradients in elastic properties: Part I. Point force,” *International Journal of Solids and Structures*, vol. 34, no. 19, pp. 2357–2392, Jul. 1997, doi: 10.1016/S0020-7683(96)00171-0.
- [10] A. E. Giannakopoulos and S. Suresh, “Indentation of solids with gradients in elastic properties: Part II. axisymmetric indentors,” *International Journal of Solids and Structures*, vol. 34, no. 19, pp. 2393–2428, Jul. 1997, doi: 10.1016/S0020-7683(96)00172-2.
- [11] H. Choi and G. Paulino, “Thermoelastic contact mechanics for a flat punch sliding over a graded coating/substrate system with frictional heat generation,” *Journal of the Mechanics and Physics of Solids*, vol. 56, no. 4, pp. 1673–1692, Apr. 2008, doi: 10.1016/j.jmps.2007.07.011.
- [12] S. Chen, C. Yan, P. Zhang, and H. Gao, “Mechanics of adhesive contact on a power-law graded elastic half-space,” *Journal of the Mechanics and Physics of Solids*, vol. 57, no. 9, pp. 1437–1448, Sep. 2009, doi: 10.1016/j.jmps.2009.06.006.
- [13] F. Jin, X. Guo, and H. Gao, “Adhesive contact on power-law graded elastic solids: The JKR–DMT transition using a double-Hertz model,” *Journal of the Mechanics*

and Physics of Solids, vol. 61, no. 12, pp. 2473–2492, Dec. 2013, doi:

10.1016/j.jmps.2013.07.015.

- [14] F. Jin, Q. Tang, X. Guo, and H. Gao, “A generalized Maugis-Dugdale solution for adhesion of power-law graded elastic materials,” *Journal of the Mechanics and Physics of Solids*, vol. 154, p. 104509, Sep. 2021, doi: 10.1016/j.jmps.2021.104509.
- [15] T.-J. Liu, C. Zhang, Y.-S. Wang, and Y.-M. Xing, “The axisymmetric stress analysis of double contact problem for functionally graded materials layer with arbitrary graded materials properties,” *International Journal of Solids and Structures*, vol. 96, pp. 229–239, Oct. 2016, doi: 10.1016/j.ijsolstr.2016.06.006.
- [16] S. J. Chidlow, W. W. F. Chong, and M. Teodorescu, “On the two-dimensional solution of both adhesive and non-adhesive contact problems involving functionally graded materials,” *European Journal of Mechanics - A/Solids*, vol. 39, pp. 86–103, May 2013, doi: 10.1016/j.euromechsol.2012.10.008.
- [17] L. Chen and W. Chen, “Surface Green’s functions of a horizontally graded elastic half-plane,” *Mechanics of Advanced Materials and Structures*, pp. 1–10, Apr. 2024, doi: 10.1080/15376494.2024.2342042.
- [18] W.-X. Zhong, *A new systematic methodology for theory of elasticity*. Dalian: Dalian University of Technology Press, 1995. (in Chinese)
- [19] L. Zhao and W. Chen, “Plane analysis for functionally graded magneto-electro-elastic materials via the symplectic framework,” *Composite Structures*, vol. 92, no. 7, pp. 1753–1761, Jun. 2010, doi: 10.1016/j.compstruct.2009.11.029.
- [20] L. Zhao, W. Q. Chen, and C. F. Lü, “Symplectic elasticity for bi-directional

- functionally graded materials,” *Mechanics of Materials*, vol. 54, pp. 32–42, Nov. 2012, doi: 10.1016/j.mechmat.2012.06.001.
- [21] W. Yao, W. Zhong, and C. W. Lim, *Symplectic elasticity*. New Jersey: World Scientific, 2009.
- [22] W. Yao and X. Li, “Symplectic duality system on plane magnetoelectroelastic solids,” *Applied Mathematics and Mechanics*, vol. 27, no. 2, pp. 195–205, Feb. 2006, doi: 10.1007/s10483-006-0207-z.
- [23] A. Y. T. Leung and J. Zheng, “Closed form stress distribution in 2D elasticity for all boundary conditions,” *Applied Mathematics and Mechanics -English Edition*, vol. 28, no. 12, pp. 1629–1642, Dec. 2007, doi: 10.1007/s10483-007-1210-z.
- [24] Q. Shu and X. Wang, “Standard orthogonal vectors in semilinear spaces and their applications,” *Linear Algebra and its Applications*, vol. 437, no. 11, pp. 2733–2754, Dec. 2012, doi: 10.1016/j.laa.2012.06.042.
- [25] G. Pietrzak and A. Curnier, “Large deformation frictional contact mechanics: continuum formulation and augmented Lagrangian treatment,” *Computer Methods in Applied Mechanics and Engineering*, vol. 177, no. 3–4, pp. 351–381, Jul. 1999, doi: 10.1016/S0045-7825(98)00388-0.
- [26] COMSOL Multiphysics® v. 6.0. cn.comsol.com. COMSOL AB, Stockholm, Sweden, 2021.

Supplementary material

S A. Constants and operator matrix

The constants in the basic formulations are

$$\begin{aligned}
a_1 &= e_{15}^0 / c_{44}^0, & a_2 &= q_{15}^0 / c_{44}^0, & a_3 &= 1 / c_{44}^0 \\
a_4 &= (c_{13}^0 b_1 + e_{31}^0 b_2 + q_{31}^0 b_3) / b_0, & a_5 &= b_1 / b_0, & a_6 &= b_2 / b_0 \\
a_7 &= b_3 / b_0, & a_8 &= (-c_{13}^0 b_2 + e_{31}^0 b_4 - q_{31}^0 b_5) / b_0, & a_9 &= b_4 / b_0 \\
a_{10} &= b_5 / b_0, & a_{11} &= (-c_{13}^0 b_3 + q_{31}^0 b_6 - e_{31}^0 b_5) / b_0, & a_{12} &= b_6 / b_0 \\
a_{13} &= -c_{11}^0 + c_{13}^0 a_4 - e_{31}^0 a_8 - q_{31}^0 a_{11}, & a_{14} &= \varepsilon_{11}^0 + (e_{15}^0)^2 / c_{44}^0, & a_{15} &= d_{11}^0 + e_{15}^0 q_{15}^0 / c_{44}^0 \\
a_{16} &= \gamma_{11}^0 + (q_{15}^0)^2 / c_{44}^0, & a_{17} &= c_{13}^0 / c_{11}^0, & a_{18} &= e_{31}^0 / c_{11}^0 \\
a_{19} &= q_{31}^0 / c_{11}^0, & b_0 &= c_{33}^0 b_1 + e_{33}^0 b_2 + q_{33}^0 b_3, & b_1 &= \gamma_{33}^0 \varepsilon_{33}^0 - (d_{33}^0)^2 \\
b_2 &= e_{33}^0 \gamma_{33}^0 - q_{33}^0 d_{33}^0, & b_3 &= \varepsilon_{33}^0 q_{33}^0 - e_{33}^0 d_{33}^0, & b_4 &= c_{33}^0 \gamma_{33}^0 + (q_{33}^0)^2 \\
b_5 &= c_{33}^0 d_{33}^0 + e_{33}^0 q_{33}^0, & b_6 &= c_{33}^0 \varepsilon_{33}^0 + (e_{33}^0)^2, & g_0 &= a_5(a_9 a_{12} - a_{10}^2) + a_6(a_6 a_{12} + a_7 a_{10}) + a_7(a_6 a_{10} + a_7 a_9) \\
g_1 &= (a_9 a_{12} - a_{10}^2) / g_0, & g_2 &= (a_6 a_{12} + a_7 a_{10}) / g_0, & g_3 &= (a_6 a_{10} + a_7 a_9) / g_0 \\
g_4 &= (a_5 a_{10} - a_6 a_7) / g_0, & g_5 &= (a_5 a_{12} + a_7^2) / g_0, & g_6 &= (a_5 a_9 + a_6^2) / g_0 \\
g_7 &= -a_4 g_1 + a_8 g_2 + a_{11} g_3, & g_8 &= a_4 g_2 + a_8 g_5 + a_{11} g_4, & g_9 &= a_4 g_3 + a_8 g_4 + a_{11} g_6 \\
k_1 &= a_{17} g_7 + g_1, & k_2 &= -a_{17} g_8 + g_2, & k_3 &= -a_{17} g_9 + g_3 \\
k_4 &= a_{18} g_7 + g_2, & k_5 &= -a_{18} g_8 - g_5, & k_6 &= -a_{18} g_9 - g_4 \\
k_7 &= a_{19} g_7 + g_3, & k_8 &= -a_{19} g_8 - g_4, & k_9 &= -a_{19} g_9 - g_6 \\
k_{10} &= a_3 k_1 - a_1 k_{11} - a_2 k_{12}, & k_{11} &= [(a_2 a_{15} - a_1 a_{16}) k_1 + a_{16} k_2 - a_{15} k_3] / (a_{15}^2 - a_{14} a_{16}), & k_{12} &= [(a_1 a_{15} - a_2 a_{14}) k_1 - a_{15} k_2 + a_{14} k_3] / (a_{15}^2 - a_{14} a_{16})
\end{aligned}$$

The quasi-Hamiltonian operator matrix is detailed as:

$$\mathcal{H} = \begin{bmatrix} 0 & -\frac{\partial}{\partial x} & -a_1 \frac{\partial}{\partial x} & -a_2 \frac{\partial}{\partial x} & a_3 & 0 & 0 & 0 \\ -a_4 \frac{\partial}{\partial x} & 0 & 0 & 0 & 0 & a_5 & a_6 & a_7 \\ a_8 \frac{\partial}{\partial x} & 0 & 0 & 0 & 0 & a_6 & -a_9 & a_{10} \\ a_{11} \frac{\partial}{\partial x} & 0 & 0 & 0 & 0 & a_7 & a_{10} & -a_{12} \\ a_{13} \left(\frac{\partial^2}{\partial x^2} + \beta \frac{\partial}{\partial x} \right) & 0 & 0 & 0 & 0 & -a_4 \left(\frac{\partial}{\partial x} + \beta \right) & a_8 \left(\frac{\partial}{\partial x} + \beta \right) & a_{11} \left(\frac{\partial}{\partial x} + \beta \right) \\ 0 & 0 & 0 & 0 & -\left(\frac{\partial}{\partial x} + \beta \right) & 0 & 0 & 0 \\ 0 & 0 & a_{14} \left(\frac{\partial^2}{\partial x^2} + \beta \frac{\partial}{\partial x} \right) & a_{15} \left(\frac{\partial^2}{\partial x^2} + \beta \frac{\partial}{\partial x} \right) & -a_1 \left(\frac{\partial}{\partial x} + \beta \right) & 0 & 0 & 0 \\ 0 & 0 & a_{15} \left(\frac{\partial^2}{\partial x^2} + \beta \frac{\partial}{\partial x} \right) & a_{16} \left(\frac{\partial^2}{\partial x^2} + \beta \frac{\partial}{\partial x} \right) & -a_2 \left(\frac{\partial}{\partial x} + \beta \right) & 0 & 0 & 0 \end{bmatrix}$$

S B. Constants for algebraic equations and relations

The parameters in [equation \(2.34\)](#) are expressed as:

$$\theta_8 = \left(a_4^2 \left(a_{10}^2 - a_9 a_{12} \right) + 2a_4 a_6 \left(a_{10} a_{11} + a_8 a_{12} \right) + a_6^2 a_{11}^2 + a_5 a_9 a_{11}^2 + 2a_5 a_8 a_{10} a_{11} + a_5 a_8^2 a_{12} + a_{12} a_{13} \left(a_6^2 + a_5 a_9 \right) - a_5 a_{10} a_{13} + a_7^2 \left(a_8^2 + a_9 a_{13} \right) + 2a_4 a_7 \left(a_8 a_{10} + a_9 a_{11} \right) + 2a_6 a_7 \left(a_{10} a_{13} - a_8 a_{11} \right) \right) \left(a_{15}^2 - a_{14} a_{16} \right) \quad (\text{B.1})$$

$$\theta_7 = 4\beta\theta_8 \quad (\text{B.2})$$

$$\begin{aligned}
\theta_6 = & \mu^2 \left(2a_8 a_{10} a_{11} a_{16} a_1^2 - a_{10}^2 a_{13} a_{16} a_1^2 + \left(a_{12} a_8^2 + a_9 \left(a_{11}^2 + a_{12} a_{13} \right) \right) a_{16} a_1^2 - a_2 a_9 a_{11}^2 a_{15} a_1 - 4a_2 a_8 a_{10} a_{11} a_{15} a_1 - a_2 a_8^2 a_{12} a_{15} a_1 \right. \\
& + 2a_2 a_{10}^2 a_{13} a_{15} a_1 - a_2 a_9 a_{12} a_{13} a_{15} a_1 + 2 \left(a_4 \left(a_8 a_{10} + a_9 a_{11} \right) + a_7 \left(a_8^2 + a_9 a_{13} \right) + a_6 \left(a_{10} a_{13} - a_8 a_{11} \right) \right) a_{15} a_1 - a_2 \left(a_{12} a_8^2 + a_9 \left(a_{11}^2 + a_{12} a_{13} \right) \right) a_{15} a_1 \\
& - 2 \left(a_4 \left(a_{10} a_{11} + a_8 a_{12} \right) + a_7 \left(a_{10} a_{13} - a_8 a_{11} \right) + a_6 \left(a_{11}^2 + a_{12} a_{13} \right) \right) a_{16} a_1 - 2 \left(a_7 \left(a_8 a_{10} + a_9 a_{11} \right) + a_6 \left(a_{10} a_{11} + a_8 a_{12} \right) + a_4 \left(a_{10}^2 - a_9 a_{12} \right) \right) a_{15}^2 \\
& + a_3 \left(a_{12} a_8^2 + 2a_{10} a_{11} a_8 - a_{10}^2 a_{13} + a_9 \left(a_{11}^2 + a_{12} a_{13} \right) \right) a_{15}^2 + a_2^2 a_9 a_{11}^2 a_{14} + 2a_2^2 a_8 a_{10} a_{11} a_{14} + a_2^2 a_8^2 a_{12} a_{14} - a_2^2 a_{10}^2 a_{13} a_{14} + a_2^2 a_9 a_{12} a_{13} a_{14} \\
& + \left(a_9 a_4^2 - 2a_6 a_8 a_4 - a_5 a_8^2 - \left(a_6^2 + a_5 a_9 \right) a_{13} \right) a_{14} - 2a_2 \left(a_4 \left(a_8 a_{10} + a_9 a_{11} \right) + a_7 \left(a_8^2 + a_9 a_{13} \right) + a_6 \left(a_{10} a_{13} - a_8 a_{11} \right) \right) a_{14} \\
& - 2 \left(a_{10} a_4^2 + \left(a_7 a_8 + a_6 a_{11} \right) a_4 + a_5 a_8 a_{11} + \left(a_6 a_7 - a_5 a_{10} \right) a_{13} \right) a_{15} + 2a_2 \left(a_4 \left(a_{10} a_{11} + a_8 a_{12} \right) + a_7 \left(a_{10} a_{13} - a_8 a_{11} \right) + a_6 \left(a_{11}^2 + a_{12} a_{13} \right) \right) a_{15} \\
& + \left(a_{12} a_4^2 - 2a_7 a_{11} a_4 - a_5 a_{11}^2 - \left(a_7^2 + a_5 a_{12} \right) a_{13} \right) a_{16} + 2 \left(a_7 \left(a_8 a_{10} + a_9 a_{11} \right) + a_6 \left(a_{10} a_{11} + a_8 a_{12} \right) + a_4 \left(a_{10}^2 - a_9 a_{12} \right) \right) a_{14} a_{16} \\
& \left. - a_3 \left(a_{12} a_8^2 + 2a_{10} a_{11} a_8 - a_{10}^2 a_{13} + a_9 \left(a_{11}^2 + a_{12} a_{13} \right) \right) a_{14} a_{16} \right) + 6\beta^2 \theta_8
\end{aligned} \quad (\text{B.3})$$

$$\theta_5 = 3\beta\mu^2\Upsilon_0 + 4\beta^3\theta_8 \quad (\text{B.4})$$

$$\begin{aligned}
\theta_4 = & \mu^4 \Upsilon_1 + \beta^2 \mu^2 \left(6a_8 a_{10} a_{11} a_{16} a_1^2 - 3a_{10}^2 a_{13} a_{16} a_1^2 + 3 \left(a_{12} a_8^2 + a_9 \left(a_{11}^2 + a_{12} a_{13} \right) \right) a_{16} a_1^2 - 3a_2 a_9 a_{11}^2 a_{15} a_1 - 12a_2 a_8 a_{10} a_{11} a_{15} a_1 \right. \\
& - 3a_2 a_8^2 a_{12} a_{15} a_1 + 6a_2 a_{10}^2 a_{13} a_{15} a_1 - 3a_2 a_9 a_{12} a_{13} a_{15} a_1 + 6a_{15} a_1 a_4 \left(a_8 a_{10} + a_9 a_{11} \right) + 6a_{15} a_1 \left(a_7 \left(a_8^2 + a_9 a_{13} \right) + a_6 \left(a_{10} a_{13} - a_8 a_{11} \right) \right) \\
& - 3a_2 \left(a_{12} a_8^2 + a_9 \left(a_{11}^2 + a_{12} a_{13} \right) \right) a_{15} a_1 - 6 \left(a_4 \left(a_{10} a_{11} + a_8 a_{12} \right) + a_7 \left(a_{10} a_{13} - a_8 a_{11} \right) + a_6 \left(a_{11}^2 + a_{12} a_{13} \right) \right) a_{16} a_1 \\
& - 7 \left(a_7 \left(a_8 a_{10} + a_9 a_{11} \right) + a_6 \left(a_{10} a_{11} + a_8 a_{12} \right) + a_4 \left(a_{10}^2 - a_9 a_{12} \right) \right) a_{15}^2 + 3a_3 \left(a_{12} a_8^2 + 2a_{10} a_{11} a_8 - a_{10}^2 a_{13} + a_9 \left(a_{11}^2 + a_{12} a_{13} \right) \right) a_{15}^2 \\
& + 3a_2^2 a_9 a_{11}^2 a_{14} + 6a_2^2 a_8 a_{10} a_{11} a_{14} + 3a_2^2 a_8^2 a_{12} a_{14} - 3a_2^2 a_{10} a_{13} a_{14} + 3a_2^2 a_9 a_{12} a_{13} a_{14} - 3 \left(-a_9 a_4^2 + 2a_6 a_8 a_4 + a_5 a_8^2 + \left(a_6^2 + a_5 a_9 \right) a_{13} \right) a_{14} \\
& - 6a_2 \left(a_4 \left(a_8 a_{10} + a_9 a_{11} \right) + a_7 \left(a_8^2 + a_9 a_{13} \right) + a_6 \left(a_{10} a_{13} - a_8 a_{11} \right) \right) a_{14} - 6 \left(a_{10} a_4^2 + \left(a_7 a_8 + a_6 a_{11} \right) a_4 + a_5 a_8 a_{11} + \left(a_6 a_7 - a_5 a_{10} \right) a_{13} \right) a_{15} \\
& + 6a_2 \left(a_4 \left(a_{10} a_{11} + a_8 a_{12} \right) + a_7 \left(a_{10} a_{13} - a_8 a_{11} \right) + a_6 \left(a_{11}^2 + a_{12} a_{13} \right) \right) a_{15} - 3 \left(-a_{12} a_4^2 + 2a_7 a_{11} a_4 + a_5 a_{11}^2 + \left(a_7^2 + a_5 a_{12} \right) a_{13} \right) a_{16} \\
& \left. + 7 \left(a_7 \left(a_8 a_{10} + a_9 a_{11} \right) + a_6 \left(a_{10} a_{11} + a_8 a_{12} \right) + a_4 \left(a_{10}^2 - a_9 a_{12} \right) \right) a_{14} a_{16} - 3a_3 \left(a_{12} a_8^2 + 2a_{10} a_{11} a_8 - a_{10}^2 a_{13} + a_9 \left(a_{11}^2 + a_{12} a_{13} \right) \right) a_{14} a_{16} \right) + \beta^4 \theta_8
\end{aligned} \tag{B.5}$$

$$\begin{aligned}
\theta_3 = & 2\beta\mu^4 \Upsilon_1 + \beta^3 \mu^2 \left(2a_8 a_{10} a_{11} a_{16} a_1^2 - a_{10}^2 a_{13} a_{16} a_1^2 + \left(a_{12} a_8^2 + a_9 \left(a_{11}^2 + a_{12} a_{13} \right) \right) a_{16} a_1^2 - a_2 a_9 a_{11}^2 a_{15} a_1 - 4a_2 a_8 a_{10} a_{11} a_{15} a_1 \right. \\
& - a_2 a_8^2 a_{12} a_{15} a_1 + 2a_2 a_{10}^2 a_{13} a_{15} a_1 - a_2 a_9 a_{12} a_{13} a_{15} a_1 + 2 \left(a_4 \left(a_8 a_{10} + a_9 a_{11} \right) + a_7 \left(a_8^2 + a_9 a_{13} \right) + a_6 \left(a_{10} a_{13} - a_8 a_{11} \right) \right) a_{15} a_1 \\
& - a_2 \left(a_{12} a_8^2 + a_9 \left(a_{11}^2 + a_{12} a_{13} \right) \right) a_{15} a_1 - 2 \left(a_4 \left(a_{10} a_{11} + a_8 a_{12} \right) + a_7 \left(a_{10} a_{13} - a_8 a_{11} \right) + a_6 \left(a_{11}^2 + a_{12} a_{13} \right) \right) a_{16} a_1 - 4a_{15}^2 a_7 \left(a_8 a_{10} + a_9 a_{11} \right) \\
& - 4a_{15}^2 \left(a_6 \left(a_{10} a_{11} + a_8 a_{12} \right) + a_4 \left(a_{10}^2 - a_9 a_{12} \right) \right) a_{15}^2 + a_3 \left(a_{12} a_8^2 + 2a_{10} a_{11} a_8 - a_{10}^2 a_{13} + a_9 \left(a_{11}^2 + a_{12} a_{13} \right) \right) a_{15}^2 + a_2^2 a_9 a_{11}^2 a_{14} + 2a_2^2 a_8 a_{10} a_{11} a_{14} + a_2^2 a_8^2 a_{12} a_{14} \\
& - a_2^2 a_{10} a_{13} a_{14} + a_2^2 a_9 a_{12} a_{13} a_{14} + \left(a_9 a_4^2 - 2a_6 a_8 a_4 - a_5 a_8^2 - \left(a_6^2 + a_5 a_9 \right) a_{13} \right) a_{14} - 2a_2 \left(a_4 \left(a_8 a_{10} + a_9 a_{11} \right) + a_7 \left(a_8^2 + a_9 a_{13} \right) + a_6 \left(a_{10} a_{13} - a_8 a_{11} \right) \right) a_{14} \\
& - 2 \left(a_{10} a_4^2 + \left(a_7 a_8 + a_6 a_{11} \right) a_4 + a_5 a_8 a_{11} + \left(a_6 a_7 - a_5 a_{10} \right) a_{13} \right) a_{15} + 2a_2 \left(a_4 \left(a_{10} a_{11} + a_8 a_{12} \right) + a_7 \left(a_{10} a_{13} - a_8 a_{11} \right) + a_6 \left(a_{11}^2 + a_{12} a_{13} \right) \right) a_{15} \\
& + \left(a_{12} a_4^2 - 2a_7 a_{11} a_4 - a_5 a_{11}^2 - \left(a_7^2 + a_5 a_{12} \right) a_{13} \right) a_{16} + 4 \left(a_7 \left(a_8 a_{10} + a_9 a_{11} \right) + a_6 \left(a_{10} a_{11} + a_8 a_{12} \right) + a_4 \left(a_{10}^2 - a_9 a_{12} \right) \right) a_{14} a_{16} \\
& \left. - a_3 \left(a_{12} a_8^2 + 2a_{10} a_{11} a_8 - a_{10}^2 a_{13} + a_9 \left(a_{11}^2 + a_{12} a_{13} \right) \right) a_{14} a_{16} \right)
\end{aligned} \tag{B.6}$$

$$\begin{aligned}
\theta_2 = & \mu^6 \Upsilon_2 + \beta^2 \mu^4 \left(\left(a_8^2 + a_9 a_{13} \right) a_1^2 + \left(-2a_6 a_{13} + 2a_2 \left(a_8 a_{11} - a_{10} a_{13} \right) - 3 \left(a_8 a_{10} + a_9 a_{11} \right) a_{15} + 3 \left(a_{10} a_{11} + a_8 a_{12} \right) a_{16} \right) a_1 \right. \\
& + a_4^2 + a_2^2 a_{11}^2 + a_{10}^2 a_{15}^2 - a_9 a_{12} a_{15}^2 - a_5 a_{13} - 2a_2 a_7 a_{13} + a_2^2 a_{12} a_{13} + a_8 \left(3a_6 - a_3 a_8 \right) a_{14} + 3a_2 a_8 a_{10} a_{14} + 3a_2 a_9 a_{11} a_{14} \\
& - a_3 a_9 a_{13} a_{14} + 3a_7 a_8 a_{15} + 3a_6 a_{11} a_{15} - 2a_3 a_8 a_{11} a_{15} - 3a_2 a_{10} a_{11} a_{15} - 3a_2 a_8 a_{12} a_{15} + 2a_3 a_{10} a_{13} a_{15} \\
& - \left(-3a_7 a_{11} + a_3 \left(a_{11}^2 + a_{12} a_{13} \right) + \left(a_{10}^2 - a_9 a_{12} \right) a_{14} \right) a_{16} - a_4 \left(2a_1 a_8 + 2a_2 a_{11} + 3a_9 a_{14} - 6a_{10} a_{15} + 3a_{12} a_{16} \right) \\
& \left. + \beta^4 \mu^2 \left(\left(-a_7 \left(a_8 a_{10} + a_9 a_{11} \right) - a_6 \left(a_{10} a_{11} + a_8 a_{12} \right) - a_4 \left(a_{10}^2 - a_9 a_{12} \right) \right) a_{15}^2 + \left(a_7 \left(a_8 a_{10} + a_9 a_{11} \right) + a_6 \left(a_{10} a_{11} + a_8 a_{12} \right) + a_4 \left(a_{10}^2 - a_9 a_{12} \right) \right) a_{14} a_{16} \right) \right)
\end{aligned} \tag{B.7}$$

$$\begin{aligned}
\theta_1 = & \beta \mu^6 \Upsilon_2 + \beta^3 \mu^4 \left(\left(a_6 a_8 - a_4 a_9 \right) a_{14} + a_2 a_8 a_{10} a_{14} + a_2 a_9 a_{11} a_{14} - a_1 a_8 a_{10} a_{15} + \left(a_7 a_8 + a_4 a_{10} \right) a_{15} - a_1 a_9 a_{11} a_{15} \right. \\
& \left. - a_2 a_{10} a_{11} a_{15} + \left(a_4 a_{10} + a_6 a_{11} \right) a_{15} - a_2 a_8 a_{12} a_{15} + a_1 a_{10} a_{11} a_{16} + a_1 a_8 a_{12} a_{16} + \left(a_7 a_{11} - a_4 a_{12} \right) a_{16} \right)
\end{aligned} \tag{B.8}$$

$$\theta_0 = \left(a_1 a_8 + a_2 a_{11} - a_4 \right) \beta^2 \mu^6 + \mu^8 \tag{B.9}$$

The parameters in equation (2.35) are given by:

$$A_0 = \theta_8 \tag{B.10}$$

$$\begin{aligned}
A_1 = & a_9 a_{11}^2 a_{14}^2 + 2a_8 a_{10} a_{11} a_{14} a_2^2 + a_8^2 a_{12} a_{14} a_2^2 - a_{10}^2 a_{13} a_{14} a_2^2 + a_9 a_{12} a_{13} a_{14} a_2^2 - 2a_7 a_8^2 a_{14} a_2 + 2a_6 a_8 a_{11} a_{14} a_2 - 2a_7 a_9 a_{13} a_{14} a_2 \\
& - 2a_6 a_{10} a_{13} a_{14} a_2 + 2a_6 a_{11}^2 a_{15} a_2 - 2a_1 a_9 a_{11}^2 a_{15} a_2 - 2a_7 a_8 a_{11} a_{15} a_2 - 4a_1 a_8 a_{10} a_{11} a_{15} a_2 - 2a_1 a_8^2 a_{12} a_{15} a_2 + 2a_1 a_{10}^2 a_{13} a_{15} a_2 + 2a_7 a_{10} a_{13} a_{15} a_2 \\
& + 2a_6 a_{12} a_{13} a_{15} a_2 - 2a_1 a_9 a_{12} a_{13} a_{15} a_2 + a_3 a_9 a_{11} a_{15}^2 - 2a_7 a_8 a_{10} a_{15}^2 - 2a_7 a_9 a_{11} a_{15}^2 - 2a_6 a_{10} a_{11} a_{15}^2 + 2a_3 a_8 a_{10} a_{11} a_{15}^2 + a_3 a_8^2 a_{12} a_{15}^2 - 2a_6 a_8 a_{12} a_{15}^2 \\
& - a_3 a_{10}^2 a_{13} a_{15}^2 + a_3 a_9 a_{12} a_{13} a_{15}^2 - a_5 a_8^2 a_{14}^2 - a_6^2 a_{13} a_{14} - a_5 a_9 a_{13} a_{14} + 2a_1 a_7 a_8^2 a_{15} - 2a_5 a_8 a_{11} a_{15} - 2a_1 a_6 a_8 a_{11} a_{15} - 2a_6 a_7 a_{13} a_{15} + 2a_1 a_7 a_9 a_{13} a_{15} \\
& + 2a_5 a_{10} a_{13} a_{15} + 2a_1 a_6 a_{10} a_{13} a_{15} \left(a_9 a_{14} - 2a_{10} a_{15} + a_{12} a_{16} \right) a_4^2 + 2 \left(-a_6 \left(a_8 a_{14} + a_{11} a_{15} \right) + a_2 \left(\left(a_{10} a_{11} + a_8 a_{12} \right) a_{15} - \left(a_8 a_{10} + a_9 a_{11} \right) a_{14} \right) \right. \\
& \left. + a_{15} \left(-a_7 a_8 + a_1 \left(a_8 a_{10} + a_9 a_{11} \right) + \left(a_9 a_{12} - a_{10}^2 \right) a_{15} \right) - \left(a_7 a_{11} + a_1 \left(a_{10} a_{11} + a_8 a_{12} \right) + \left(a_9 a_{12} - a_{10}^2 \right) a_{14} \right) a_{16} \right) a_4 + a_5 a_{11}^2 + a_7^2 a_{13} + a_5 a_{12} a_{13} \\
& - \left. - \left(\left(a_{12} a_8^2 + 2a_{10} a_{11} a_8 - a_{10}^2 a_{13} + a_9 \left(a_{11}^2 + a_{12} a_{13} \right) \right) a_1^2 + 2 \left(a_7 \left(a_{10} a_{13} - a_8 a_{11} \right) + a_6 \left(a_{11}^2 + a_{12} a_{13} \right) \right) a_1 + \left(-2a_7 \left(a_8 a_{10} + a_9 a_{11} \right) \right. \right. \\
& \left. \left. - 2a_6 \left(a_{10} a_{11} + a_8 a_{12} \right) + a_3 \left(a_{12} a_8^2 + 2a_{10} a_{11} a_8 + a_9 a_{11}^2 + \left(a_9 a_{12} - a_{10}^2 \right) a_{13} \right) \right) a_{14} \right) a_{16}
\end{aligned} \tag{B.11}$$

$$A_2 = -\theta_8 \quad (B.12)$$

$$\begin{aligned} A_3 = & \left(a_8^2 + a_9 a_{13} \right) a_1^2 + 2 \left(-a_6 a_{13} + a_2 \left(a_8 a_{11} - a_{10} a_{13} \right) - \left(a_8 a_{10} + a_9 a_{11} \right) a_{15} + \left(a_{10} a_{11} + a_8 a_{12} \right) a_{16} \right) a_1 + a_4^2 + a_2^2 a_{11}^2 + a_{10}^2 a_{15}^2 - a_9 a_{12} a_{15}^2 \\ & - a_5 a_{13} - 2 a_2 a_7 a_{13} + a_2^2 a_{12} a_{13} + a_8 \left(2 a_6 - a_3 a_8 \right) a_{14} + 2 a_2 a_8 a_{10} a_{14} + 2 a_2 a_9 a_{11} a_{14} - a_3 a_9 a_{13} a_{14} + 2 a_7 a_8 a_{15} + 2 a_6 a_{11} a_{15} - 2 a_3 a_8 a_{11} a_{15} \\ & - 2 a_2 a_{10} a_{11} a_{15} - 2 a_2 a_8 a_{12} a_{15} + 2 a_3 a_{10} a_{13} a_{15} - \left(-2 a_7 a_{11} + a_3 \left(a_{11}^2 + a_{12} a_{13} \right) + \left(a_{10}^2 - a_9 a_{12} \right) a_{14} \right) a_{16} - 2 a_4 \left(a_1 a_8 + a_2 a_{11} + a_9 a_{14} - 2 a_{10} a_{15} + a_{12} a_{16} \right) \end{aligned} \quad (B.13)$$

$$\begin{aligned} A_4 = & \left(-3 a_9 a_{11}^2 a_{14} a_2^2 - 6 a_8 a_{10} a_{11} a_{14} a_2^2 - 3 a_8^2 a_{12} a_{14} a_2^2 + 3 a_{10}^2 a_{13} a_{14} a_2^2 - 3 a_9 a_{12} a_{13} a_{14} a_2^2 + 6 a_7 a_8^2 a_{14} a_2 - 6 a_6 a_8 a_{11} a_{14} a_2 + 6 a_7 a_9 a_{13} a_{14} a_2 \right. \\ & + 6 a_6 a_{10} a_{13} a_{14} a_2 - 6 a_6 a_{11}^2 a_{15} a_2 + 6 a_1 a_9 a_{11}^2 a_{15} a_2 + 6 a_7 a_8 a_{11} a_{15} a_2 + 12 a_1 a_8 a_{10} a_{11} a_{15} a_2 + 6 a_1 a_8^2 a_{12} a_{15} a_2 - 6 a_1 a_{10}^2 a_{13} a_{15} a_2 - 6 a_7 a_{10} a_{13} a_{15} a_2 \\ & - 6 a_6 a_{12} a_{13} a_{15} a_2 + 6 a_1 a_9 a_{12} a_{13} a_{15} a_2 - 3 a_3 a_9 a_{11}^2 a_{15} a_2 + 2 a_7 a_8 a_{10} a_{15}^2 + 2 a_6 a_{10} a_{11} a_{15}^2 - 6 a_3 a_8 a_{10} a_{11} a_{15}^2 - 3 a_3 a_8^2 a_{12} a_{15}^2 + 2 a_6 a_8 a_{12} a_{15}^2 \\ & + 3 a_3 a_{10}^2 a_{13} a_{15}^2 - 3 a_3 a_9 a_{12} a_{13} a_{15}^2 + 3 a_5 a_8^2 a_{14} + 3 a_6^2 a_{13} a_{14} + 3 a_5 a_9 a_{13} a_{14} - 6 a_1 a_7 a_8^2 a_{15} + 6 a_5 a_8 a_{11} a_{15} + 6 a_1 a_6 a_8 a_{11} a_{15} + 6 a_6 a_7 a_{13} a_{15} - 6 a_1 a_7 a_9 a_{13} a_{15} \\ & - 6 a_5 a_{10} a_{13} a_{15} - 6 a_1 a_6 a_{10} a_{13} a_{15} - 3 \left(a_9 a_{14} - 2 a_{10} a_{15} + a_{12} a_{16} \right) a_4^2 + 2 \left(3 a_6 \left(a_8 a_{14} + a_{11} a_{15} \right) + a_{15} \left(3 a_7 a_8 - 3 a_1 \left(a_8 a_{10} + a_9 a_{11} \right) + \left(a_{10}^2 - a_9 a_{12} \right) a_{15} \right) \right. \\ & + 3 a_2 \left(\left(a_8 a_{10} + a_9 a_{11} \right) a_{14} - \left(a_{10} a_{11} + a_8 a_{12} \right) a_{15} \right) + \left(3 \left(a_7 + a_1 a_{10} \right) a_{11} + 3 a_1 a_8 a_{12} + \left(a_9 a_{12} - a_{10}^2 \right) a_{14} \right) a_{16} \left. \right) a_4 + \left(-3 a_1^2 a_{12} a_8^2 \right. \\ & + 3 a_{11} \left(\left(a_5 + a_1 \left(2 a_6 - a_1 a_9 \right) \right) a_{11} - 2 a_1 a_8 \left(a_7 + a_1 a_{10} \right) \right) + 3 \left(\left(a_7 + a_1 a_{10} \right)^2 + \left(a_5 + a_1 \left(2 a_6 - a_1 a_9 \right) \right) a_{12} \right) a_{13} \\ & \left. + \left(-2 a_7 \left(a_8 a_{10} + a_9 a_{11} \right) - 2 a_6 \left(a_{10} a_{11} + a_8 a_{12} \right) + 3 a_3 \left(a_{12} a_8^2 + 2 a_{10} a_{11} a_8 + a_9 a_{11}^2 + \left(a_9 a_{12} - a_{10}^2 \right) a_{13} \right) \right) a_{14} \right) a_{16} \Big) / 4 \end{aligned} \quad (B.14)$$

$$A_5 = 3 \theta_8 / 8 \quad (B.15)$$

$$A_6 = \Upsilon_2 \quad (B.16)$$

$$\begin{aligned} A_7 = & \left(- \left(a_8^2 + a_9 a_{13} \right) a_1^2 \right) + 2 \left(\left(a_6 + a_2 a_{10} \right) a_{13} - a_2 a_8 a_{11} \right) a_1 - a_4^2 - a_2^2 a_{11}^2 - a_{10}^2 a_{15}^2 + a_9 a_{12} a_{15}^2 + 2 a_4 \left(a_1 a_8 + a_2 a_{11} \right) + a_5 a_{13} + 2 a_2 a_7 a_{13} \\ & - a_2^2 a_{12} a_{13} + a_3 a_8^2 a_{14} + a_3 a_9 a_{13} a_{14} + 2 a_3 a_8 a_{11} a_{15} - 2 a_3 a_{10} a_{13} a_{15} + \left(a_3 \left(a_{11}^2 + a_{12} a_{13} \right) + \left(a_{10}^2 - a_9 a_{12} \right) a_{14} \right) a_{16} \right) / 2 \end{aligned} \quad (B.17)$$

$$\begin{aligned}
A_8 = & \left(3a_9 a_{11}^2 a_{14} a_2^2 + 6a_8 a_{10} a_{11} a_{14} a_2^2 + 3a_8^2 a_{12} a_{14} a_2^2 - 3a_{10}^2 a_{13} a_{14} a_2^2 + 3a_9 a_{12} a_{13} a_{14} a_2^2 - 6a_7 a_8^2 a_{14} a_2 + 6a_6 a_8 a_{11} a_{14} a_2 - 6a_7 a_9 a_{13} a_{14} a_2 \right. \\
& - 6a_6 a_{10} a_{13} a_{14} a_2 + 6a_6 a_{11}^2 a_{15} a_2 - 6a_1 a_9 a_{11}^2 a_{15} a_2 - 6a_7 a_8 a_{11} a_{15} a_2 - 12a_1 a_8 a_{10} a_{11} a_{15} a_2 - 6a_1 a_8^2 a_{12} a_{15} a_2 + 6a_1 a_{10}^2 a_{13} a_{15} a_2 + 6a_7 a_{10} a_{13} a_{15} a_2 \\
& + 6a_6 a_{12} a_{13} a_{15} a_2 - 6a_1 a_9 a_{12} a_{13} a_{15} a_2 + 3a_3 a_9 a_{11}^2 a_{15} + 2a_7 a_8 a_{10} a_{15}^2 + 2a_6 a_{10} a_{11} a_{15}^2 + 6a_3 a_8 a_{10} a_{11} a_{15}^2 + 3a_3 a_8^2 a_{12} a_{15}^2 + 2a_6 a_8 a_{12} a_{15}^2 \\
& - 3a_3 a_{10}^2 a_{13} a_{15}^2 + 3a_3 a_9 a_{12} a_{13} a_{15}^2 - 3a_6^2 a_{13} a_{14} + 6a_1 a_7 a_8^2 a_{15} - 6a_1 a_6 a_8 a_{11} a_{15} - 6a_6 a_7 a_{13} a_{15} + 6a_1 a_7 a_9 a_{13} a_{15} + 6a_1 a_6 a_{10} a_{13} a_{15} + 3(a_9 a_{14} - 2a_{10} a_{15} + a_{12} a_{16}) a_4^2 \\
& + 2(-3a_6(a_8 a_{14} + a_{11} a_{15}) + 3a_2((a_{10} a_{11} + a_8 a_{12}) a_{15} - (a_8 a_{10} + a_9 a_{11}) a_{14}) + a_{15}(-3a_7 a_8 + 3a_1(a_8 a_{10} + a_9 a_{11}) + (a_{10}^2 - a_9 a_{12}) a_{15}) \\
& - (3(a_7 + a_1 a_{10}) a_{11} + 3a_1 a_8 a_{12} + (a_{10}^2 - a_9 a_{12}) a_{14}) a_{16} - (-3a_1^2 a_{12} a_8^2 - 3a_1 a_{11}(2a_8(a_7 + a_1 a_{10}) + (a_1 a_9 - 2a_6) a_{11}) + 3((a_7 + a_1 a_{10})^2 + a_1(2a_6 - a_1 a_9) a_{12}) a_{13} \\
& + (2a_7(a_8 a_{10} + a_9 a_{11}) + 2a_6(a_{10} a_{11} + a_8 a_{12}) + 3a_3(a_{12} a_8^2 + 2a_{10} a_{11} a_8 + a_9 a_{11}^2 + (a_9 a_{12} - a_{10}^2) a_{13})) a_{14}) a_{16} \\
& \left. - 3a_5(a_{14} a_8^2 + 2a_{11} a_{15} a_8 + a_{11}^2 a_{16} + a_{13}(a_9 a_{14} - 2a_{10} a_{15} + a_{12} a_{16})) \right) / 16
\end{aligned} \tag{B.18}$$

$$A_9 = -\theta_8 / 16 \tag{B.19}$$

$$A_{10} = 1 \tag{B.20}$$

$$A_{11} = (-2a_4 + 2a_1 a_8 + 2a_2 a_{11} + a_3 a_{13} - a_9 a_{14} + 2a_{10} a_{15} - a_{12} a_{16}) / 4 \tag{B.21}$$

$$\begin{aligned}
A_{12} = & \left((a_8^2 + a_9 a_{13}) a_1^2 + 2(-a_6 a_{13} + a_2(a_8 a_{11} - a_{10} a_{13}) + (a_8 a_{10} + a_9 a_{11}) a_{15} - (a_{10} a_{11} + a_8 a_{12}) a_{16}) a_1 + a_4^2 + a_2^2 a_{11}^2 + a_{10}^2 a_{15}^2 - a_9 a_{12} a_{15}^2 \right. \\
& - a_5 a_{13} - 2a_2 a_7 a_{13} + a_2^2 a_{12} a_{13} - a_8(2a_6 + a_3 a_8) a_{14} - 2a_2 a_8 a_{10} a_{14} - 2a_2 a_9 a_{11} a_{14} - a_3 a_9 a_{13} a_{14} - 2a_7 a_8 a_{15} - 2a_6 a_{11} a_{15} - 2a_3 a_8 a_{11} a_{15} \\
& \left. + 2a_2 a_{10} a_{11} a_{15} + 2a_2 a_8 a_{12} a_{15} + 2a_3 a_{10} a_{13} a_{15} - (2a_7 a_{11} + a_3(a_{11}^2 + a_{12} a_{13}) + (a_{10}^2 - a_9 a_{12}) a_{14}) a_{16} - 2a_4(a_1 a_8 + a_2 a_{11} - a_9 a_{14} + 2a_{10} a_{15} - a_{12} a_{16}) \right) / 16
\end{aligned} \tag{B.22}$$

$$\begin{aligned}
A_{13} = & \left(-a_9 a_{11}^2 a_{14} a_2^2 - 2a_8 a_{10} a_{11} a_{14} a_2^2 - a_8^2 a_{12} a_{14} a_2^2 + a_{10}^2 a_{13} a_{14} a_2^2 - a_9 a_{12} a_{13} a_{14} a_2^2 + 2a_7 a_8^2 a_{14} a_2 - 2a_6 a_8 a_{11} a_{14} a_2 + 2a_7 a_9 a_{13} a_{14} a_2 \right. \\
& + 2a_6 a_{10} a_{13} a_{14} a_2 - 2a_6 a_{11}^2 a_{15} a_2 + 2a_1 a_9 a_{11}^2 a_{15} a_2 + 2a_7 a_8 a_{11} a_{15} a_2 + 4a_1 a_8 a_{10} a_{11} a_{15} a_2 + 2a_1 a_8^2 a_{12} a_{15} a_2 - 2a_1 a_{10}^2 a_{13} a_{15} a_2 - 2a_7 a_{10} a_{13} a_{15} a_2 \\
& - 2a_6 a_{12} a_{13} a_{15} a_2 + 2a_1 a_9 a_{12} a_{13} a_{15} a_2 - a_3 a_9 a_{11}^2 a_{15}^2 - 2a_7 a_8 a_{10} a_{15}^2 - 2a_7 a_9 a_{11} a_{15}^2 - 2a_6 a_{10} a_{11} a_{15}^2 - 2a_3 a_8 a_{10} a_{11} a_{15}^2 - a_3 a_8^2 a_{12} a_{15}^2 - 2a_6 a_8 a_{12} a_{15}^2 \\
& + a_3 a_{10}^2 a_{13} a_{15}^2 - a_3 a_9 a_{12} a_{13} a_{15}^2 + a_5 a_8^2 a_{14} + a_6^2 a_{13} a_{14} + a_5 a_9 a_{13} a_{14} - 2a_1 a_7 a_8^2 a_{15} + 2a_5 a_8 a_{11} a_{15} + 2a_1 a_6 a_8 a_{11} a_{15} + 2a_6 a_7 a_{13} a_{15} - 2a_1 a_7 a_9 a_{13} a_{15} \\
& - 2a_5 a_{10} a_{13} a_{15} - 2a_1 a_6 a_{10} a_{13} a_{15} - (a_9 a_{14} - 2a_{10} a_{15} + a_{12} a_{16}) a_4^2 + 2 \left(a_6 (a_8 a_{14} + a_{11} a_{15}) - a_{15} (-a_7 a_8 + a_1 (a_8 a_{10} + a_9 a_{11}) + (a_{10}^2 - a_9 a_{12}) a_{15}) \right. \\
& + a_2 ((a_8 a_{10} + a_9 a_{11}) a_{14} - (a_{10} a_{11} + a_8 a_{12}) a_{15}) + (a_7 a_{11} + a_1 (a_{10} a_{11} + a_8 a_{12}) + (a_{10}^2 - a_9 a_{12}) a_{14}) a_{16} \Big) a_4 + a_5 a_{11}^2 + a_7^2 a_{13} + a_5 a_{12} a_{13} \\
& + \left. - \left((a_{12} a_8^2 + 2a_{10} a_{11} a_8 - a_{10}^2 a_{13} + a_9 (a_{11}^2 + a_{12} a_{13})) a_1^2 + 2 (a_7 (a_{10} a_{13} - a_8 a_{11}) + a_6 (a_{11}^2 + a_{12} a_{13})) a_1 + (2a_7 (a_8 a_{10} + a_9 a_{11}) \right. \right. \\
& \left. \left. + 2a_6 (a_{10} a_{11} + a_8 a_{12}) + a_3 (a_{12} a_8^2 + 2a_{10} a_{11} a_8 + a_9 a_{11}^2 + (a_9 a_{12} - a_{10}^2) a_{13}) \right) a_{14} \right) a_{16} \Big) / 64
\end{aligned} \tag{B.23}$$

$$A_{14} = \theta_8 / 256 \tag{B.24}$$

The parameters in equation (2.37) are:

$$\chi_{1t} = (\eta_t^6 \Upsilon_3 + 3\eta_t^5 \beta \Upsilon_3 + \eta_t^4 (3\beta^2 \Upsilon_3 + \mu^2 \Upsilon_4) + \eta_t^3 (\beta^3 \Upsilon_3 + 2\beta\mu^2 \Upsilon_4) + \eta_t^2 (\mu^4 \Upsilon_5 + \beta^2 \mu^2 \Upsilon_4) + \eta_t \beta \mu^4 \Upsilon_5 + a_3 \mu^6) / (\mu \Theta) \tag{B.25}$$

$$\begin{aligned}
\chi_{2t} = & \left(\eta_t^5 \Upsilon_8 + \eta_t^4 \beta \Upsilon_9 + \eta_t^3 \left(\mu^2 \left(- \left((a_6 a_8 - a_4 a_9) a_1^2 \right) - a_5 a_8 a_1 - a_2 (a_7 a_8 + 2 a_4 a_{10}) a_1 - a_6 (a_4 + a_2 a_{11}) a_1 + a_7 a_9 a_{15} a_1 + a_6 a_{10} a_{15} a_1 \right. \right. \right. \right. \\
& - a_7 a_{10} a_{16} a_1 - a_6 a_{12} a_{16} a_1 - a_2 a_4 a_7 - a_2 a_5 a_{11} - a_2^2 a_7 a_{11} + a_2^2 a_4 a_{12} - a_6^2 a_{14} + a_3 a_6 a_8 a_{14} - a_3 a_4 a_9 a_{14} - a_5 a_9 a_{14} - a_2 a_7 a_9 a_{14} - a_2 a_6 a_{10} a_{14} \\
& - 2 a_6 a_7 a_{15} + a_3 a_7 a_8 a_{15} + 2 a_3 a_4 a_{10} a_{15} + 2 a_5 a_{10} a_{15} + a_2 a_7 a_{10} a_{15} + a_3 a_6 a_{11} a_{15} + a_2 a_6 a_{12} a_{15} - a_7^2 a_{16} + a_3 a_7 a_{11} a_{16} - a_3 a_4 a_{12} a_{16} - a_5 a_{12} a_{16} \Big) \right. \\
& + \beta^2 \left(- \left(a_7 (a_8 a_{10} + a_9 a_{11}) + a_6 (a_{10} a_{11} + a_8 a_{12}) + a_4 (a_{10}^2 - a_9 a_{12}) \right) a_{16} a_1^2 \right) + a_4 a_7 a_9 a_{15} a_1 + a_6^2 a_{11} a_{15} a_1 - a_6 (a_8 (a_7 - 2 a_2 a_{12}) - a_{10} (a_4 + 2 a_2 a_{11})) a_{15} a_1 \\
& + 2 a_2 (a_7 (a_8 a_{10} + a_9 a_{11}) + a_4 (a_{10}^2 - a_9 a_{12})) a_{15} a_1 - a_7^2 a_8 a_{16} a_1 - a_4 a_7 a_{10} a_{16} a_1 + a_6 a_7 a_{11} a_{16} a_1 - a_4 a_6 a_{12} a_{16} a_1 - a_5 a_{11} (a_{10} a_{16} - a_9 a_{15}) a_1 \\
& - a_5 a_8 (a_{12} a_{16} - a_{10} a_{15}) a_1 - a_3 a_4 a_{10}^2 a_{15}^2 + 3 a_7^2 a_9 a_{15}^2 + 6 a_6 a_7 a_{10} a_{15}^2 - a_3 a_6 a_{10} a_{11} a_{15}^2 - a_3 a_7 (a_8 a_{10} + a_9 a_{11}) a_{15}^2 + 3 a_6^2 a_{12} a_{15}^2 - a_3 a_6 a_8 a_{12} a_{15}^2 \\
& + a_3 a_4 a_9 a_{12} a_{15}^2 + 3 a_5 a_9 a_{12} a_{15}^2 - a_2^2 a_4 a_{10}^2 a_{14} + a_2 a_6 a_7 a_8 a_{14} - a_2 a_4 a_7 a_9 a_{14} - a_2 a_4 a_6 a_{10} a_{14} - a_2^2 a_7 a_8 a_{10} a_{14} - a_2 a_6^2 a_{11} a_{14} - a_2^2 a_7 a_9 a_{11} a_{14} \\
& - a_2^2 a_6 a_{10} a_{11} a_{14} - a_2^2 a_6 a_8 a_{12} a_{14} + a_2^2 a_4 a_9 a_{12} a_{14} + a_2 a_7^2 a_8 a_{15} + a_2 a_4 a_7 a_{10} a_{15} - a_2 a_6 a_7 a_{11} a_{15} + a_2 a_4 a_6 a_{12} a_{15} - a_2 a_5 a_{11} (a_9 a_{14} - a_{10} a_{15}) \\
& - a_2 a_5 a_8 (a_{10} a_{14} - a_{12} a_{15}) + a_3 a_4 a_{10}^2 a_{14} a_{16} + a_3 a_6 a_{10} a_{11} a_{14} a_{16} + a_3 a_7 (a_8 a_{10} + a_9 a_{11}) a_{14} a_{16} + a_3 a_6 a_8 a_{12} a_{14} a_{16} - a_3 a_4 a_9 a_{12} a_{14} a_{16} - 3 a_5 a_9 a_{12} a_{14} a_{16} \\
& - 3 (a_{12} a_6^2 + 2 a_7 a_{10} a_6 + a_7^2 a_9) a_{14} a_{16} - 3 a_5 a_{10}^2 (a_{15}^2 - a_{14} a_{16}) \Big) \right) + \eta_t^2 \left(\beta \mu^2 \left(- \left((a_6 a_8 - a_4 a_9) a_1^2 \right) - a_5 a_8 a_1 - a_2 (a_7 a_8 + 2 a_4 a_{10}) a_1 - a_6 (a_4 + a_2 a_{11}) a_1 \right. \right. \\
& + 2 a_7 a_9 a_{15} a_1 + 2 a_6 a_{10} a_{15} a_1 - 2 a_7 a_{10} a_{16} a_1 - 2 a_6 a_{12} a_{16} a_1 - a_2 a_4 a_7 - a_2 a_5 a_{11} - a_2^2 a_7 a_{11} + a_2^2 a_4 a_{12} - 2 a_6^2 a_{14} + a_3 a_6 a_8 a_{14} - a_3 a_4 a_9 a_{14} - 2 a_5 a_9 a_{14} \\
& - 2 a_2 a_7 a_9 a_{14} - 2 a_2 a_6 a_{10} a_{14} - 4 a_6 a_7 a_{15} + a_3 a_7 a_8 a_{15} + 2 a_3 a_4 a_{10} a_{15} + 4 a_5 a_{10} a_{15} + 2 a_2 a_7 a_{10} a_{15} + a_3 a_6 a_{11} a_{15} + 2 a_2 a_6 a_{12} a_{15} - 2 a_7^2 a_{16} + a_3 a_7 a_{11} a_{16} \\
& - a_3 a_4 a_{12} a_{16} - 2 a_5 a_{12} a_{16} \Big) + \beta^3 \left(- a_5 (a_{15}^2 - a_{14} a_{16}) a_{10}^2 + 2 a_6 a_7 a_{15}^2 a_{10} + a_7^2 a_9 a_{15}^2 + a_6^2 a_{12} a_{15}^2 + a_5 a_9 a_{12} a_{15}^2 - a_5 a_9 a_{12} a_{14} a_{16} + (- a_{12} a_6^2 - 2 a_7 a_{10} a_6 - a_7^2 a_9) a_{14} a_{16} \right) \Big) \\
& + \eta_t \left(\mu^4 (-a_3 a_4 - a_5 - a_1 a_6 - a_2 a_7) + \beta^2 \mu^2 (-a_2 a_{10} a_{14} a_6 - 2 a_7 a_{15} a_6 + a_1 a_{10} a_{15} a_6 + a_2 a_{12} a_{15} a_6 - a_1 a_{12} a_{16} a_6 - a_6^2 a_{14} - a_5 a_9 a_{14} - a_2 a_7 a_9 a_{14} \right. \\
& \left. \left. + a_1 a_7 a_9 a_{15} + 2 a_5 a_{10} a_{15} + a_2 a_7 a_{10} a_{15} - a_7^2 a_{16} - a_1 a_7 a_{10} a_{16} - a_5 a_{12} a_{16} \right) \right) - \beta \mu^4 (a_5 + a_1 a_6 + a_2 a_7) \Big) / \Theta \quad (B.26)
\end{aligned}$$

$$\begin{aligned}
\chi_{3t} = & \left(\eta_t^5 \Upsilon_{10} + 2 \eta_t^4 \beta \Upsilon_{10} + \eta_t^3 (\beta^2 \Upsilon_{10} + \mu^2 \Upsilon_{11}) + \eta_t^2 \mu^2 \beta \left(- \left((a_{10} a_{11} + a_8 a_{12}) a_2^2 \right) - a_6 a_{11} a_2 + (2 a_7 a_8 + (a_4 + a_1 a_8) a_{10} + a_1 a_9 a_{11}) a_2 \right. \right. \right. \\
& + 2 (a_{10}^2 - a_9 a_{12}) a_{15} a_2 + a_4 a_6 + a_5 a_8 + a_1 a_6 a_8 - a_1 a_4 a_9 + 2 a_7 a_9 a_{15} + 2 a_6 a_{10} a_{15} - 2 a_7 a_{10} a_{16} - 2 a_6 a_{12} a_{16} - 2 a_1 (a_{10}^2 - a_9 a_{12}) a_{16} \\
& + a_3 a_{11} (a_{10} a_{16} - a_9 a_{15}) + a_3 a_8 (a_{12} a_{16} - a_{10} a_{15}) \Big) + \eta_t \left(\mu^4 (-a_6 + a_3 a_8 + a_1 a_9 - a_2 a_{10}) + \beta^2 \mu^2 (a_7 a_9 a_{15} + a_6 a_{10} a_{15} + a_2 (a_{10}^2 - a_9 a_{12}) a_{15} \right. \\
& \left. \left. - a_7 a_{10} a_{16} - a_6 a_{12} a_{16} - a_1 (a_{10}^2 - a_9 a_{12}) a_{16} \right) \right) + \mu^4 \beta (-a_6 + a_1 a_9 - a_2 a_{10}) \Big) / \Theta \quad (B.27)
\end{aligned}$$

$$\begin{aligned}
\chi_{4t} = & \left(\eta_t^5 \Upsilon_{12} + 2\eta_t^4 \beta \Upsilon_{12} + \eta_t^3 (\mu^2 \Upsilon_{13} + \beta^2 \Upsilon_{12}) \right) + \eta_t^2 \mu^2 \beta \left(- \left((a_8 a_{10} + a_9 a_{11}) a_1^2 \right) - a_7 a_8 a_1 + a_{10} (a_4 + a_2 a_{11}) a_1 + (2a_6 a_{11} + a_2 a_8 a_{12}) a_1 \right. \\
& + 2a_{10}^2 a_{15} a_1 - 2a_9 a_{12} a_{15} a_1 + a_4 a_7 + a_5 a_{11} + a_2 a_7 a_{11} - a_2 a_4 a_{12} - 2a_2 a_{10}^2 a_{14} - 2a_7 a_9 a_{14} - 2a_6 a_{10} a_{14} + a_3 a_8 a_{10} a_{14} + a_3 a_9 a_{11} a_{14} + 2a_2 a_9 a_{12} a_{14} \\
& + 2a_7 a_{10} a_{15} - a_3 a_{10} a_{11} a_{15} + 2a_6 a_{12} a_{15} - a_3 a_8 a_{12} a_{15} \Big) + \eta_t \left(\mu^4 (-a_7 - a_1 a_{10} + a_3 a_{11} + a_2 a_{12}) + \beta^2 \mu^2 (-a_2 a_{14} a_{10}^2 + a_1 a_{15} a_{10}^2 - a_6 a_{14} a_{10} \right. \\
& \left. \left. + a_7 a_{15} a_{10} - a_7 a_9 a_{14} + a_2 a_9 a_{12} a_{14} + a_6 a_{12} a_{15} - a_1 a_9 a_{12} a_{15}) \right) + \mu^4 \beta (-a_7 - a_1 a_{10} + a_2 a_{12}) \right) / \Theta
\end{aligned} \tag{B.28}$$

$$\chi_{5t} = -(\beta + \eta_t) / \mu \tag{B.29}$$

$$\begin{aligned}
\chi_{6t} = & \left(\eta_t^7 \Upsilon_{14} + 3\eta_t^6 \beta \Upsilon_{14} + \eta_t^5 (3\beta^2 \Upsilon_{14} + \mu^2 \Upsilon_{15}) \right) + \eta_t^4 \left(\beta^3 \Upsilon_{14} + 2\beta \mu^2 \left(-2(a_{10} a_{11} + a_8 a_{12}) a_{16} a_1^2 - 2(2a_8 (a_7 - a_2 a_{12}) - (a_6 + 2a_2 a_{10}) a_{11}) a_{15} a_1 \right. \right. \\
& - 2a_7 a_{11} a_{16} a_1 - 2a_4 (a_{10} a_{15} - a_{12} a_{16}) a_1 + 3a_7 a_{10} a_{15}^2 - 2a_3 a_{10} a_{11} a_{15}^2 + 3a_6 a_{12} a_{15}^2 - 2a_3 a_8 a_{12} a_{15}^2 + 2a_5 a_8 a_{14} - 2a_6 (a_2 a_{11} - a_4) a_{14} \\
& - 2a_2^2 (a_{10} a_{11} + a_8 a_{12}) a_{14} + 2a_4 a_7 a_{15} + 2a_5 a_{11} a_{15} + 2a_2 a_7 (2a_8 a_{14} + a_{11} a_{15}) + 2a_2 a_4 (a_{10} a_{14} - a_{12} a_{15}) - 3a_7 a_{10} a_{14} a_{16} + 2a_3 a_{10} a_{11} a_{14} a_{16} \\
& \left. \left. - 3a_6 a_{12} a_{14} a_{16} + 2a_3 a_8 a_{12} a_{14} a_{16} \right) + \eta_t^3 \left(\mu^4 (-a_8 a_1^2 + a_4 a_1 - a_2 a_{11} a_1 + a_{10} a_{15} a_1 - a_{12} a_{16} a_1 - a_6 a_{14} + a_3 a_8 a_{14} - a_7 a_{15} + a_3 a_{11} a_{15} - a_2 (a_{10} a_{14} - a_{12} a_{15})) \right. \right. \\
& + \beta^2 \mu^2 \left(-((a_{10} a_{11} + a_8 a_{12}) a_{16} a_1^2) - (2a_8 (a_7 - a_2 a_{12}) - (a_6 + 2a_2 a_{10}) a_{11}) a_{15} a_1 - a_7 a_{11} a_{16} a_1 - a_4 (a_{10} a_{15} - a_{12} a_{16}) a_1 + 3a_7 a_{10} a_{15}^2 - a_3 a_{10} a_{11} a_{15}^2 \right. \\
& + 3a_6 a_{12} a_{15}^2 - a_3 a_8 a_{12} a_{15}^2 + a_5 a_8 a_{14} - a_6 (a_2 a_{11} - a_4) a_{14} - a_2^2 (a_{10} a_{11} + a_8 a_{12}) a_{14} + a_4 a_7 a_{15} + a_5 a_{11} a_{15} + a_2 a_7 (2a_8 a_{14} + a_{11} a_{15}) + a_2 a_4 (a_{10} a_{14} - a_{12} a_{15}) \\
& \left. \left. - 3a_7 a_{10} a_{14} a_{16} + a_3 a_{10} a_{11} a_{14} a_{16} - 3a_6 a_{12} a_{14} a_{16} + a_3 a_8 a_{12} a_{14} a_{16}) \right) + \eta_t^2 \left(\beta \mu^4 (-a_8 a_1^2 + a_4 a_1 - a_2 a_{11} a_1 + 2a_{10} a_{15} a_1 - 2a_{12} a_{16} a_1 - 2a_6 a_{14} + a_3 a_8 a_{14} \right. \\
& - 2a_7 a_{15} + a_3 a_{11} a_{15} - 2a_2 (a_{10} a_{14} - a_{12} a_{15})) + \beta^3 \mu^2 \left(a_7 a_{10} a_{15}^2 + a_6 a_{12} a_{15}^2 - a_7 a_{10} a_{14} a_{16} - a_6 a_{12} a_{14} a_{16} \right) \Big) + \eta_t \left(\beta^2 \mu^4 (-a_6 a_{14} - a_7 a_{15} + a_1 a_{10} a_{15} \right. \\
& \left. \left. - a_2 (a_{10} a_{14} - a_{12} a_{15}) - a_1 a_{12} a_{16}) - \mu^6 a_1 \right) - \beta \mu^6 a_1 \right) / (\mu \Theta)
\end{aligned} \tag{B.30}$$

$$\begin{aligned}
\chi_{7t} = & \left(\eta_t^7 \Upsilon_{16} + 3\eta_t^6 \beta \Upsilon_{16} + \eta_t^5 (3\beta^2 \Upsilon_{16} + \mu^2 \Upsilon_{17}) + \eta_t^4 (\beta^3 \Upsilon_{16} + \beta \mu^2 (-2(a_8 a_{10} + a_9 a_{11}) a_{14} a_2^2 - 2a_6 a_8 a_{14} a_2 + 4a_1 (a_8 a_{10} + a_9 a_{11}) a_{15} a_2 \right. \right. \\
& + 2(a_7 a_8 - 2a_6 a_{11}) a_{15} a_2 - 2a_4 (a_{10} a_{15} - a_9 a_{14}) a_2 + 3a_7 a_9 a_{15}^2 + 3a_6 a_{10} a_{15}^2 - 2a_3 (a_8 a_{10} + a_9 a_{11}) a_{15}^2 + 2a_5 a_8 a_{15} + 2a_6 (a_4 + a_1 a_8) a_{15} \\
& \left. \left. - 2a_1 a_4 a_9 a_{15} - 2(a_1 a_8 - a_4) (a_7 + a_1 a_{10}) a_{16} + 4a_1 a_6 a_{11} a_{16} - 2(a_1^2 a_9 - a_5) a_{11} a_{16} - 3a_7 a_9 a_{14} a_{16} - 3a_6 a_{10} a_{14} a_{16} + 2a_3 (a_8 a_{10} + a_9 a_{11}) a_{14} a_{16}) \right) \right) \\
& + \eta_t^3 (\mu^4 (-a_{11} a_2^2 + a_4 a_2 - a_1 a_8 a_2 - a_9 a_{14} a_2 + a_{10} a_{15} a_2 - a_6 a_{15} + a_3 a_8 a_{15} + a_1 a_9 a_{15} + (-a_7 - a_1 a_{10}) a_{16} + a_3 a_{11} a_{16}) + \beta^2 \mu^2 (-((a_8 a_{10} + a_9 a_{11}) a_{14} a_2^2) \\
& + 2a_1 (a_8 a_{10} + a_9 a_{11}) a_{15} a_2 + (a_7 a_8 - 2a_6 a_{11}) a_{15} a_2 - a_4 (a_{10} a_{15} - a_9 a_{14}) a_2 + 3a_7 a_9 a_{15}^2 + 3a_6 a_{10} a_{15}^2 - a_3 (a_8 a_{10} + a_9 a_{11}) a_{15}^2 - a_2 a_6 a_8 a_{14} + a_5 a_8 a_{15} \\
& + a_6 (a_4 + a_1 a_8) a_{15} - a_1 a_4 a_9 a_{15} + (a_4 - a_1 a_8) (a_7 + a_1 a_{10}) a_{16} + 2a_1 a_6 a_{11} a_{16} + (a_5 - a_1^2 a_9) a_{11} a_{16} - 3a_7 a_9 a_{14} a_{16} - 3a_6 a_{10} a_{14} a_{16} + a_3 (a_8 a_{10} + a_9 a_{11}) a_{14} a_{16}) \right) \\
& + \eta_t^2 (\beta^3 \mu^2 (a_7 a_9 a_{15}^2 + a_6 a_{10} a_{15}^2 - a_7 a_9 a_{14} a_{16} - a_6 a_{10} a_{14} a_{16}) + \beta \mu^4 (-a_{11} a_2^2 + a_4 a_2 - a_1 a_8 a_2 - 2a_9 a_{14} a_2 + 2a_{10} a_{15} a_2 - 2a_6 a_{15} + a_3 a_8 a_{15} + 2a_1 a_9 a_{15} \\
& \left. \left. - 2(a_7 + a_1 a_{10}) a_{16} + a_3 a_{11} a_{16}) \right) + \eta_t (\beta^2 \mu^4 (-a_2 a_9 a_{14} - a_6 a_{15} + a_1 a_9 a_{15} + a_2 a_{10} a_{15} + (-a_7 - a_1 a_{10}) a_{16}) - \mu^6 a_2) - \beta \mu^6 a_2 \right) / (\mu \Theta) \tag{B.31}
\end{aligned}$$

where

$$\begin{aligned}
\Theta = & \eta_t^6 \Upsilon_6 + 2\eta_t^5 \beta \Upsilon_6 + \eta_t^4 (\beta^2 \Upsilon_6 + \mu^2 \Upsilon_7) + \eta_t^3 \beta^2 \mu \Upsilon_7 + \eta_t^2 (\mu^4 (-a_4 + a_1 a_8 + a_2 a_{11} + a_9 a_{14} - 2a_{10} a_{15} + a_{12} a_{16}) \\
& + \beta^2 \mu^2 (a_{15}^2 a_{10}^2 - a_{14} a_{16} a_{10}^2 - a_9 a_{12} a_{15}^2 + a_9 a_{12} a_{14} a_{16})) + \eta_t \beta \mu^4 (a_9 a_{14} - 2a_{10} a_{15} + a_{12} a_{16}) + \mu^6 \tag{B.32}
\end{aligned}$$

$$\Upsilon_0 = \theta_6 - 6\beta^2 \theta_8 \tag{B.33}$$

$$\begin{aligned}
\Upsilon_1 = & \left((a_8^2 + a_9 a_{13}) a_1^2 + 2(-a_6 a_{13} + a_2 (a_8 a_{11} - a_{10} a_{13}) - (a_8 a_{10} + a_9 a_{11}) a_{15} + (a_{10} a_{11} + a_8 a_{12}) a_{16}) a_1 + a_4^2 + a_2^2 a_{11}^2 + a_{10}^2 a_{15}^2 \right. \\
& - a_9 a_{12} a_{15}^2 - a_5 a_{13} - 2a_2 a_7 a_{13} + a_2^2 a_{12} a_{13} + a_8 (2a_6 - a_3 a_8) a_{14} + 2a_2 a_8 a_{10} a_{14} + 2a_2 a_9 a_{11} a_{14} - a_3 a_9 a_{13} a_{14} + 2a_7 a_8 a_{15} + 2a_6 a_{11} a_{15} \\
& \left. - 2a_3 a_8 a_{11} a_{15} - 2a_2 a_{10} a_{11} a_{15} - 2a_2 a_8 a_{12} a_{15} + 2a_3 a_{10} a_{13} a_{15} - (-2a_7 a_{11} + a_3 (a_{11}^2 + a_{12} a_{13}) + (a_{10}^2 - a_9 a_{12}) a_{14}) a_{16} \right. \\
& \left. - 2a_4 (a_1 a_8 + a_2 a_{11} + a_9 a_{14} - 2a_{10} a_{15} + a_{12} a_{16}) \right) \tag{B.34}
\end{aligned}$$

$$\Upsilon_2 = -2a_4 + 2a_1 a_8 + 2a_2 a_{11} - a_3 a_{13} + a_9 a_{14} - 2a_{10} a_{15} + a_{12} a_{16} \tag{B.35}$$

$$\Upsilon_3 = a_5 a_{15}^2 a_{10}^2 - a_5 a_{14} a_{16} a_{10}^2 - 2 a_6 a_7 a_{15}^2 a_{10} - a_7^2 a_9 a_{15}^2 - a_6^2 a_{12} a_{15}^2 - a_5 a_9 a_{12} a_{15}^2 + a_5 a_9 a_{12} a_{14} a_{16} + \left(a_{12} a_6^2 + 2 a_7 a_{10} a_6 + a_7^2 a_9 \right) a_{14} a_{16} \quad (\text{B.36})$$

$$\begin{aligned} \Upsilon_4 = & \left(a_{10}^2 - a_9 a_{12} \right) a_{16} a_1^2 - 2 a_6 a_{10} a_{15} a_1 - 2 a_2 \left(a_{10}^2 - a_9 a_{12} \right) a_{15} a_1 + 2 a_6 a_{12} a_{16} a_1 + 2 a_7 \left(a_{10} a_{16} - a_9 a_{15} \right) a_1 + a_3 a_{10}^2 a_{15}^2 - a_3 a_9 a_{12} a_{15}^2 \\ & + a_6^2 a_{14} + a_2^2 a_{10}^2 a_{14} + a_5 a_9 a_{14} + 2 a_2 a_7 a_9 a_{14} + 2 a_2 a_6 a_{10} a_{14} - a_2^2 a_9 a_{12} a_{14} + 2 a_6 a_7 a_{15} - 2 a_5 a_{10} a_{15} - 2 a_2 a_7 a_{10} a_{15} - 2 a_2 a_6 a_{12} a_{15} + a_7^2 a_{16} \\ & + a_5 a_{12} a_{16} - a_3 a_{10}^2 a_{14} a_{16} + a_3 a_9 a_{12} a_{14} a_{16} \end{aligned} \quad (\text{B.37})$$

$$\Upsilon_5 = -a_9 a_1^2 + 2 a_6 a_1 + 2 a_2 a_{10} a_1 + a_5 + 2 a_2 a_7 - a_2^2 a_{12} + a_3 a_9 a_{14} - 2 a_3 a_{10} a_{15} + a_3 a_{12} a_{16} \quad (\text{B.38})$$

$$\begin{aligned} \Upsilon_6 = & -a_4 a_{15}^2 a_{10}^2 + a_4 a_{14} a_{16} a_{10}^2 - a_7 a_8 a_{15}^2 a_{10} - a_6 a_{11} a_{15}^2 a_{10} + a_7 a_8 a_{14} a_{16} a_{10} + a_6 a_{11} a_{14} a_{16} a_{10} - a_7 a_9 a_{11} a_{15}^2 \\ & - a_6 a_8 a_{12} a_{15}^2 + a_4 a_9 a_{12} a_{15}^2 + a_7 a_9 a_{11} a_{14} a_{16} + a_6 a_8 a_{12} a_{14} a_{16} - a_4 a_9 a_{12} a_{14} a_{16} \end{aligned} \quad (\text{B.39})$$

$$\begin{aligned} \Upsilon_7 = & a_{15}^2 a_{10}^2 - a_{14} a_{16} a_{10}^2 + 2 a_4 a_{15} a_{10} - a_9 a_{12} a_{15}^2 + a_6 a_8 a_{14} - a_4 a_9 a_{14} + a_7 a_8 a_{15} + a_6 a_{11} a_{15} + a_2 a_{11} \left(a_9 a_{14} - a_{10} a_{15} \right) \\ & + a_2 a_8 \left(a_{10} a_{14} - a_{12} a_{15} \right) + a_7 a_{11} a_{16} - a_4 a_{12} a_{16} + a_9 a_{12} a_{14} a_{16} + a_1 a_{11} \left(a_{10} a_{16} - a_9 a_{15} \right) + a_1 a_8 \left(a_{12} a_{16} - a_{10} a_{15} \right) \end{aligned} \quad (\text{B.40})$$

$$\begin{aligned} \Upsilon_8 = & - \left(\left(a_7 \left(a_8 a_{10} + a_9 a_{11} \right) + a_6 \left(a_{10} a_{11} + a_8 a_{12} \right) + a_4 \left(a_{10}^2 - a_9 a_{12} \right) \right) a_{16} a_1^2 \right) + a_4 a_7 a_9 a_{15} a_1 + a_6^2 a_{11} a_{15} a_1 \\ & - a_6 \left(a_8 \left(a_7 - 2 a_2 a_{12} \right) - a_{10} \left(a_4 + 2 a_2 a_{11} \right) \right) a_{15} a_1 + 2 a_2 \left(a_7 \left(a_8 a_{10} + a_9 a_{11} \right) + a_4 \left(a_{10}^2 - a_9 a_{12} \right) \right) a_{15} a_1 - a_7^2 a_8 a_{16} a_1 \\ & - a_4 a_7 a_{10} a_{16} a_1 + a_6 a_7 a_{11} a_{16} a_1 - a_4 a_6 a_{12} a_{16} a_1 - a_5 a_{11} \left(a_{10} a_{16} - a_9 a_{15} \right) a_1 - a_5 a_8 \left(a_{12} a_{16} - a_{10} a_{15} \right) a_1 - a_3 a_4 a_{10}^2 a_{15}^2 \\ & + a_7^2 a_9 a_{15}^2 + 2 a_6 a_7 a_{10} a_{15}^2 - a_3 a_6 a_{10} a_{11} a_{15}^2 - a_3 a_7 \left(a_8 a_{10} + a_9 a_{11} \right) a_{15}^2 + a_6^2 a_{12} a_{15}^2 - a_3 a_6 a_8 a_{12} a_{15}^2 + a_3 a_4 a_9 a_{12} a_{15}^2 \\ & + a_5 a_9 a_{12} a_{15}^2 - a_2^2 a_4 a_{10}^2 a_{14} + a_2 a_6 a_7 a_8 a_{14} - a_2 a_4 a_7 a_9 a_{14} - a_2 a_4 a_6 a_{10} a_{14} - a_2^2 a_7 a_8 a_{10} a_{14} - a_2 a_6^2 a_{11} a_{14} - a_2^2 a_7 a_9 a_{11} a_{14} \\ & - a_2^2 a_6 a_{10} a_{11} a_{14} - a_2^2 a_6 a_8 a_{12} a_{14} + a_2^2 a_4 a_9 a_{12} a_{14} + a_2 a_7^2 a_8 a_{15} + a_2 a_4 a_7 a_{10} a_{15} - a_2 a_6 a_7 a_{11} a_{15} + a_2 a_4 a_6 a_{12} a_{15} \\ & - a_2 a_5 a_{11} \left(a_9 a_{14} - a_{10} a_{15} \right) - a_2 a_5 a_8 \left(a_{10} a_{14} - a_{12} a_{15} \right) + a_3 a_4 a_{10}^2 a_{14} a_{16} + a_3 a_6 a_{10} a_{11} a_{14} a_{16} + a_3 a_7 \left(a_8 a_{10} + a_9 a_{11} \right) a_{14} a_{16} \\ & + a_3 a_6 a_8 a_{12} a_{14} a_{16} - a_3 a_4 a_9 a_{12} a_{14} a_{16} - a_5 a_9 a_{12} a_{14} a_{16} + \left(-a_{12} a_6^2 - 2 a_7 a_{10} a_6 - a_7^2 a_9 \right) a_{14} a_{16} - a_5 a_{10}^2 \left(a_{15}^2 - a_{14} a_{16} \right) \end{aligned} \quad (\text{B.41})$$

$$\begin{aligned}
\Upsilon_9 = & -2 \left(a_7 (a_8 a_{10} + a_9 a_{11}) + a_6 (a_{10} a_{11} + a_8 a_{12}) + a_4 (a_{10}^2 - a_9 a_{12}) \right) a_{16} a_1^2 + 2 a_1 \left(\left(-a_6 a_7 a_8 + a_5 a_{10} a_8 + a_4 a_7 a_9 + a_4 a_6 a_{10} + (a_6^2 + a_5 a_9) a_{11} \right) a_{15} \right. \\
& \left. - (a_8 a_7^2 + (a_4 a_{10} - a_6 a_{11}) a_7 + a_5 a_{10} a_{11} + (a_4 a_6 + a_5 a_8) a_{12}) a_{16} \right) - 2 a_2^2 \left(a_7 (a_8 a_{10} + a_9 a_{11}) + a_6 (a_{10} a_{11} + a_8 a_{12}) + a_4 (a_{10}^2 - a_9 a_{12}) \right) a_{14} \\
& + 2 a_2 \left((a_8 a_7^2 + ((a_4 + 2 a_1 a_8) a_{10} - (a_6 - 2 a_1 a_9) a_{11}) a_7 + a_{10} (2 a_1 a_4 a_{10} + (a_5 + 2 a_1 a_6) a_{11}) + ((a_5 + 2 a_1 a_6) a_8 + a_4 (a_6 - 2 a_1 a_9)) a_{12}) a_{15} \right. \\
& \left. - (-a_6 a_7 a_8 + a_5 a_{10} a_8 + a_4 a_7 a_9 + a_4 a_6 a_{10} + (a_6^2 + a_5 a_9) a_{11}) a_{14} \right) + (3 a_9 a_7^2 + (6 a_6 a_{10} - 2 a_3 (a_8 a_{10} + a_9 a_{11})) a_7 - 3 a_5 a_{10}^2 + 3 (a_6^2 + a_5 a_9) a_{12} \\
& \left. - 2 a_3 (a_6 (a_{10} a_{11} + a_8 a_{12}) + a_4 (a_{10}^2 - a_9 a_{12})) \right) (a_{15}^2 - a_{14} a_{16})
\end{aligned} \tag{B.42}$$

$$\begin{aligned}
\Upsilon_{10} = & -a_{11} a_{15} a_6^2 + a_7 a_8 a_{15} a_6 - a_2 a_{10} a_{11} a_{15} a_6 - a_2 a_8 a_{12} a_{15} a_6 - (a_7 - a_1 a_{10}) a_{11} a_{16} a_6 + a_1 a_8 a_{12} a_{16} a_6 + a_4 (a_{12} a_{16} - a_{10} a_{15}) a_6 - a_4 a_7 a_9 a_{15} - a_2 a_7 (a_8 a_{10} + a_9 a_{11}) a_{15} \\
& - a_2 a_4 (a_{10}^2 - a_9 a_{12}) a_{15} + a_7^2 a_8 a_{16} + a_7 (a_4 + a_1 a_8) a_{10} a_{16} + a_1 a_7 a_9 a_{11} a_{16} + a_1 a_4 (a_{10}^2 - a_9 a_{12}) a_{16} - a_5 a_{11} (a_9 a_{15} - a_{10} a_{16}) - a_5 a_8 (a_{10} a_{15} - a_{12} a_{16})
\end{aligned} \tag{B.43}$$

$$\begin{aligned}
\Upsilon_{11} = & -((a_{10} a_{11} + a_8 a_{12}) a_2^2) - a_6 a_{11} a_2 + (2 a_7 a_8 + (a_4 + a_1 a_8) a_{10} + a_1 a_9 a_{11}) a_2 + (a_{10}^2 - a_9 a_{12}) a_{15} a_2 + a_4 a_6 + a_5 a_8 + a_1 a_6 a_8 \\
& - a_1 a_4 a_9 + a_7 a_9 a_{15} + a_6 a_{10} a_{15} - a_7 a_{10} a_{16} - a_6 a_{12} a_{16} - a_1 (a_{10}^2 - a_9 a_{12}) a_{16} + a_3 a_{11} (a_{10} a_{16} - a_9 a_{15}) + a_3 a_8 (a_{12} a_{16} - a_{10} a_{15})
\end{aligned} \tag{B.44}$$

$$\begin{aligned}
\Upsilon_{12} = & a_{11} a_{14} a_6^2 + a_4 a_{10} a_{14} a_6 + a_2 a_{10} a_{11} a_{14} a_6 + a_2 a_8 a_{12} a_{14} a_6 - a_1 a_{10} a_{11} a_{15} a_6 - a_4 a_{12} a_{15} a_6 - a_1 a_8 a_{12} a_{15} a_6 + a_2 a_4 a_{10}^2 a_{14} \\
& - a_6 a_7 a_8 a_{14} + a_5 a_8 a_{10} a_{14} + a_2 a_7 a_8 a_{10} a_{14} + a_5 a_9 a_{11} a_{14} + a_2 a_7 a_9 a_{11} a_{14} - a_2 a_4 a_9 a_{12} a_{14} - a_1 a_4 a_{10}^2 a_{15} - a_7^2 a_8 a_{15} - a_1 a_7 a_8 a_{10} a_{15} \\
& + a_7 (a_6 - a_1 a_9) a_{11} a_{15} - a_5 a_{10} a_{11} a_{15} - a_5 a_8 a_{12} a_{15} + a_1 a_4 a_9 a_{12} a_{15} + a_4 a_7 (a_9 a_{14} - a_{10} a_{15})
\end{aligned} \tag{B.45}$$

$$\begin{aligned}
\Upsilon_{13} = & -((a_8 a_{10} + a_9 a_{11}) a_1^2) - a_7 a_8 a_1 + a_{10} (a_4 + a_2 a_{11}) a_1 + (2 a_6 a_{11} + a_2 a_8 a_{12}) a_1 + a_{10}^2 a_{15} a_1 - a_9 a_{12} a_{15} a_1 + a_4 a_7 + a_5 a_{11} + a_2 a_7 a_{11} \\
& - a_2 a_4 a_{12} - a_2 a_{10}^2 a_{14} - a_7 a_9 a_{14} - a_6 a_{10} a_{14} + a_3 a_8 a_{10} a_{14} + a_3 a_9 a_{11} a_{14} + a_2 a_9 a_{12} a_{14} + a_7 a_{10} a_{15} - a_3 a_{10} a_{11} a_{15} + a_6 a_{12} a_{15} - a_3 a_8 a_{12} a_{15}
\end{aligned} \tag{B.46}$$

$$\begin{aligned}
\Upsilon_{14} = & a_8 a_{14} a_{16} a_7^2 - a_4 a_{10} a_{15}^2 a_7 + a_6 a_{11} a_{15}^2 a_7 + a_4 a_{10} a_{14} a_{16} a_7 - a_6 a_{11} a_{14} a_{16} a_7 - a_7^2 a_8 a_{15}^2 - a_5 a_{10} a_{11} a_{15}^2 \\
& - a_4 a_6 a_{12} a_{15}^2 - a_5 a_8 a_{12} a_{15}^2 + a_5 a_{10} a_{11} a_{14} a_{16} + a_4 a_6 a_{12} a_{14} a_{16} + a_5 a_8 a_{12} a_{14} a_{16}
\end{aligned} \tag{B.47}$$

$$\begin{aligned}\Upsilon_{15} = & -\left(\left(a_{10}a_{11} + a_8a_{12}\right)a_{16}a_1^2\right) - \left(2a_8\left(a_7 - a_2a_{12}\right) - \left(a_6 + 2a_2a_{10}\right)a_{11}\right)a_{15}a_1 - a_7a_{11}a_{16}a_1 - a_4\left(a_{10}a_{15} - a_{12}a_{16}\right)a_1 + a_7a_{10}a_{15}^2 \\ & - a_3a_{10}a_{11}a_{15}^2 + a_6a_{12}a_{15}^2 - a_3a_8a_{12}a_{15}^2 + a_5a_8a_{14} - a_6\left(a_2a_{11} - a_4\right)a_{14} - a_2^2\left(a_{10}a_{11} + a_8a_{12}\right)a_{14} + a_4a_7a_{15} + a_5a_{11}a_{15} \\ & + a_2a_7\left(2a_8a_{14} + a_{11}a_{15}\right) + a_2a_4\left(a_{10}a_{14} - a_{12}a_{15}\right) - a_7a_{10}a_{14}a_{16} + a_3a_{10}a_{11}a_{14}a_{16} - a_6a_{12}a_{14}a_{16} + a_3a_8a_{12}a_{14}a_{16}\end{aligned}\tag{B.48}$$

$$\begin{aligned}\Upsilon_{16} = & -a_{11}\left(a_{15}^2 - a_{14}a_{16}\right)a_6^2 + a_7a_8a_{15}^2a_6 - a_4a_{10}a_{15}^2a_6 - a_7a_8a_{14}a_{16}a_6 + a_4a_{10}a_{14}a_{16}a_6 \\ & - a_4a_7a_9a_{15}^2 - a_5\left(a_8a_{10} + a_9a_{11}\right)a_{15}^2 + a_4a_7a_9a_{14}a_{16} + a_5\left(a_8a_{10} + a_9a_{11}\right)a_{14}a_{16}\end{aligned}\tag{B.49}$$

$$\begin{aligned}\Upsilon_{17} = & -\left(\left(a_8a_{10} + a_9a_{11}\right)a_{14}a_2^2\right) + 2a_1\left(a_8a_{10} + a_9a_{11}\right)a_{15}a_2 + \left(a_7a_8 - 2a_6a_{11}\right)a_{15}a_2 - a_4\left(a_{10}a_{15} - a_9a_{14}\right)a_2 + a_7a_9a_{15}^2 + a_6a_{10}a_{15}^2 \\ & - a_3\left(a_8a_{10} + a_9a_{11}\right)a_{15}^2 - a_2a_6a_8a_{14} + a_5a_8a_{15} + a_6\left(a_4 + a_1a_8\right)a_{15} - a_1a_4a_9a_{15} + \left(a_4 - a_1a_8\right)\left(a_7 + a_1a_{10}\right)a_{16} + 2a_1a_6a_{11}a_{16} \\ & + \left(a_5 - a_1^2a_9\right)a_{11}a_{16} - a_7a_9a_{14}a_{16} - a_6a_{10}a_{14}a_{16} + a_3\left(a_8a_{10} + a_9a_{11}\right)a_{14}a_{16}\end{aligned}\tag{B.50}$$

The parameters in equation (2.41) are:

$$\left[\Omega_{1i} \quad \Omega_{2i} \quad \Omega_{3i} \quad \Omega_{4i} \quad \Omega_{5i} \quad \Omega_{6i} \quad \Omega_{7i}\right] = -\left[\begin{array}{ccccccc} \varpi_{12i}e^{-\eta_{2i}l} & \varpi_{13i}e^{-\eta_{3i}l} & \varpi_{14i}e^{-\eta_{4i}l} & \varpi_{15i}e^{-\eta_{5i}l} & \varpi_{16i}e^{-\eta_{6i}l} & \varpi_{17i}e^{-\eta_{7i}l} & \varpi_{18i}e^{-\eta_{8i}l} \\ \varpi_{22i}e^{\eta_{2i}l} & \varpi_{23i}e^{\eta_{3i}l} & \varpi_{24i}e^{\eta_{4i}l} & \varpi_{25i}e^{\eta_{5i}l} & \varpi_{26i}e^{\eta_{6i}l} & \varpi_{27i}e^{\eta_{7i}l} & \varpi_{28i}e^{\eta_{8i}l} \\ \varpi_{22i}e^{-\eta_{2i}l} & \varpi_{23i}e^{-\eta_{3i}l} & \varpi_{24i}e^{-\eta_{4i}l} & \varpi_{25i}e^{-\eta_{5i}l} & \varpi_{26i}e^{-\eta_{6i}l} & \varpi_{27i}e^{-\eta_{7i}l} & \varpi_{28i}e^{-\eta_{8i}l} \\ \varpi_{32i}e^{\eta_{2i}l} & \varpi_{33i}e^{\eta_{3i}l} & \varpi_{34i}e^{\eta_{4i}l} & \varpi_{35i}e^{\eta_{5i}l} & \varpi_{36i}e^{\eta_{6i}l} & \varpi_{37i}e^{\eta_{7i}l} & \varpi_{38i}e^{\eta_{8i}l} \\ \varpi_{32i}e^{-\eta_{2i}l} & \varpi_{33i}e^{-\eta_{3i}l} & \varpi_{34i}e^{-\eta_{4i}l} & \varpi_{35i}e^{-\eta_{5i}l} & \varpi_{36i}e^{-\eta_{6i}l} & \varpi_{37i}e^{-\eta_{7i}l} & \varpi_{38i}e^{-\eta_{8i}l} \\ \varpi_{42i}e^{\eta_{2i}l} & \varpi_{43i}e^{\eta_{3i}l} & \varpi_{44i}e^{\eta_{4i}l} & \varpi_{45i}e^{\eta_{5i}l} & \varpi_{46i}e^{\eta_{6i}l} & \varpi_{47i}e^{\eta_{7i}l} & \varpi_{48i}e^{\eta_{8i}l} \\ \varpi_{42i}e^{-\eta_{2i}l} & \varpi_{43i}e^{-\eta_{3i}l} & \varpi_{44i}e^{-\eta_{4i}l} & \varpi_{45i}e^{-\eta_{5i}l} & \varpi_{46i}e^{-\eta_{6i}l} & \varpi_{47i}e^{-\eta_{7i}l} & \varpi_{48i}e^{-\eta_{8i}l} \end{array}\right]^{-1} \left[\begin{array}{c} \varpi_{11i}e^{-\eta_{1i}l} \\ \varpi_{21i}e^{\eta_{1i}l} \\ \varpi_{21i}e^{-\eta_{1i}l} \\ \varpi_{31i}e^{\eta_{1i}l} \\ \varpi_{31i}e^{-\eta_{1i}l} \\ \varpi_{41i}e^{\eta_{1i}l} \\ \varpi_{41i}e^{-\eta_{1i}l} \end{array}\right]\tag{B.51}$$

S C. Constants for scenario 1

The relations among the constants are derived as:

$$\begin{cases} \mathcal{A}_{in} = \frac{1}{E_0 \mu_n (\eta_{in} + \beta)} \left[\mu_n \nu_0 - \frac{(\eta_{in} + \beta)^2}{\mu_n} \right] \mathcal{D}_{in} \\ \mathcal{B}_{in} = -\frac{1}{E_0 \eta_{in} (\eta_{in} + \beta)} \left[\mu_n - \nu_0 \frac{(\eta_{in} + \beta)^2}{\mu_n} \right] \mathcal{D}_{in} \\ \mathcal{C}_{in} = -\frac{\eta_{in} + \beta}{\mu_n} \mathcal{D}_{in} \end{cases}$$

After solving the eigenvalues μ_n from equation (3.8), the constants of nontrivial solutions are deduced as

$$\begin{cases} \mathcal{D}_{1n} = E_0 \mu_n \\ \mathcal{D}_{2n} = -E_0 \mu_n \\ \mathcal{D}_{3n} = E_0 \mu_n \Xi_{1n} \\ \mathcal{D}_{4n} = E_0 \mu_n \Xi_{2n} \end{cases}$$

$$\begin{aligned} & \frac{(\eta_{1n} - \eta_{4n}) e^{\eta_{1n} l} \sinh[(\eta_{3n} - \eta_{4n})l]}{\beta + \eta_{1n}} + \frac{(\eta_{4n} - \eta_{3n}) e^{\eta_{3n} l} \sinh[(\eta_{1n} - \eta_{4n})l]}{\beta + \eta_{3n}} \\ & \frac{(\eta_{2n} - \eta_{4n}) e^{\eta_{2n} l} \sinh[(\eta_{3n} - \eta_{4n})l]}{\beta + \eta_{2n}} + \frac{(\eta_{4n} - \eta_{3n}) e^{\eta_{3n} l} \sinh[(\eta_{2n} - \eta_{4n})l]}{\beta + \eta_{3n}} \end{aligned}$$

where

$$\Xi_{1n} = \frac{(\beta + \eta_{3n})e^{(\eta_{3n} - \eta_{1n})l} \left(\beta \eta_{1n} e^{2(\eta_{1n} + \eta_{2n})l} - \beta \eta_{1n} e^{2(\eta_{1n} + \eta_{4n})l} - \beta \eta_{2n} e^{2(\eta_{1n} + \eta_{2n})l} + (\eta_{2n} - \eta_{4n})(\beta + \eta_{1n})e^{2(\eta_{2n} + \eta_{4n})l} + \beta \eta_{4n} e^{2(\eta_{1n} + \eta_{4n})l} - \eta_{1n} \eta_{2n} e^{2(\eta_{1n} + \eta_{4n})l} + \eta_{1n} \eta_{4n} e^{2(\eta_{1n} + \eta_{2n})l} - \eta_{2n} \eta_{4n} e^{2(\eta_{1n} + \eta_{2n})l} + \eta_{2n} \eta_{4n} e^{2(\eta_{1n} + \eta_{4n})l} \right)}{(\beta + \eta_{1n})(\beta \eta_{2n} e^{2(\eta_{2n} + \eta_{3n})l} - \beta \eta_{2n} e^{2(\eta_{2n} + \eta_{4n})l} - \beta \eta_{3n} e^{2(\eta_{2n} + \eta_{3n})l} + (\eta_{3n} - \eta_{4n})(\beta + \eta_{2n})e^{2(\eta_{3n} + \eta_{4n})l} + \beta \eta_{4n} e^{2(\eta_{2n} + \eta_{4n})l} - \eta_{2n} \eta_{3n} e^{2(\eta_{2n} + \eta_{4n})l} + \eta_{2n} \eta_{4n} e^{2(\eta_{2n} + \eta_{3n})l} - \eta_{3n} \eta_{4n} e^{2(\eta_{2n} + \eta_{3n})l} + \eta_{3n} \eta_{4n} e^{2(\eta_{2n} + \eta_{4n})l})}$$

$$\Xi_{2n} = \frac{(\beta + \eta_{4n})e^{(\eta_{4n} - \eta_{1n})l} \left(\beta \eta_{1n} e^{2(\eta_{1n} + \eta_{3n})l} - \beta \eta_{1n} e^{2(\eta_{1n} + \eta_{2n})l} + \beta \eta_{2n} e^{2(\eta_{1n} + \eta_{2n})l} - (\eta_{2n} - \eta_{3n})(\beta + \eta_{1n})e^{2(\eta_{2n} + \eta_{3n})l} - \beta \eta_{3n} e^{2(\eta_{1n} + \eta_{3n})l} + \eta_{1n} \eta_{2n} e^{2(\eta_{1n} + \eta_{3n})l} - \eta_{1n} \eta_{3n} e^{2(\eta_{1n} + \eta_{2n})l} + \eta_{2n} \eta_{3n} e^{2(\eta_{1n} + \eta_{2n})l} - \eta_{2n} \eta_{3n} e^{2(\eta_{1n} + \eta_{3n})l} \right)}{(\beta + \eta_{1n})(\beta \eta_{2n} e^{2(\eta_{2n} + \eta_{3n})l} - \beta \eta_{2n} e^{2(\eta_{2n} + \eta_{4n})l} - \beta \eta_{3n} e^{2(\eta_{2n} + \eta_{3n})l} + (\eta_{3n} - \eta_{4n})(\beta + \eta_{2n})e^{2(\eta_{3n} + \eta_{4n})l} + \beta \eta_{4n} e^{2(\eta_{2n} + \eta_{4n})l} - \eta_{2n} \eta_{3n} e^{2(\eta_{2n} + \eta_{4n})l} + \eta_{2n} \eta_{4n} e^{2(\eta_{2n} + \eta_{3n})l} - \eta_{3n} \eta_{4n} e^{2(\eta_{2n} + \eta_{3n})l} + \eta_{3n} \eta_{4n} e^{2(\eta_{2n} + \eta_{4n})l})}$$

Codes

- Codes
 - 1.Symplectic Analysis
 - 2.Zeros & Chebfun
 - 3.FEM

1.Symplectic Analysis

```
%%%=====Copyright=====
%%% Version Oct. 17, 2024
%%%
%%% Lizichen Chen <lzcchen@zju.edu.cn>
%%% Department of Engineering Mechanics, Zhejiang University
%%%
%%%=====Description=====
%%% Symplectic contact analysis
%%%
%%%=====

clear; clc; format long;

nu= 0.25;
E = 1;
beta = 0.1;
a = -0.5;
b = 0.5;
l = 10;
h = 10;
d = 0.02; %maximum indentation depth

xi = l*cosh(beta*l)/sinh(beta*l)-1/beta;

syms x z mu real

vec = [1 1 exp(beta*x) exp(beta*x)];
Mt = diag(vec);

% bar = waitbar(0,'Start...');

% eigenvectors and eigen-solutions for zero eigenvalue

% Saint-Venant solutions only require this part

phi0s_0 = [1 0 0 0].';
phi0a_0 = [0 1 0 0].';
phi0s_1 = vpa([0 -nu*x E 0].');
phi0a_1 = [-x 0 0 0].';
phi0a_2 = vpa([0 (nu*x.^2)/2 -E*x 0].');
phi0_3 = vpa([(2*(1+nu))/E*(-E*l*exp(-beta*x))/(beta^2*sinh(beta*l))+
```

```
(E*x.^2)/(2*beta)-(xi*E/beta+E/beta^2)*x)-nu*x^3/6+(xi*nu*x^2)/2) 0 0 (E*l*exp(-
beta*x)/(beta*sinh(beta*l))+E*x/beta-(xi*E/beta+E/beta^2))].');

f0s_0 = phi0s_0;
f0a_0 = phi0a_0;
f0s_1 = phi0s_1 + z*phi0s_0;
f0a_1 = phi0a_1 + z*phi0a_0;
f0a_2 = phi0a_2 + z*phi0a_1 + (z^2)*phi0a_0/2;
f0_3 = vpa(phi0_3 + z*phi0a_2 + (z^2)*phi0a_1/2 + (z^3)*phi0a_0/factorial(3) + xi*
(z*phi0s_1 + (z^2)*phi0s_0/2));

%% eigenvectors and eigen-solutions for general eigenvalues

% the corresponding eigenvalues are derived through chebfun[1]
mu_num1 = [ 0.216770703063582 + 0.107139620004182i
0.378795349308418 + 0.134884827323222i
0.538497796737552 + 0.152222782289058i
0.697264749719046 + 0.164961556015475i
0.855540207813688 + 0.175063152082181i
1.01351974051428 + 0.183444051676859i
1.17130518761091 + 0.190610170120139i
1.32895553408938 + 0.196871496153662i
1.48650759360047 + 0.202432161302456i
1.64398566053789 + 0.207433908702813i
1.80140647972292 + 0.211979256700566i
1.95878200270734 + 0.216144794762847i
2.11612100859733 + 0.219989271520295i
2.27343010345277 + 0.223558750075335i
2.43071436122255 + 0.226890022828818i
2.58797774865504 + 0.230012947581372i
2.74522341511208 + 0.232952090178354i
2.90245389516800 + 0.235727907232762i
3.05967125332764 + 0.238357615465374i
3.21687718938876 + 0.240855842412500i
3.37407311646433 + 0.243235121396738i
3.53126021964467 + 0.245506273491593i
3.68843950071283 + 0.247678706117715i
3.84561181265540 + 0.249760649212011i
4.00277788660121 + 0.251759344015567i
4.15993835306842 + 0.253681195455886i
4.31709375888278 + 0.255531896240977i
4.47424458076788 + 0.257316528745475i
4.63139123635102 + 0.259039649296082i
4.78853409314339 + 0.260705358385119i
4.94567347591917 + 0.262317359541845i
5.10280967281849 + 0.263879008992454i
5.25994294042609 + 0.265393357786577i
5.41707350802170 + 0.266863187721901i
5.57420158115649 + 0.268291042131689i
5.73132734467771 + 0.269679252392493i
5.88845096529876 + 0.271029960846979i
6.04557259379307 + 0.272345140708481i
6.20269236687458 + 0.273626613412135i
6.35981040881639 + 0.274876063795931i
```

6.51692683284908 + 0.276095053429523i
6.67404174237337 + 0.277285032355608i
6.83115523201516 + 0.278447349465525i
6.98826738854668 + 0.279583261695419i
7.14537829169310 + 0.280693942200320i
7.30248801484104 + 0.281780487639536i
7.45959662566274 + 0.282843924686832i
7.61670418666728 + 0.283885215862355i
7.77381075568887 + 0.284905264769371i
7.93091638632029 + 0.285904920807295i
8.08802112829864 + 0.286884983422585i
8.24512502784955 + 0.287846205950889i
8.40222812799476 + 0.288789299096715i
8.55933046882782 + 0.289714934090879i
8.71643208776158 + 0.290623745560942i
8.87353301975074 + 0.291516334145325i
9.03063329749260 + 0.292393268878157i
9.18773295160813 + 0.293255089368516i
9.34483201080592 + 0.294102307795008i
9.50193050203066 + 0.294935410734140i
9.65902845059789 + 0.295754860838849i
9.81612588031655 + 0.296561098381653i
9.97322281360052 + 0.297354542675364i
10.1303192715703 + 0.298135593382812i
10.2874152741460 + 0.298904631725828i
10.4445108401322 + 0.299662021602654i
10.6016059872956 + 0.300408110621975i
10.7587007324367 + 0.301143231060922i
10.9157950914548 + 0.301867700753675i
11.0728890794087 + 0.302581823916593i
11.2299827105717 + 0.303285891915252i
11.3870759984827 + 0.303980183978222i
11.5441689559935 + 0.304664967861964i
11.7012615953120 + 0.305340500470808i
11.8583539280428 + 0.306007028435598i
12.0154459652238 + 0.306664788654295i
12.1725377173614 + 0.307314008797460i
12.3296291944618 + 0.307954907781353i
12.4867204060611 + 0.308587696211090i
12.6438113612526 + 0.309212576796101i
12.8009020687127 + 0.309829744739967i
12.9579925367247 + 0.310439388106467i
13.1150827732008 + 0.311041688163590i
13.2721727857030 + 0.311636819707074i
13.4292625814627 + 0.312224951364918i
13.5863521673981 + 0.312806245884183i
13.7434415501319 + 0.313380860401332i
13.9005307360067 + 0.313948946697183i
14.0576197310994 + 0.314510651437577i
14.2147085412360 + 0.315066116400656i
14.3717971720037 + 0.315615478691656i
14.5288856287636 + 0.316158870946031i
14.6859739166620 + 0.316696421521670i
14.8430620406411 + 0.317228254680875i

```

15.0001500054491 + 0.317754490762767i
15.1572378156500 + 0.318275246346727i
15.3143254756321 + 0.318790634407391i
15.4714129896168 + 0.319300764461766i
15.6285003616662 + 0.319805742708898i
15.7855875956911 + 0.320305672162549i
15.9426746954575 + 0.320800652777339i
16.0997616645938 + 0.321290781568682i
16.2568485065966 + 0.321776152726898i
16.4139352248371 + 0.322256857725865i
16.5710218225665 + 0.322732985426466i
16.7281083029215 + 0.323204622175180i
16.8851946689291 + 0.323671851898058i
17.0422809235116 + 0.324134756190349i
17.1993670694912 + 0.324593414402023i
17.3564531095938 + 0.325047903719392i
17.5135390464540 + 0.325498299243074i
17.6706248826179 + 0.325944674062460i
17.8277106205477 + 0.326387099326902i
17.9847962626245 + 0.326825644313766i
18.1418818111521 + 0.327260376493525i
18.2989672683599 + 0.327691361592067i
18.4560526364059 + 0.328118663650328i
18.6131379173798 + 0.328542345081382i
18.7702231133055 + 0.328962466725174i
18.9273082261435 + 0.329379087900919i];

mu_num = [-conj(mu_num1); mu_num1];

eta = [(-beta/2 + sqrt(beta^2-4*mu.^2-4*mu*beta*sqrt(nu))/2) (-beta/2 -
sqrt(beta^2-4*mu.^2-4*mu*beta*sqrt(nu))/2) (-beta/2 + sqrt(beta^2-
4*mu.^2+4*mu*beta*sqrt(nu))/2) (-beta/2 - sqrt(beta^2-
4*mu.^2+4*mu*beta*sqrt(nu))/2)].';

CharaM = [exp(eta(2)*1) exp(eta(3)*1) exp(eta(4)*1); exp(-eta(2)*1) exp(-eta(3)*1)
exp(-eta(4)*1); exp(eta(2)*1)/(eta(2)+beta) exp(eta(3)*1)/(eta(3)+beta)
exp(eta(4)*1)/(eta(4)+beta)];
D1 = E*mu;
D1vecctor = -D1*[exp(eta(1)*1) exp(-eta(1)*1) exp(eta(1)*1)/(eta(1)+beta)].';
Dtemp = inv(CharaM)*D1vecctor;
Dvec = [D1;Dtemp];

Avec = vpa((mu*nu-(eta+beta).^2/mu)./(E*mu*(eta+beta)).*Dvec);
Bvec = vpa(-(mu-nu*(eta+beta).^2/mu)./(E*eta.* (eta+beta)).*Dvec);
Cvec = vpa(-(eta+beta).*Dvec/mu);

phii = vpa(simplify([sum(Avec.*exp(eta*x)) sum(Bvec.*exp(eta*x))
sum(Cvec.*exp(eta*x)) sum(Dvec.*exp(eta*x))]..'));
% f_trivali = exp(mu*z).*phii;

f_trival = [];

for k_ = 1:length(mu_num)

```

```

if k_ > length(mu_num)/2
    f_trival = [f_trival vpa(real(Mt*subs(exp(-mu*h).*((real(subs(exp(mu*z),mu,mu_num(k_)))+imag(subs(exp(mu*z),mu,mu_num(k_)))*1i).*((real(simplify(subs(phi,mu,mu_num(k_)), 'Criterion', 'preferReal', 'Steps', 100))+imag(simplify(subs(phi,mu,mu_num(k_)), 'Criterion', 'preferReal', 'Steps', 100))*1i)),mu,mu_num(k_))) vpa(imag(Mt*subs(exp(-mu*h).*((real(subs(exp(mu*z),mu,mu_num(k_)))+imag(subs(exp(mu*z),mu,mu_num(k_)))*1i).*((real(simplify(subs(phi,mu,mu_num(k_)), 'Criterion', 'preferReal', 'Steps', 100))+imag(simplify(subs(phi,mu,mu_num(k_)), 'Criterion', 'preferReal', 'Steps', 100))*1i)),mu,mu_num(k_))))];
else
    f_trival = [f_trival
vpa(real(Mt*subs((real(subs(exp(mu*z),mu,mu_num(k_)))+imag(subs(exp(mu*z),mu,mu_num(k_)))*1i).*((real(simplify(subs(phi,mu,mu_num(k_)), 'Criterion', 'preferReal', 'Steps', 100))+imag(simplify(subs(phi,mu,mu_num(k_)), 'Criterion', 'preferReal', 'Steps', 100))*1i),mu,mu_num(k_)))
vpa(imag(Mt*subs((real(subs(exp(mu*z),mu,mu_num(k_)))+imag(subs(exp(mu*z),mu,mu_num(k_)))*1i).*((real(simplify(subs(phi,mu,mu_num(k_)), 'Criterion', 'preferReal', 'Steps', 100))+imag(simplify(subs(phi,mu,mu_num(k_)), 'Criterion', 'preferReal', 'Steps', 100))*1i),mu,mu_num(k_))))];
end
end

f_special0 = vpa([Mt*f0s_0 Mt*f0a_0 Mt*f0s_1 Mt*f0a_1 Mt*f0a_2 Mt*f0_3]);

f = [f_special0 f_trival];

%% derivation of coefficients via calculus of variations

%parallel computing
pa=parpool(20);

Em = [];
Fm = [];

num_len = length(f(1,:));

parfor i_ = 1:num_len
    for j_ = 1:num_len
        temp1 = matlabFunction(transpose(f(3:4,i_))*f(1:2,j_), 'vars',{x,z});
        temp2 = matlabFunction(f(3,i_)*f(1,j_), 'vars',{x,z});
        temp3 = matlabFunction(f(2,i_)*f(4,j_), 'vars',{x,z});
        temp4 = matlabFunction(f(1,i_)*f(3,j_), 'vars',{x,z});
        Em(i_,j_) = -integral(@(x) temp1(x,h),-1,1,'ArrayValued',true,'RelTol',0,'AbsTol',1e-20) + integral(@(x) temp2(x,0),a,b,'ArrayValued',true,'RelTol',0,'AbsTol',1e-20) - integral(@(x) temp3(x,0),-1,1,'ArrayValued',true,'RelTol',0,'AbsTol',1e-20) - integral(@(x) temp4(x,0),-1,a,'ArrayValued',true,'RelTol',0,'AbsTol',1e-20) - integral(@(x) temp4(x,0),b,1,'ArrayValued',true,'RelTol',0,'AbsTol',1e-20);
    end
    temp5 = matlabFunction(f(3,i_), 'vars',{x,z});
    Fm(i_) = integral(@(x)

```

```

d*temp5(x,0),a,b,'ArrayValued',true,'RelTol',0,'AbsTol',1e-20);
    % str=['Waiting...',num2str(100*i_/num_len),'%'];
    % waitbar(i_/num_len,bar,str)
end
delete(pa);

Mm = inv(Em)*(Fm.');
ansvec = vpa(f*Mm)

%% plot results on the surface
w = ansvec(1)
ww = matlabFunction(w);
fplot(@(x) ww(x,0),[-1,1])
set(gca,'YDir','reverse');

figure;
u = ansvec(2);
uu = matlabFunction(u);
fplot(@(x) uu(x,0),[-1,1])
set(gca,'YDir','reverse');

figure;
sigma = ansvec(3);
ss = matlabFunction(sigma);
fplot(@(x) ss(x,0),[-1,1])
set(gca,'YDir','reverse');

figure;
tau = ansvec(4);
tt = matlabFunction(tau);
fplot(@(x) tt(x,0),[-1,1])
set(gca,'YDir','reverse');

%% Reference
% [1] Chebfun Team (2024). Chebfun - current version
% (https://github.com/chebfun/chebfun), GitHub. Retrieved October 16, 2024.

```

2.Zeros & Chebfun

```

clear; clc; format long;

nu= 0.25;
E = 1;
beta = 0.1;
l = 10;
h = 10;

syms mu

eta1 = -beta/2 + sqrt(beta^2-4*mu.^2-4*mu*beta*sqrt(nu))/2;
eta2 = -beta/2 - sqrt(beta^2-4*mu.^2-4*mu*beta*sqrt(nu))/2;

```

```

eta3 = -beta/2 + sqrt(beta^2-4*mu.^2+4*mu*beta*sqrt(nu))/2;
eta4 = -beta/2 - sqrt(beta^2-4*mu.^2+4*mu*beta*sqrt(nu))/2;

equa = (eta1-eta2).*(eta3-eta4)+(eta1-eta4).*(eta2-eta3).*cosh((eta1-eta2-
eta3+eta4)*l)+(eta1-eta3).*(eta4-eta2).*cosh((eta1-eta2+eta3-eta4)*l);
funct = matlabFunction(equa, 'vars',mu);

Zerostemp = chebfun(funct,[0.1 5],'splitting','on')
mu_zerotemp = roots(Zerostemp, 'complex','norecursion');
Verifications1 = double(vpa(subs(equa,mu,mu_zerotemp)));
index = find(abs(real(Verifications1))<=1e-6 & abs(imag(Verifications1))<=1e-6);
mu_zeros1 = mu_zerotemp(index);
AN1 = Verifications1(index);
index1 = find(real(mu_zeros1)>=0 & imag(mu_zeros1)>=0);
mu_zeros1_fin = mu_zeros1(index1);
VerificationsX = double(abs(vpa(subs(equa,mu,mu_zeros1_fin))));
```

3.FEM

```

function out = model

import com.comsol.model.*
import com.comsol.model.util.*

model = ModelUtil.create('Model');

model.modelPath('C:\Users\Administrator\Downloads');

model.label('FEM_symplectic_analysis.mph');

model.param.set('nu', '0.25', ['Possion' native2unicode(hex2dec({'20' '18'})),
'unicode') 's rato']);

model.param.set('y_max', '0.1', [native2unicode(hex2dec({'53' '8b'})), 'unicode')
native2unicode(hex2dec({'59' '34'})), 'unicode') native2unicode(hex2dec({'67'
'00'})), 'unicode') native2unicode(hex2dec({'59' '27'})), 'unicode')
native2unicode(hex2dec({'53' '8b'})), 'unicode') native2unicode(hex2dec({'51'
'65'})), 'unicode') native2unicode(hex2dec({'6d' 'f1'})), 'unicode')
native2unicode(hex2dec({'5e' 'a6'})), 'unicode') native2unicode(hex2dec({'ff'
'08'})), 'unicode') native2unicode(hex2dec({'5e' '94'})), 'unicode')
native2unicode(hex2dec({'8b' 'e5'})), 'unicode') native2unicode(hex2dec({'66'
'2f'})), 'unicode') '0.1-0.05=0.05m' native2unicode(hex2dec({'ff' '09'})),
'unicode') ]);

model.param.set('par', '0', [native2unicode(hex2dec({'6c' '42'})), 'unicode')
native2unicode(hex2dec({'89' 'e3'})), 'unicode') native2unicode(hex2dec({'53'
'c2'})), 'unicode') native2unicode(hex2dec({'65' '70'})), 'unicode') ]);

model.component.create('comp1', true);

model.component('comp1').geom.create('geom1', 2);

model.result.table.create('ev12', 'Table');
```

```
model.result.table.create('tbl1', 'Table');
model.result.table.create('tbl2', 'Table');
model.result.table.create('tbl3', 'Table');

model.func.create('an1', 'Analytic');
model.func.create('rm1', 'Ramp');
model.func('an1').set('funcname', 'gradient_exp');
model.func('an1').set('expr', 'exp(0.1*x)');
model.func('an1').set('fununit', 'Pa');
model.func('an1').set('argunit', {'m'});
model.func('an1').set('plotfixedvalue', {'-10'});
model.func('an1').set('plotargs', {'x' '-10' '10'});
model.func('rm1').set('funcname', 'rm');
model.func('rm1').set('cutoffactive', true);
model.func('rm1').set('smoothzonelocactive', true);
model.func('rm1').set('smoothzonecutoffactive', true);

model.component('comp1').mesh.create('mesh1');

model.component('comp1').geom('geom1').create('r1', 'Rectangle');
model.component('comp1').geom('geom1').feature('r1').set('pos', [-10 -10]);
model.component('comp1').geom('geom1').feature('r1').set('size', [20 10]);
model.component('comp1').geom('geom1').create('r2', 'Rectangle');
model.component('comp1').geom('geom1').feature('r2').set('pos', [-0.5 0.05]);
model.component('comp1').geom('geom1').feature('r2').set('size', [1 2]);
model.component('comp1').geom('geom1').feature('fin').label([native2unicode(hex2dec({'5f' '62'}), 'unicode') native2unicode(hex2dec({'62' '10'}), 'unicode') native2unicode(hex2dec({'88' 'c5'}), 'unicode') native2unicode(hex2dec({'91' '4d'}), 'unicode') ]);
model.component('comp1').geom('geom1').feature('fin').set('action', 'assembly');
model.component('comp1').geom('geom1').feature('fin').set('imprint', true);
model.component('comp1').geom('geom1').feature('fin').set('pairtype', 'contact');
model.component('comp1').geom('geom1').run;
model.component('comp1').geom('geom1').run('fin');

model.component('comp1').pair.create('p1', 'Contact');
model.component('comp1').pair('p1').source.set([6]);
model.component('comp1').pair('p1').destination.set([3]);

model.component('comp1').physics.create('solid', 'SolidMechanics', 'geom1');
model.component('comp1').physics('solid').create('rd1', 'RigidDomain', 2);
model.component('comp1').physics('solid').feature('rd1').selection.set([2]);
model.component('comp1').physics('solid').feature('rd1').create('pdr1',
'PrescribedDispRot', -1);
model.component('comp1').physics('solid').feature('rd1').feature('pdr1').set('RotationType', 'PrescribedRotationGroup');
model.component('comp1').physics('solid').create('fix1', 'Fixed', 1);
model.component('comp1').physics('solid').feature('fix1').selection.set([2]);

model.component('comp1').mesh('mesh1').create('map1', 'Map');
model.component('comp1').mesh('mesh1').create('ftri1', 'FreeTri');
model.component('comp1').mesh('mesh1').feature('map1').selection.geom('geom1', 2);
model.component('comp1').mesh('mesh1').feature('map1').selection.set([1]);
model.component('comp1').mesh('mesh1').feature('map1').create('dis1',
```

```
'Distribution');
model.component('comp1').mesh('mesh1').feature('map1').create('dis2',
'Distribution');
model.component('comp1').mesh('mesh1').feature('map1').feature('dis1').selection.set([2 3]);
model.component('comp1').mesh('mesh1').feature('map1').feature('dis2').selection.set([1 4]);
model.component('comp1').mesh('mesh1').feature('ftri1').selection.geom('geom1',
2);
model.component('comp1').mesh('mesh1').feature('ftri1').selection.set([2]);
model.component('comp1').mesh('mesh1').feature('ftri1').create('size1', 'Size');

model.result.table('evl2').label('Evaluation 2D');
model.result.table('evl2').comments([native2unicode(hex2dec({'4e' 'a4'})),
'unicode') native2unicode(hex2dec({'4e' '92'}), 'unicode')
native2unicode(hex2dec({'76' '84'}), 'unicode') native2unicode(hex2dec({'4e' '8c'}),
'unicode') native2unicode(hex2dec({'7e' 'f4'}), 'unicode')
native2unicode(hex2dec({'50' '3c'}), 'unicode') ]);
model.result.table('tbl1').comments([native2unicode(hex2dec({'7e' 'bf'}),
'unicode') native2unicode(hex2dec({'79' 'ef'}), 'unicode')
native2unicode(hex2dec({'52' '06'}), 'unicode') ' 1']);
model.result.table('tbl2').label([native2unicode(hex2dec({'88' '68'}), 'unicode')
native2unicode(hex2dec({'68' '3c'}), 'unicode') ' 2']);
model.result.table('tbl2').comments([native2unicode(hex2dec({'7e' 'bf'}),
'unicode') native2unicode(hex2dec({'79' 'ef'}), 'unicode')
native2unicode(hex2dec({'52' '06'}), 'unicode') ' 2']);
model.result.table('tbl3').comments('sigma_all');

model.component('comp1').view('view1').axis.set('xmin', -10.499998092651367);
model.component('comp1').view('view1').axis.set('xmax', 10.499998092651367);
model.component('comp1').view('view1').axis.set('ymin', -10.934999465942383);
model.component('comp1').view('view1').axis.set('ymax', 2.9849982261657715);

model.component('comp1').pair('p1').searchMethod('fast');

model.component('comp1').physics('solid').prop('Type2D').set('Type2D',
'PlaneStress');
model.component('comp1').physics('solid').prop('AdvancedSettings').set('GroupPhysO
desRc', false);
model.component('comp1').physics('solid').prop('AdvancedSettings').set('GroupPhysO
desAtt', false);
model.component('comp1').physics('solid').prop('AdvancedSettings').set('GroupPhysO
desRd', false);
model.component('comp1').physics('solid').feature('lemm1').set('E_mat',
'userdef');
model.component('comp1').physics('solid').feature('lemm1').set('E',
'gradient_exp(x)');
model.component('comp1').physics('solid').feature('lemm1').set('nu_mat',
'userdef');
model.component('comp1').physics('solid').feature('lemm1').set('nu', 'nu');
model.component('comp1').physics('solid').feature('lemm1').set('rho_mat',
'userdef');
model.component('comp1').physics('solid').feature('lemm1').set('rho', 7850);
model.component('comp1').physics('solid').feature('dcnt1').set('ContactMethodCtrl'
```

```
, 'AugmentedLagrange');

model.component('comp1').physics('solid').feature('rd1').set('rho_mat',
'userdef');

model.component('comp1').physics('solid').feature('rd1').set('rho', 7850);
model.component('comp1').physics('solid').feature('rd1').label([native2unicode(hex
2dec({'52' '1a'})), 'unicode']) native2unicode(hex2dec({'60' '27'}), 'unicode')
native2unicode(hex2dec({'57' 'df'}), 'unicode') ' 1']);

model.component('comp1').physics('solid').feature('rd1').feature('init1').set('Cen
terOfRotationType', 'CentroidOfSelectedEntities');

model.component('comp1').physics('solid').feature('rd1').feature('init1').set('u',
{'0'; '-rm(par)*y_max'; '0'});

model.component('comp1').physics('solid').feature('rd1').feature('pdr1').set('U0',
{'0'; '-rm(par)*y_max'; '0'});

model.component('comp1').physics('solid').feature('rd1').feature('pdr1').set('Dire
ction', [1; 1; 0]);

model.component('comp1').mesh('mesh1').feature('size').set('hauto', 2);
model.component('comp1').mesh('mesh1').feature('map1').feature('dis1').set('type',
'predefined');
model.component('comp1').mesh('mesh1').feature('map1').feature('dis1').set('elemco
unt', 200);
model.component('comp1').mesh('mesh1').feature('map1').feature('dis1').set('elemra
tio', 0.1);
model.component('comp1').mesh('mesh1').feature('map1').feature('dis1').set('growth
rate', 'exponential');
model.component('comp1').mesh('mesh1').feature('map1').feature('dis1').set('symmet
ric', true);
model.component('comp1').mesh('mesh1').feature('map1').feature('dis2').set('type',
'predefined');
model.component('comp1').mesh('mesh1').feature('map1').feature('dis2').set('revers
e', true);
model.component('comp1').mesh('mesh1').feature('map1').feature('dis2').set('elemco
unt', 50);
model.component('comp1').mesh('mesh1').feature('map1').feature('dis2').set('elemra
tio', 9);
model.component('comp1').mesh('mesh1').feature('ftri1').feature('size1').set('haut
o', 1);
model.component('comp1').mesh('mesh1').run;

model.study.create('std1');
model.study('std1').create('stat', 'Stationary');

model.sol.create('sol1');
model.sol('sol1').study('std1');
model.sol('sol1').attach('std1');
model.sol('sol1').create('st1', 'StudyStep');
model.sol('sol1').create('v1', 'Variables');
model.sol('sol1').create('s1', 'Stationary');
model.sol('sol1').feature('s1').create('p1', 'Parametric');
model.sol('sol1').feature('s1').create('se1', 'Segregated');
model.sol('sol1').feature('s1').feature('se1').create('ss1', 'SegregatedStep');
model.sol('sol1').feature('s1').feature('se1').create('ls1', 'LumpedStep');
model.sol('sol1').feature('s1').feature('se1').feature.remove('ssDef');
model.sol('sol1').feature('s1').feature.remove('fcDef');
```

```
model.result.dataset.create('cln1', 'CutLine2D');
model.result.dataset.create('cln2', 'CutLine2D');
model.result.numerical.create('int1', 'IntLine');
model.result.numerical.create('int2', 'IntLine');
model.result.numerical.create('int3', 'IntLine');
model.result.create('pg1', 'PlotGroup2D');
model.result.create('pg2', 'PlotGroup2D');
model.result.create('pg4', 'PlotGroup2D');
model.result.create('pg5', 'PlotGroup2D');
model.result.create('pg6', 'PlotGroup2D');
model.result.create('pg7', 'PlotGroup2D');
model.result.create('pg8', 'PlotGroup1D');
model.result('pg1').create('surf1', 'Surface');
model.result('pg1').feature('surf1').set('expr', 'solid.mises');
model.result('pg1').feature('surf1').create('def', 'Deform');
model.result('pg2').create('arwl1', 'ArrowLine');
model.result('pg2').create('surf1', 'Surface');
model.result('pg2').feature('arwl1').create('col', 'Color');
model.result('pg2').feature('arwl1').create('def', 'Deform');
model.result('pg2').feature('arwl1').feature('col').set('expr',
'comp1.solid.dcnt1.Tn');
model.result('pg2').feature('surf1').set('expr', '1');
model.result('pg2').feature('surf1').create('def', 'Deform');
model.result('pg2').feature('surf1').create('sel1', 'Selection');
model.result('pg2').feature('surf1').feature('sel1').selection.set([1 2]);
model.result('pg4').selection.geom('geom1', 2);
model.result('pg4').selection.set([1]);
model.result('pg4').create('surf1', 'Surface');
model.result('pg4').create('con1', 'Contour');
model.result('pg4').feature('surf1').set('expr', 'v');
model.result('pg4').feature('surf1').create('def', 'Deform');
model.result('pg4').feature('con1').set('expr', 'v');
model.result('pg4').feature('con1').create('def1', 'Deform');
model.result('pg5').selection.geom('geom1', 2);
model.result('pg5').selection.set([1]);
model.result('pg5').create('surf1', 'Surface');
model.result('pg5').create('con1', 'Contour');
model.result('pg5').feature('surf1').set('expr', 'u');
model.result('pg5').feature('surf1').create('def', 'Deform');
model.result('pg5').feature('con1').set('expr', 'u');
model.result('pg5').feature('con1').create('def1', 'Deform');
model.result('pg6').create('surf1', 'Surface');
model.result('pg6').create('con1', 'Contour');
model.result('pg6').create('mesh1', 'Mesh');
model.result('pg6').feature('surf1').set('expr', 'solid.sy');
model.result('pg6').feature('surf1').create('def', 'Deform');
model.result('pg6').feature('con1').set('expr', 'solid.sy');
model.result('pg6').feature('con1').create('def1', 'Deform');
model.result('pg7').create('surf1', 'Surface');
model.result('pg7').create('con1', 'Contour');
model.result('pg7').create('mesh1', 'Mesh');
model.result('pg7').feature('surf1').set('expr', 'solid.sxy');
model.result('pg7').feature('surf1').create('def', 'Deform');
```

```

model.result('pg7').feature('con1').set('expr', 'solid.sxy');
model.result('pg7').feature('con1').create('def1', 'Deform');
model.result('pg8').create('lngr1', 'LineGraph');
model.result('pg8').feature('lngr1').set('expr', '-solid.sxy');
model.result.export.create('data1', 'Data');
model.result.export.create('data2', 'Data');
model.result.export.create('data3', 'Data');
model.result.export.create('data4', 'Data');

model.study('std1').feature('stat').set('useparam', true);
model.study('std1').feature('stat').set('pname', {'par'});
model.study('std1').feature('stat').set('plistarr', {'range(0,0.1,1)'});
model.study('std1').feature('stat').set('punit', {''});

model.sol('sol1').attach('std1');
model.sol('sol1').feature('st1').label([native2unicode(hex2dec({'7f' '16'})),
'unicode') native2unicode(hex2dec({'8b' 'd1'}), 'unicode')
native2unicode(hex2dec({'65' 'b9'}), 'unicode') native2unicode(hex2dec({'7a' '0b'}), 'unicode') ': ' native2unicode(hex2dec({'7a' '33'}), 'unicode')
native2unicode(hex2dec({'60' '01'}), 'unicode') ]);
model.sol('sol1').feature('v1').label([native2unicode(hex2dec({'56' 'e0'}),
'unicode') native2unicode(hex2dec({'53' 'd8'}), 'unicode')
native2unicode(hex2dec({'91' 'cf'}), 'unicode') ' 1.1']]);
model.sol('sol1').feature('v1').set('clistctrl', {'p1'});
model.sol('sol1').feature('v1').set('cname', {'par'});
model.sol('sol1').feature('v1').set('clist', {'range(0,0.1,1)'});
model.sol('sol1').feature('v1').feature('comp1_solid_Tn_p1').set('scalemethod',
'manual');
model.sol('sol1').feature('v1').feature('comp1_solid_Tn_p1').set('scaleval',
100000000);
model.sol('sol1').feature('v1').feature('comp1_solid_wZ').set('scalemethod',
'manual');
model.sol('sol1').feature('v1').feature('comp1_solid_wZ').set('scaleval', '1e-2');
model.sol('sol1').feature('v1').feature('comp1_u').set('scalemethod', 'manual');
model.sol('sol1').feature('v1').feature('comp1_u').set('scaleval', '1e-
2*23.349571730547865');
model.sol('sol1').feature('v1').feature('comp1_solid_rd1_u').set('scalemethod',
'manual');
model.sol('sol1').feature('v1').feature('comp1_solid_rd1_u').set('scaleval', '1e-
2*23.349571730547865');
model.sol('sol1').feature('v1').feature('comp1_solid_rd1_phi').set('scalemethod',
'manual');
model.sol('sol1').feature('v1').feature('comp1_solid_rd1_phi').set('scaleval',
'1e-1');
model.sol('sol1').feature('s1').label([native2unicode(hex2dec({'7a' '33'}),
'unicode') native2unicode(hex2dec({'60' '01'}), 'unicode')
native2unicode(hex2dec({'6c' '42'}), 'unicode') native2unicode(hex2dec({'89' 'e3'}),
'unicode') native2unicode(hex2dec({'56' '68'}), 'unicode') ' 1.1']]);
model.sol('sol1').feature('s1').set('probesel', 'none');
model.sol('sol1').feature('s1').feature('dDef').label([native2unicode(hex2dec({'76' 'f4'}),
'unicode') native2unicode(hex2dec({'63' 'a5'}), 'unicode') ' 1']);
model.sol('sol1').feature('s1').feature('aDef').label([native2unicode(hex2dec({'9a' 'd8'}),
'unicode') native2unicode(hex2dec({'7e' 'a7'}), 'unicode') ' 1']);
model.sol('sol1').feature('s1').feature('aDef').set('cachepattern', true);

```

```

model.sol('sol1').feature('s1').feature('p1').label([native2unicode(hex2dec({'53' 'c2'})), 'unicode']) native2unicode(hex2dec({'65' '70'}), 'unicode')
native2unicode(hex2dec({'53' '16'}), 'unicode') ' 1.1']);
model.sol('sol1').feature('s1').feature('p1').set('pname', {'par'});
model.sol('sol1').feature('s1').feature('p1').set('plistarr', {'range(0,0.1,1)'});
model.sol('sol1').feature('s1').feature('p1').set('punit', {''});
model.sol('sol1').feature('s1').feature('p1').set('porder', 'constant');
model.sol('sol1').feature('s1').feature('p1').set('continuationlsqall', false);
model.sol('sol1').feature('s1').feature('se1').label([native2unicode(hex2dec({'52' '06'})), 'unicode']) native2unicode(hex2dec({'79' 'bb'}), 'unicode') ' 1.1']);
model.sol('sol1').feature('s1').feature('se1').set('maxsegiter', 15);
model.sol('sol1').feature('s1').feature('se1').feature('ss1').label([native2unicode(hex2dec({'56' 'fa'})), 'unicode']) native2unicode(hex2dec({'4f' '53'})), 'unicode') native2unicode(hex2dec({'52' '9b'}), 'unicode')
native2unicode(hex2dec({'5b' '66'}), 'unicode']);
model.sol('sol1').feature('s1').feature('se1').feature('ss1').set('segvar', {'comp1_u' 'comp1_solid_wZ' 'comp1_solid_rd1_u' 'comp1_solid_rd1_phi'});
model.sol('sol1').feature('s1').feature('se1').feature('ss1').set('subdtech', 'ddog');
model.sol('sol1').feature('s1').feature('se1').feature('ss1').set('subiter', 7);
model.sol('sol1').feature('s1').feature('se1').feature('ss1').set('subtermauto', 'itertol');
model.sol('sol1').feature('s1').feature('se1').feature('ss1').set('subntolfact', 1);
model.sol('sol1').feature('s1').feature('se1').feature('ls1').label([native2unicode(hex2dec({'96' 'c6'})), 'unicode']) native2unicode(hex2dec({'60' '3b'}), 'unicode') native2unicode(hex2dec({'6b' '65'}), 'unicode')
native2unicode(hex2dec({'9a' 'a4'}), 'unicode') ' 1.1']);
model.sol('sol1').feature('s1').feature('se1').feature('ls1').set('segvar', {'comp1_solid_Tn_p1'});
model.sol('sol1').runAll;

model.result.dataset('cln1').label('-10,10');
model.result.dataset('cln1').set('genpoints', [-10 0; 10 0]);
model.result.dataset('cln2').label(-0.5,0.5);
model.result.dataset('cln2').set('genpoints', [-0.5 0; 0.5 0]);
model.result.numerical('int1').label('sigma_normal');
model.result.numerical('int1').set('data', 'cln2');
model.result.numerical('int1').set('looplevelinput', {'manualindices'});
model.result.numerical('int1').set('looplevelindices', [8]);
model.result.numerical('int1').set('table', 'tbl1');
model.result.numerical('int1').set('expr', {'solid.sy'});
model.result.numerical('int1').set('unit', {'N/m'});
model.result.numerical('int1').set('descr', {[native2unicode(hex2dec({'5e' '94'})), 'unicode']) native2unicode(hex2dec({'52' '9b'}), 'unicode')
native2unicode(hex2dec({'5f' '20'}), 'unicode') native2unicode(hex2dec({'91' 'cf'}), 'unicode') native2unicode(hex2dec({'ff' '0c'}), 'unicode') 'y '
native2unicode(hex2dec({'52' '06'}), 'unicode') native2unicode(hex2dec({'91' 'cf'}), 'unicode') ]});
model.result.numerical('int1').set('const', {'solid.refpntx' '0'
[native2unicode(hex2dec({'52' '9b'}), 'unicode')] native2unicode(hex2dec({'77' 'e9'}), 'unicode') native2unicode(hex2dec({'8b' 'a1'}), 'unicode')
native2unicode(hex2dec({'7b' '97'}), 'unicode') native2unicode(hex2dec({'53' 'c2'}), 'unicode') native2unicode(hex2dec({'80' '03'}), 'unicode')})

```

```

native2unicode(hex2dec({'70' 'b9'}), 'unicode') ' x ' native2unicode(hex2dec({'57'
'50'}), 'unicode') native2unicode(hex2dec({'68' '07'}), 'unicode') ];
'solid.refpnty' '0' [native2unicode(hex2dec({'52' '9b'}), 'unicode')
native2unicode(hex2dec({'77' 'e9'}), 'unicode') native2unicode(hex2dec({'8b'
'a1'}), 'unicode') native2unicode(hex2dec({'7b' '97'}), 'unicode')
native2unicode(hex2dec({'53' 'c2'}), 'unicode') native2unicode(hex2dec({'80'
'03'}), 'unicode') native2unicode(hex2dec({'70' 'b9'}), 'unicode') ' y '
native2unicode(hex2dec({'57' '50'}), 'unicode') native2unicode(hex2dec({'68'
'07'}), 'unicode') ]; 'solid.refpntz' '0' [native2unicode(hex2dec({'52' '9b'}),
'unicode') native2unicode(hex2dec({'77' 'e9'}), 'unicode')
native2unicode(hex2dec({'8b' 'a1'}), 'unicode') native2unicode(hex2dec({'7b'
'97'}), 'unicode') native2unicode(hex2dec({'53' 'c2'}), 'unicode')
native2unicode(hex2dec({'80' '03'}), 'unicode') native2unicode(hex2dec({'70'
'b9'}), 'unicode') ' z ' native2unicode(hex2dec({'57' '50'}), 'unicode')
native2unicode(hex2dec({'68' '07'}), 'unicode') ]});
model.result.numerical('int2').label('tau');
model.result.numerical('int2').set('data', 'cln2');
model.result.numerical('int2').set('looplevelinput', {'manualindices'});
model.result.numerical('int2').set('looplevelindices', [8]);
model.result.numerical('int2').set('table', 'tbl2');
model.result.numerical('int2').set('expr', {'solid.sxy'});
model.result.numerical('int2').set('unit', {'N/m'});
model.result.numerical('int2').set('descr', {[native2unicode(hex2dec({'5e' '94'}),
'unicode') native2unicode(hex2dec({'52' '9b'}), 'unicode')
native2unicode(hex2dec({'5f' '20'}), 'unicode') native2unicode(hex2dec({'91'
'cf'}), 'unicode') native2unicode(hex2dec({'ff' '0c'}), 'unicode') 'xy '
native2unicode(hex2dec({'52' '06'}), 'unicode') native2unicode(hex2dec({'91'
'cf'}), 'unicode')]}));
model.result.numerical('int2').set('const', {'solid.refpntx' '0'
[native2unicode(hex2dec({'52' '9b'}), 'unicode') native2unicode(hex2dec({'77'
'e9'}), 'unicode') native2unicode(hex2dec({'8b' 'a1'}), 'unicode')
native2unicode(hex2dec({'7b' '97'}), 'unicode') native2unicode(hex2dec({'53'
'c2'}), 'unicode') native2unicode(hex2dec({'80' '03'}), 'unicode')
native2unicode(hex2dec({'70' 'b9'}), 'unicode') ' x ' native2unicode(hex2dec({'57'
'50'}), 'unicode') native2unicode(hex2dec({'68' '07'}), 'unicode') ];
'solid.refpnty' '0' [native2unicode(hex2dec({'52' '9b'}), 'unicode')
native2unicode(hex2dec({'77' 'e9'}), 'unicode') native2unicode(hex2dec({'8b'
'a1'}), 'unicode') native2unicode(hex2dec({'7b' '97'}), 'unicode')
native2unicode(hex2dec({'53' 'c2'}), 'unicode') native2unicode(hex2dec({'80'
'03'}), 'unicode') native2unicode(hex2dec({'70' 'b9'}), 'unicode') ' y '
native2unicode(hex2dec({'57' '50'}), 'unicode') native2unicode(hex2dec({'68'
'07'}), 'unicode') ]; 'solid.refpntz' '0' [native2unicode(hex2dec({'52' '9b'}),
'unicode') native2unicode(hex2dec({'77' 'e9'}), 'unicode')
native2unicode(hex2dec({'8b' 'a1'}), 'unicode') native2unicode(hex2dec({'7b'
'97'}), 'unicode') native2unicode(hex2dec({'53' 'c2'}), 'unicode')
native2unicode(hex2dec({'80' '03'}), 'unicode') native2unicode(hex2dec({'70'
'b9'}), 'unicode') ' z ' native2unicode(hex2dec({'57' '50'}), 'unicode')
native2unicode(hex2dec({'68' '07'}), 'unicode') ]});
model.result.numerical('int3').label('sigma_all');
model.result.numerical('int3').set('data', 'cln1');
model.result.numerical('int3').set('table', 'tbl3');
model.result.numerical('int3').set('expr', {'solid.sy'});
model.result.numerical('int3').set('unit', {'N/m'});
model.result.numerical('int3').set('descr', {[native2unicode(hex2dec({'5e' '94'}),

```

```

'unicode') native2unicode(hex2dec({'52' '9b'}), 'unicode')
native2unicode(hex2dec({'5f' '20'}), 'unicode') native2unicode(hex2dec({'91'
'cf'}), 'unicode') native2unicode(hex2dec({'ff' '0c'}), 'unicode') 'y '
native2unicode(hex2dec({'52' '06'}), 'unicode') native2unicode(hex2dec({'91'
'cf'}), 'unicode') ]});
model.result.numerical('int3').set('const', {'solid.refpntx' '0'
[native2unicode(hex2dec({'52' '9b'}), 'unicode') native2unicode(hex2dec({'77'
'e9'}), 'unicode') native2unicode(hex2dec({'8b' 'a1'}), 'unicode')
native2unicode(hex2dec({'7b' '97'}), 'unicode') native2unicode(hex2dec({'53'
'c2'}), 'unicode') native2unicode(hex2dec({'80' '03'}), 'unicode')
native2unicode(hex2dec({'70' 'b9'}), 'unicode') 'x' native2unicode(hex2dec({'57'
'50'}), 'unicode') native2unicode(hex2dec({'68' '07'}), 'unicode') ];
'solid.refpnty' '0' [native2unicode(hex2dec({'52' '9b'}), 'unicode')
native2unicode(hex2dec({'77' 'e9'}), 'unicode') native2unicode(hex2dec({'8b'
'a1'}), 'unicode') native2unicode(hex2dec({'7b' '97'}), 'unicode')
native2unicode(hex2dec({'53' 'c2'}), 'unicode') native2unicode(hex2dec({'80'
'03'}), 'unicode') native2unicode(hex2dec({'70' 'b9'}), 'unicode') 'y '
native2unicode(hex2dec({'57' '50'}), 'unicode') native2unicode(hex2dec({'68'
'07'}), 'unicode')]; 'solid.refpntz' '0' [native2unicode(hex2dec({'52' '9b'}),
'unicode') native2unicode(hex2dec({'77' 'e9'}), 'unicode')
native2unicode(hex2dec({'8b' 'a1'}), 'unicode') native2unicode(hex2dec({'7b'
'97'}), 'unicode') native2unicode(hex2dec({'53' 'c2'}), 'unicode')
native2unicode(hex2dec({'80' '03'}), 'unicode') native2unicode(hex2dec({'70'
'b9'}), 'unicode') 'z' native2unicode(hex2dec({'57' '50'}), 'unicode')
native2unicode(hex2dec({'68' '07'}), 'unicode') ]]);
model.result.numerical('int1').setResult;
model.result.numerical('int2').setResult;
model.result.numerical('int3').setResult;
model.result('pg1').label([native2unicode(hex2dec({'5e' '94'}), 'unicode')
native2unicode(hex2dec({'52' '9b'}), 'unicode') ' (solid)' ]);
model.result('pg1').set('looplevel', [8]);
model.result('pg1').set('frametype', 'spatial');
model.result('pg1').feature('surf1').set('const', {'solid.refpntx' '0'
[native2unicode(hex2dec({'52' '9b'}), 'unicode') native2unicode(hex2dec({'77'
'e9'}), 'unicode') native2unicode(hex2dec({'8b' 'a1'}), 'unicode')
native2unicode(hex2dec({'7b' '97'}), 'unicode') native2unicode(hex2dec({'53'
'c2'}), 'unicode') native2unicode(hex2dec({'80' '03'}), 'unicode')
native2unicode(hex2dec({'70' 'b9'}), 'unicode') 'x' native2unicode(hex2dec({'57'
'50'}), 'unicode') native2unicode(hex2dec({'68' '07'}), 'unicode') ];
'solid.refpnty' '0' [native2unicode(hex2dec({'52' '9b'}), 'unicode')
native2unicode(hex2dec({'77' 'e9'}), 'unicode') native2unicode(hex2dec({'8b'
'a1'}), 'unicode') native2unicode(hex2dec({'7b' '97'}), 'unicode')
native2unicode(hex2dec({'53' 'c2'}), 'unicode') native2unicode(hex2dec({'80'
'03'}), 'unicode') native2unicode(hex2dec({'70' 'b9'}), 'unicode') 'y '
native2unicode(hex2dec({'57' '50'}), 'unicode') native2unicode(hex2dec({'68'
'07'}), 'unicode')]; 'solid.refpntz' '0' [native2unicode(hex2dec({'52' '9b'}),
'unicode') native2unicode(hex2dec({'77' 'e9'}), 'unicode')
native2unicode(hex2dec({'8b' 'a1'}), 'unicode') native2unicode(hex2dec({'7b'
'97'}), 'unicode') native2unicode(hex2dec({'53' 'c2'}), 'unicode')
native2unicode(hex2dec({'80' '03'}), 'unicode') native2unicode(hex2dec({'70'
'b9'}), 'unicode') 'z' native2unicode(hex2dec({'57' '50'}), 'unicode')
native2unicode(hex2dec({'68' '07'}), 'unicode') ]]);
model.result('pg1').feature('surf1').set('colortable', 'Prism');
model.result('pg1').feature('surf1').set('threshold', 'manual');

```

```
model.result('pg1').feature('surf1').set('thresholdvalue', 0.2);
model.result('pg1').feature('surf1').set('resolution', 'normal');
model.result('pg1').feature('surf1').feature('def').set('scaleactive', true);
model.result('pg2').label([native2unicode(hex2dec({'63' 'a5'})), 'unicode'])
native2unicode(hex2dec({'89' 'e6'}), 'unicode') native2unicode(hex2dec({'52'
'9b'}), 'unicode') '(solid)');
model.result('pg2').set('looplevel', [8]);
model.result('pg2').set('titletype', 'label');
model.result('pg2').set('frametype', 'spatial');
model.result('pg2').set('showlegendsunit', true);
model.result('pg2').feature('arw11').label([native2unicode(hex2dec({'63' 'a5'})),
'unicode') native2unicode(hex2dec({'89' 'e6'}), 'unicode') ' 1,
native2unicode(hex2dec({'53' '8b'}), 'unicode') native2unicode(hex2dec({'52'
'9b'}), 'unicode') ]);
model.result('pg2').feature('arw11').set('expr', {'solid.dcnt1.Tnx'
'solid.dcnt1.Tny'});
model.result('pg2').feature('arw11').set('descr', [native2unicode(hex2dec({'63'
'a5'}), 'unicode') native2unicode(hex2dec({'89' 'e6'}), 'unicode')
native2unicode(hex2dec({'53' '8b'}), 'unicode') native2unicode(hex2dec({'52'
'9b'}), 'unicode') '' native2unicode(hex2dec({'ff' '08'}), 'unicode')
native2unicode(hex2dec({'7a' '7a'}), 'unicode') native2unicode(hex2dec({'95'
'f4'}), 'unicode') native2unicode(hex2dec({'57' '50'}), 'unicode')
native2unicode(hex2dec({'68' '07'}), 'unicode') native2unicode(hex2dec({'7c'
'fb'}), 'unicode') native2unicode(hex2dec({'ff' '09'}), 'unicode') ]);
model.result('pg2').feature('arw11').set('const', {'solid.refpntx' '0'
[native2unicode(hex2dec({'52' '9b'}), 'unicode') native2unicode(hex2dec({'77'
'e9'}), 'unicode') native2unicode(hex2dec({'8b' 'a1'}), 'unicode')
native2unicode(hex2dec({'7b' '97'}), 'unicode') native2unicode(hex2dec({'53'
'c2'}), 'unicode') native2unicode(hex2dec({'80' '03'}), 'unicode')
native2unicode(hex2dec({'70' 'b9'}), 'unicode') ' x ' native2unicode(hex2dec({'57'
'50'}), 'unicode') native2unicode(hex2dec({'68' '07'}), 'unicode') ];
'solid.refpnty' '0' [native2unicode(hex2dec({'52' '9b'}), 'unicode')
native2unicode(hex2dec({'77' 'e9'}), 'unicode') native2unicode(hex2dec({'8b'
'a1'}), 'unicode') native2unicode(hex2dec({'7b' '97'}), 'unicode')
native2unicode(hex2dec({'53' 'c2'}), 'unicode') native2unicode(hex2dec({'80'
'03'}), 'unicode') native2unicode(hex2dec({'70' 'b9'}), 'unicode') ' y '
native2unicode(hex2dec({'57' '50'}), 'unicode') native2unicode(hex2dec({'68'
'07'}), 'unicode') ]; 'solid.refpntz' '0' [native2unicode(hex2dec({'52' '9b'}),
'unicode') native2unicode(hex2dec({'77' 'e9'}), 'unicode')
native2unicode(hex2dec({'8b' 'a1'}), 'unicode') native2unicode(hex2dec({'7b'
'97'}), 'unicode') native2unicode(hex2dec({'53' 'c2'}), 'unicode')
native2unicode(hex2dec({'80' '03'}), 'unicode') native2unicode(hex2dec({'70'
'b9'}), 'unicode') ' z ' native2unicode(hex2dec({'57' '50'}), 'unicode')
native2unicode(hex2dec({'68' '07'}), 'unicode') ]});
model.result('pg2').feature('arw11').set('placement', 'gausspoints');
model.result('pg2').feature('arw11').set('gporder', 4);
model.result('pg2').feature('arw11').set('arrowbase', 'head');
model.result('pg2').feature('arw11').set('scale', 20.212635521142257);
model.result('pg2').feature('arw11').set('scaleactive', false);
model.result('pg2').feature('arw11').feature('col').set('coloring', 'gradient');
model.result('pg2').feature('arw11').feature('col').set('topcolor', 'green');
model.result('pg2').feature('arw11').feature('col').set('bottomcolor', 'custom');
model.result('pg2').feature('arw11').feature('col').set('custombottomcolor',
[0.509804 0.54902 0.509804]);
```

```

model.result('pg2').feature('arw11').feature('def').set('scaleactive', true);
model.result('pg2').feature('surf1').label([native2unicode(hex2dec({'70' '70'})),
'unicode') native2unicode(hex2dec({'82' '72'}), 'unicode')
native2unicode(hex2dec({'88' '68'}), 'unicode') native2unicode(hex2dec({'97' '62'}), 'unicode') ]);
model.result('pg2').feature('surf1').set('const', {'solid.refpntx' '0'
[native2unicode(hex2dec({'52' '9b'}), 'unicode') native2unicode(hex2dec({'77' 'e9'}), 'unicode')
native2unicode(hex2dec({'8b' 'a1'}), 'unicode')
native2unicode(hex2dec({'7b' '97'}), 'unicode') native2unicode(hex2dec({'53' 'c2'}), 'unicode')
native2unicode(hex2dec({'80' '03'}), 'unicode')
native2unicode(hex2dec({'70' 'b9'}), 'unicode') 'x' native2unicode(hex2dec({'57' '50'}), 'unicode')
native2unicode(hex2dec({'68' '07'}), 'unicode') ];
'solid.refpnty' '0' [native2unicode(hex2dec({'52' '9b'}), 'unicode')
native2unicode(hex2dec({'77' 'e9'}), 'unicode') native2unicode(hex2dec({'8b' 'a1'}), 'unicode')
native2unicode(hex2dec({'7b' '97'}), 'unicode')
native2unicode(hex2dec({'53' 'c2'}), 'unicode') native2unicode(hex2dec({'80' '03'}), 'unicode')
native2unicode(hex2dec({'70' 'b9'}), 'unicode') 'y'
native2unicode(hex2dec({'57' '50'}), 'unicode') native2unicode(hex2dec({'68' '07'}), 'unicode') ];
'solid.refpntz' '0' [native2unicode(hex2dec({'52' '9b'}), 'unicode')
native2unicode(hex2dec({'77' 'e9'}), 'unicode')
native2unicode(hex2dec({'8b' 'a1'}), 'unicode')
native2unicode(hex2dec({'7b' '97'}), 'unicode')
native2unicode(hex2dec({'53' 'c2'}), 'unicode') native2unicode(hex2dec({'80' '03'}), 'unicode')
native2unicode(hex2dec({'70' 'b9'}), 'unicode') 'z'
native2unicode(hex2dec({'57' '50'}), 'unicode')
native2unicode(hex2dec({'68' '07'}), 'unicode') ]]);
model.result('pg2').feature('surf1').set('coloring', 'uniform');
model.result('pg2').feature('surf1').set('color', 'gray');
model.result('pg2').feature('surf1').set('resolution', 'normal');
model.result('pg2').feature('surf1').feature('def').set('scaleactive', true);
model.result('pg4').label([native2unicode(hex2dec({'4f' '4d'}), 'unicode')
native2unicode(hex2dec({'79' 'fb'}), 'unicode') 'V_direction']);
model.result('pg4').set('looplevel', [8]);
model.result('pg4').set('titletype', 'none');
model.result('pg4').set(' xlabel', 'x-axis');
model.result('pg4').set(' xlabelactive', true);
model.result('pg4').set(' ylabel', 'z-axis (reverse)');
model.result('pg4').set(' ylabelactive', true);
model.result('pg4').set('frametype', 'spatial');
model.result('pg4').set('legendpos', 'bottom');
model.result('pg4').feature('surf1').set('const', {'solid.refpntx' '0'
[native2unicode(hex2dec({'52' '9b'}), 'unicode') native2unicode(hex2dec({'77' 'e9'}), 'unicode')
native2unicode(hex2dec({'8b' 'a1'}), 'unicode')
native2unicode(hex2dec({'7b' '97'}), 'unicode') native2unicode(hex2dec({'53' 'c2'}), 'unicode')
native2unicode(hex2dec({'80' '03'}), 'unicode')
native2unicode(hex2dec({'70' 'b9'}), 'unicode') 'x' native2unicode(hex2dec({'57' '50'}), 'unicode')
native2unicode(hex2dec({'68' '07'}), 'unicode') ];
'solid.refpnty' '0' [native2unicode(hex2dec({'52' '9b'}), 'unicode')
native2unicode(hex2dec({'77' 'e9'}), 'unicode') native2unicode(hex2dec({'8b' 'a1'}), 'unicode')
native2unicode(hex2dec({'7b' '97'}), 'unicode')
native2unicode(hex2dec({'53' 'c2'}), 'unicode') native2unicode(hex2dec({'80' '03'}), 'unicode')
native2unicode(hex2dec({'70' 'b9'}), 'unicode') 'y'
native2unicode(hex2dec({'57' '50'}), 'unicode') native2unicode(hex2dec({'68' '07'}), 'unicode') ];
'solid.refpntz' '0' [native2unicode(hex2dec({'52' '9b'}), 'unicode')
native2unicode(hex2dec({'77' 'e9'}), 'unicode')
native2unicode(hex2dec({'8b' 'a1'}), 'unicode')
native2unicode(hex2dec({'7b' '97'}), 'unicode')
native2unicode(hex2dec({'53' 'c2'}), 'unicode') native2unicode(hex2dec({'80' '03'}), 'unicode')
native2unicode(hex2dec({'70' 'b9'}), 'unicode') 'z'
native2unicode(hex2dec({'57' '50'}), 'unicode')
native2unicode(hex2dec({'68' '07'}), 'unicode') ]]);

```

```

native2unicode(hex2dec({'8b' 'a1'}), 'unicode') native2unicode(hex2dec({'7b'
'97'}), 'unicode') native2unicode(hex2dec({'53' 'c2'}), 'unicode')
native2unicode(hex2dec({'80' '03'}), 'unicode') native2unicode(hex2dec({'70'
'b9'}), 'unicode') ' z ' native2unicode(hex2dec({'57' '50'}), 'unicode')
native2unicode(hex2dec({'68' '07'}), 'unicode') ]});
model.result('pg4').feature('surf1').set('colortable', 'Magma');
model.result('pg4').feature('surf1').set('colortabletrans', 'nonlinear');
model.result('pg4').feature('surf1').set('colorcalibration', 1.5);
model.result('pg4').feature('surf1').set('threshold', 'manual');
model.result('pg4').feature('surf1').set('thresholdvalue', 0.2);
model.result('pg4').feature('surf1').set('resolution', 'normal');
model.result('pg4').feature('surf1').feature('def').set('scaleactive', true);
model.result('pg4').feature('con1').set('const', {'solid.refpntx' '0'
[native2unicode(hex2dec({'52' '9b'}), 'unicode') native2unicode(hex2dec({'77'
'e9'}), 'unicode') native2unicode(hex2dec({'7b' '97'}), 'unicode') native2unicode(hex2dec({'53'
'c2'}), 'unicode') native2unicode(hex2dec({'80' '03'}), 'unicode')
native2unicode(hex2dec({'70' 'b9'}), 'unicode') ' x ' native2unicode(hex2dec({'57'
'50'}), 'unicode') native2unicode(hex2dec({'68' '07'}), 'unicode') ];
'solid.refpnty' '0' [native2unicode(hex2dec({'52' '9b'}), 'unicode')
native2unicode(hex2dec({'77' 'e9'}), 'unicode') native2unicode(hex2dec({'8b'
'a1'}), 'unicode') native2unicode(hex2dec({'7b' '97'}), 'unicode')
native2unicode(hex2dec({'53' 'c2'}), 'unicode') native2unicode(hex2dec({'80'
'03'}), 'unicode') native2unicode(hex2dec({'70' 'b9'}), 'unicode') ' y '
native2unicode(hex2dec({'57' '50'}), 'unicode') native2unicode(hex2dec({'68'
'07'}), 'unicode')]; 'solid.refpntz' '0' [native2unicode(hex2dec({'52' '9b'}),
'unicode') native2unicode(hex2dec({'77' 'e9'}), 'unicode')
native2unicode(hex2dec({'8b' 'a1'}), 'unicode') native2unicode(hex2dec({'7b'
'97'}), 'unicode') native2unicode(hex2dec({'53' 'c2'}), 'unicode')
native2unicode(hex2dec({'80' '03'}), 'unicode') native2unicode(hex2dec({'70'
'b9'}), 'unicode') ' z ' native2unicode(hex2dec({'57' '50'}), 'unicode')
native2unicode(hex2dec({'68' '07'}), 'unicode') ]});
model.result('pg4').feature('con1').set('number', 25);
model.result('pg4').feature('con1').set('contourtype', 'tubes');
model.result('pg4').feature('con1').set('radiusexpr', '0.027');
model.result('pg4').feature('con1').set('tuberadiusscaleactive', true);
model.result('pg4').feature('con1').set('colortable', 'WaveLight');
model.result('pg4').feature('con1').set('resolution', 'custom');
model.result('pg4').feature('con1').set('refine', 10);
model.result('pg4').feature('con1').set('smooth', 'everywhere');
model.result('pg4').feature('con1').set('threshold', 'manual');
model.result('pg4').feature('con1').set('thresholdvalue', '0.000000000001');
model.result('pg4').feature('con1').set('resolution', 'custom');
model.result('pg4').feature('con1').set('refine', 10);
model.result('pg4').feature('con1').feature('def1').set('scaleactive', true);
model.result('pg5').label([native2unicode(hex2dec({'4f' '4d'}), 'unicode')
native2unicode(hex2dec({'79' 'fb'}), 'unicode') 'U']);
model.result('pg5').set('looplevel', [8]);
model.result('pg5').set('titletype', 'none');
model.result('pg5').set('xlabel', 'x-axis');
model.result('pg5').set(' xlabelactive', true);
model.result('pg5').set('ylabel', 'z-axis (reverse)');
model.result('pg5').set(' ylabelactive', true);
model.result('pg5').set('frametype', 'spatial');
```

```

model.result('pg5').set('legendpos', 'bottom');
model.result('pg5').feature('surf1').set('const', {'solid.refpntx' : 0
[native2unicode(hex2dec({'52' '9b'}), 'unicode') native2unicode(hex2dec({'77'
'e9'}), 'unicode') native2unicode(hex2dec({'8b' 'a1'}), 'unicode')
native2unicode(hex2dec({'7b' '97'}), 'unicode') native2unicode(hex2dec({'53'
'c2'}), 'unicode') native2unicode(hex2dec({'80' '03'}), 'unicode')
native2unicode(hex2dec({'70' 'b9'}), 'unicode') 'x' native2unicode(hex2dec({'57'
'50'}), 'unicode') native2unicode(hex2dec({'68' '07'}), 'unicode') ];
'solid.refpnty' : 0 [native2unicode(hex2dec({'52' '9b'}), 'unicode')
native2unicode(hex2dec({'77' 'e9'}), 'unicode') native2unicode(hex2dec({'8b'
'a1'}), 'unicode') native2unicode(hex2dec({'7b' '97'}), 'unicode')
native2unicode(hex2dec({'53' 'c2'}), 'unicode') native2unicode(hex2dec({'80'
'03'}), 'unicode') native2unicode(hex2dec({'70' 'b9'}), 'unicode') 'y'
native2unicode(hex2dec({'57' '50'}), 'unicode') native2unicode(hex2dec({'68'
'07'}), 'unicode') ]; 'solid.refpntz' : 0 [native2unicode(hex2dec({'52' '9b'}),
'unicode') native2unicode(hex2dec({'77' 'e9'}), 'unicode')
native2unicode(hex2dec({'8b' 'a1'}), 'unicode') native2unicode(hex2dec({'7b'
'97'}), 'unicode') native2unicode(hex2dec({'53' 'c2'}), 'unicode')
native2unicode(hex2dec({'80' '03'}), 'unicode') native2unicode(hex2dec({'70'
'b9'}), 'unicode') 'z' native2unicode(hex2dec({'57' '50'}), 'unicode')
native2unicode(hex2dec({'68' '07'}), 'unicode') ]});
model.result('pg5').feature('surf1').set('colortable', 'Magma');
model.result('pg5').feature('surf1').set('threshold', 'manual');
model.result('pg5').feature('surf1').set('thresholdvalue', 0.2);
model.result('pg5').feature('surf1').set('resolution', 'normal');
model.result('pg5').feature('surf1').feature('def').set('scaleactive', true);
model.result('pg5').feature('con1').set('const', {'solid.refpntx' : 0
[native2unicode(hex2dec({'52' '9b'}), 'unicode') native2unicode(hex2dec({'77'
'e9'}), 'unicode') native2unicode(hex2dec({'8b' 'a1'}), 'unicode')
native2unicode(hex2dec({'7b' '97'}), 'unicode') native2unicode(hex2dec({'53'
'c2'}), 'unicode') native2unicode(hex2dec({'80' '03'}), 'unicode')
native2unicode(hex2dec({'70' 'b9'}), 'unicode') 'x' native2unicode(hex2dec({'57'
'50'}), 'unicode') native2unicode(hex2dec({'68' '07'}), 'unicode') ];
'solid.refpnty' : 0 [native2unicode(hex2dec({'52' '9b'}), 'unicode')
native2unicode(hex2dec({'77' 'e9'}), 'unicode') native2unicode(hex2dec({'8b'
'a1'}), 'unicode') native2unicode(hex2dec({'7b' '97'}), 'unicode')
native2unicode(hex2dec({'53' 'c2'}), 'unicode') native2unicode(hex2dec({'80'
'03'}), 'unicode') native2unicode(hex2dec({'70' 'b9'}), 'unicode') 'y'
native2unicode(hex2dec({'57' '50'}), 'unicode') native2unicode(hex2dec({'68'
'07'}), 'unicode') ]; 'solid.refpntz' : 0 [native2unicode(hex2dec({'52' '9b'}),
'unicode') native2unicode(hex2dec({'77' 'e9'}), 'unicode')
native2unicode(hex2dec({'8b' 'a1'}), 'unicode') native2unicode(hex2dec({'7b'
'97'}), 'unicode') native2unicode(hex2dec({'53' 'c2'}), 'unicode')
native2unicode(hex2dec({'80' '03'}), 'unicode') native2unicode(hex2dec({'70'
'b9'}), 'unicode') 'z' native2unicode(hex2dec({'57' '50'}), 'unicode')
native2unicode(hex2dec({'68' '07'}), 'unicode') ]]);
model.result('pg5').feature('con1').set('number', 25);
model.result('pg5').feature('con1').set('contourtype', 'tubes');
model.result('pg5').feature('con1').set('radiusexpr', '0.025');
model.result('pg5').feature('con1').set('tuberadiusscaleactive', true);
model.result('pg5').feature('con1').set('colortable', 'WaveLight');
model.result('pg5').feature('con1').set('resolution', 'custom');
model.result('pg5').feature('con1').set('refine', 10);
model.result('pg5').feature('con1').set('smooth', 'everywhere');

```

```
model.result('pg5').feature('con1').set('threshold', 'manual');
model.result('pg5').feature('con1').set('resolution', 'custom');
model.result('pg5').feature('con1').set('refine', 10);
model.result('pg5').feature('def1').set('scaleactive', true);
model.result('pg6').label([native2unicode(hex2dec({'5e' '94'})), 'unicode'])
native2unicode(hex2dec({'52' '9b'}), 'unicode') 'sigma']);
model.result('pg6').set('looplevel', [8]);
model.result('pg6').set('titletype', 'none');
model.result('pg6').set(' xlabel', 'x-axis');
model.result('pg6').set(' xlabelactive', true);
model.result('pg6').set(' ylabel', 'z-axis (reverse)');
model.result('pg6').set(' ylabelactive', true);
model.result('pg6').set('frametype', 'spatial');
model.result('pg6').set('legendpos', 'bottom');
model.result('pg6').feature('surf1').set('const', {'solid.refpntx' '0'
[native2unicode(hex2dec({'52' '9b'}), 'unicode') native2unicode(hex2dec({'77'
'e9'}), 'unicode') native2unicode(hex2dec({'8b' 'a1'}), 'unicode')
native2unicode(hex2dec({'7b' '97'}), 'unicode') native2unicode(hex2dec({'53'
'c2'}), 'unicode') native2unicode(hex2dec({'80' '03'}), 'unicode')
native2unicode(hex2dec({'70' 'b9'}), 'unicode') ' x ' native2unicode(hex2dec({'57'
'50'}), 'unicode') native2unicode(hex2dec({'68' '07'}), 'unicode') ];
'solid.refpnty' '0' [native2unicode(hex2dec({'52' '9b'}), 'unicode')
native2unicode(hex2dec({'77' 'e9'}), 'unicode') native2unicode(hex2dec({'8b'
'a1'}), 'unicode') native2unicode(hex2dec({'7b' '97'}), 'unicode')
native2unicode(hex2dec({'53' 'c2'}), 'unicode') native2unicode(hex2dec({'80'
'03'}), 'unicode') native2unicode(hex2dec({'70' 'b9'}), 'unicode') ' y '
native2unicode(hex2dec({'57' '50'}), 'unicode') native2unicode(hex2dec({'68'
'07'}), 'unicode') ]; 'solid.refpntz' '0' [native2unicode(hex2dec({'52' '9b'}),
'unicode') native2unicode(hex2dec({'77' 'e9'}), 'unicode')
native2unicode(hex2dec({'8b' 'a1'}), 'unicode') native2unicode(hex2dec({'7b'
'97'}), 'unicode') native2unicode(hex2dec({'53' 'c2'}), 'unicode')
native2unicode(hex2dec({'80' '03'}), 'unicode') native2unicode(hex2dec({'70'
'b9'}), 'unicode') ' z ' native2unicode(hex2dec({'57' '50'}), 'unicode')
native2unicode(hex2dec({'68' '07'}), 'unicode') ]});
model.result('pg6').feature('surf1').set('colortable', 'Magma');
model.result('pg6').feature('surf1').set('colortabletrans', 'nonlinear');
model.result('pg6').feature('surf1').set('colorcalibration', 1.2);
model.result('pg6').feature('surf1').set('threshold', 'manual');
model.result('pg6').feature('surf1').set('thresholdvalue', 0.2);
model.result('pg6').feature('surf1').set('resolution', 'normal');
model.result('pg6').feature('surf1').feature('def').set('scaleactive', true);
model.result('pg6').feature('con1').set('const', {'solid.refpntx' '0'
[native2unicode(hex2dec({'52' '9b'}), 'unicode') native2unicode(hex2dec({'77'
'e9'}), 'unicode') native2unicode(hex2dec({'8b' 'a1'}), 'unicode')
native2unicode(hex2dec({'7b' '97'}), 'unicode') native2unicode(hex2dec({'53'
'c2'}), 'unicode') native2unicode(hex2dec({'80' '03'}), 'unicode')
native2unicode(hex2dec({'70' 'b9'}), 'unicode') ' x ' native2unicode(hex2dec({'57'
'50'}), 'unicode') native2unicode(hex2dec({'68' '07'}), 'unicode') ];
'solid.refpnty' '0' [native2unicode(hex2dec({'52' '9b'}), 'unicode')
native2unicode(hex2dec({'77' 'e9'}), 'unicode') native2unicode(hex2dec({'8b'
'a1'}), 'unicode') native2unicode(hex2dec({'7b' '97'}), 'unicode')
native2unicode(hex2dec({'53' 'c2'}), 'unicode') native2unicode(hex2dec({'80'
'03'}), 'unicode') native2unicode(hex2dec({'70' 'b9'}), 'unicode') ' y '
native2unicode(hex2dec({'57' '50'}), 'unicode') native2unicode(hex2dec({'68'
'07'}), 'unicode') ]});
```

```
'07'}), 'unicode') ]; 'solid.refpntz' '0' [native2unicode(hex2dec({'52' '9b'})),  

'unicode') native2unicode(hex2dec({'77' 'e9'})), 'unicode')  

native2unicode(hex2dec({'8b' 'a1'})), 'unicode') native2unicode(hex2dec({'7b'  

'97'})), 'unicode') native2unicode(hex2dec({'53' 'c2'})), 'unicode')  

native2unicode(hex2dec({'80' '03'})), 'unicode') native2unicode(hex2dec({'70'  

'b9'})), 'unicode') 'z' native2unicode(hex2dec({'57' '50'})), 'unicode')  

native2unicode(hex2dec({'68' '07'})), 'unicode') ]});  

model.result('pg6').feature('con1').set('number', 25);  

model.result('pg6').feature('con1').set('contourtype', 'tubes');  

model.result('pg6').feature('con1').set('radiusexpr', '0.025');  

model.result('pg6').feature('con1').set('tuberadiusscaleactive', true);  

model.result('pg6').feature('con1').set('colortable', 'WaveLight');  

model.result('pg6').feature('con1').set('resolution', 'custom');  

model.result('pg6').feature('con1').set('refine', 10);  

model.result('pg6').feature('con1').set('smooth', 'everywhere');  

model.result('pg6').feature('con1').set('resolution', 'custom');  

model.result('pg6').feature('con1').set('refine', 10);  

model.result('pg6').feature('con1').feature('def1').set('scaleactive', true);  

model.result('pg6').feature('mesh1').set('elemcolor', 'none');  

model.result('pg6').feature('mesh1').set('wireframecolor', 'custom');  

model.result('pg6').feature('mesh1').set('customwireframecolor',  

[0.2078431397676468 0.2078431397676468 0.21568627655506134]);  

model.result('pg6').feature('mesh1').set('resolution', 'extrafine');  

model.result('pg7').label([native2unicode(hex2dec({'5e' '94'})), 'unicode')  

native2unicode(hex2dec({'52' '9b'})), 'unicode') 'tau']);  

model.result('pg7').set('looplevel', [8]);  

model.result('pg7').set('titletype', 'none');  

model.result('pg7').set(' xlabel', 'x-axis');  

model.result('pg7').set(' xlabelactive', true);  

model.result('pg7').set(' ylabel', 'z-axis (reverse)');  

model.result('pg7').set(' ylabelactive', true);  

model.result('pg7').set('frametype', 'spatial');  

model.result('pg7').set('legendpos', 'bottom');  

model.result('pg7').feature('surf1').set('const', {'solid.refpntx' '0'  

[native2unicode(hex2dec({'52' '9b'})), 'unicode') native2unicode(hex2dec({'77'  

'e9'})), 'unicode') native2unicode(hex2dec({'8b' 'a1'})), 'unicode')  

native2unicode(hex2dec({'7b' '97'})), 'unicode') native2unicode(hex2dec({'53'  

'c2'})), 'unicode') native2unicode(hex2dec({'80' '03'})), 'unicode')  

native2unicode(hex2dec({'70' 'b9'})), 'unicode') 'x' native2unicode(hex2dec({'57'  

'50'})), 'unicode') native2unicode(hex2dec({'68' '07'})), 'unicode')];  

'solid.refpnty' '0' [native2unicode(hex2dec({'52' '9b'})), 'unicode')  

native2unicode(hex2dec({'77' 'e9'})), 'unicode') native2unicode(hex2dec({'8b'  

'a1'})), 'unicode') native2unicode(hex2dec({'7b' '97'})), 'unicode')  

native2unicode(hex2dec({'53' 'c2'})), 'unicode') native2unicode(hex2dec({'80'  

'03'})), 'unicode') native2unicode(hex2dec({'70' 'b9'})), 'unicode') 'y'  

native2unicode(hex2dec({'57' '50'})), 'unicode') native2unicode(hex2dec({'68'  

'07'})); 'solid.refpntz' '0' [native2unicode(hex2dec({'52' '9b'})),  

'unicode') native2unicode(hex2dec({'77' 'e9'})), 'unicode')  

native2unicode(hex2dec({'8b' 'a1'})), 'unicode') native2unicode(hex2dec({'7b'  

'97'})), 'unicode') native2unicode(hex2dec({'53' 'c2'})), 'unicode')  

native2unicode(hex2dec({'80' '03'})), 'unicode') native2unicode(hex2dec({'70'  

'b9'})), 'unicode') 'z' native2unicode(hex2dec({'57' '50'})), 'unicode')  

native2unicode(hex2dec({'68' '07'})), 'unicode') ]);  

model.result('pg7').feature('surf1').set('colortable', 'Magma');
```

```

model.result('pg7').feature('surf1').set('colortabletrans', 'nonlinear');
model.result('pg7').feature('surf1').set('colorcalibration', -1.3);
model.result('pg7').feature('surf1').set('threshold', 'manual');
model.result('pg7').feature('surf1').set('thresholdvalue', 0.2);
model.result('pg7').feature('surf1').set('resolution', 'normal');
model.result('pg7').feature('surf1').feature('def').set('scaleactive', true);
model.result('pg7').feature('con1').set('const', {'solid.refpntx' '0'
[native2unicode(hex2dec({'52' '9b'}), 'unicode') native2unicode(hex2dec({'77'
'e9'})), 'unicode']) native2unicode(hex2dec({'8b' 'a1'}), 'unicode')
native2unicode(hex2dec({'7b' '97'}), 'unicode') native2unicode(hex2dec({'53'
'c2'}), 'unicode') native2unicode(hex2dec({'80' '03'}), 'unicode')
native2unicode(hex2dec({'70' 'b9'}), 'unicode') 'x' native2unicode(hex2dec({'57'
'50'}), 'unicode') native2unicode(hex2dec({'68' '07'}), 'unicode') ];
'solid.refpnty' '0' [native2unicode(hex2dec({'52' '9b'}), 'unicode')
native2unicode(hex2dec({'77' 'e9'}), 'unicode') native2unicode(hex2dec({'8b'
'a1'}), 'unicode') native2unicode(hex2dec({'7b' '97'}), 'unicode')
native2unicode(hex2dec({'53' 'c2'}), 'unicode') native2unicode(hex2dec({'80'
'03'}), 'unicode') native2unicode(hex2dec({'70' 'b9'}), 'unicode') 'y'
native2unicode(hex2dec({'57' '50'}), 'unicode') native2unicode(hex2dec({'68'
'07'}), 'unicode')] ; 'solid.refpntz' '0' [native2unicode(hex2dec({'52' '9b'}),
'unicode') native2unicode(hex2dec({'77' 'e9'}), 'unicode')
native2unicode(hex2dec({'8b' 'a1'}), 'unicode') native2unicode(hex2dec({'7b'
'97'}), 'unicode') native2unicode(hex2dec({'53' 'c2'}), 'unicode')
native2unicode(hex2dec({'80' '03'}), 'unicode') native2unicode(hex2dec({'70'
'b9'}), 'unicode') 'z' native2unicode(hex2dec({'57' '50'}), 'unicode')
native2unicode(hex2dec({'68' '07'}), 'unicode') ]});
model.result('pg7').feature('con1').set('titletype', 'none');
model.result('pg7').feature('con1').set('number', 25);
model.result('pg7').feature('con1').set('contourtype', 'tubes');
model.result('pg7').feature('con1').set('radiusexpr', '0.025');
model.result('pg7').feature('con1').set('tuberadiuscaleactive', true);
model.result('pg7').feature('con1').set('colortable', 'WaveLight');
model.result('pg7').feature('con1').set('resolution', 'custom');
model.result('pg7').feature('con1').set('refine', 10);
model.result('pg7').feature('con1').set('smooth', 'everywhere');
model.result('pg7').feature('con1').set('resolution', 'custom');
model.result('pg7').feature('con1').set('refine', 10);
model.result('pg7').feature('con1').feature('def1').set('scaleactive', true);
model.result('pg7').feature('mesh1').set('elemcolor', 'none');
model.result('pg7').feature('mesh1').set('wireframecolor', 'custom');
model.result('pg7').feature('mesh1').set('customwireframecolor',
[0.2078431397676468 0.2078431397676468 0.21568627655506134]);
model.result('pg7').feature('mesh1').set('resolution', 'extrafine');
model.result('pg8').set('looplevelinput', {'manualindices'});
model.result('pg8').set('looplevelindices', [8]);
model.result('pg8').set(' xlabel', [native2unicode(hex2dec({'5f' '27'}), 'unicode')
native2unicode(hex2dec({'95' '7f'}), 'unicode') ' (m)']);
model.result('pg8').set(' ylabel', '-solid.sxy (N/m<sup>2</sup>)');
model.result('pg8').set(' xlabelactive', false);
model.result('pg8').set(' ylabelactive', false);
model.result('pg8').feature('lngr1').set('data', 'cln1');
model.result('pg8').feature('lngr1').set('looplevelinput', {'manualindices'});
model.result('pg8').feature('lngr1').set('looplevelindices', [8]);
model.result('pg8').feature('lngr1').set('const', {'solid.refpntx' '0'}

```

```
[native2unicode(hex2dec({'52' '9b'}), 'unicode') native2unicode(hex2dec({'77' 'e9'}), 'unicode') native2unicode(hex2dec({'8b' 'a1'}), 'unicode')
native2unicode(hex2dec({'7b' '97'}), 'unicode') native2unicode(hex2dec({'53' 'c2'}), 'unicode') native2unicode(hex2dec({'80' '03'}), 'unicode')
native2unicode(hex2dec({'70' 'b9'}), 'unicode') 'x' native2unicode(hex2dec({'57' '50'}), 'unicode') native2unicode(hex2dec({'68' '07'}), 'unicode') ];
'solid.refpnty' '0' [native2unicode(hex2dec({'52' '9b'}), 'unicode')
native2unicode(hex2dec({'77' 'e9'}), 'unicode') native2unicode(hex2dec({'8b' 'a1'}), 'unicode') native2unicode(hex2dec({'7b' '97'}), 'unicode')
native2unicode(hex2dec({'53' 'c2'}), 'unicode') native2unicode(hex2dec({'80' '03'}), 'unicode') native2unicode(hex2dec({'70' 'b9'}), 'unicode') 'y'
native2unicode(hex2dec({'57' '50'}), 'unicode') native2unicode(hex2dec({'68' '07'}), 'unicode')]; 'solid.refpntz' '0' [native2unicode(hex2dec({'52' '9b'}), 'unicode')
native2unicode(hex2dec({'77' 'e9'}), 'unicode') native2unicode(hex2dec({'8b' 'a1'}), 'unicode') native2unicode(hex2dec({'7b' '97'}), 'unicode')
native2unicode(hex2dec({'53' 'c2'}), 'unicode') native2unicode(hex2dec({'80' '03'}), 'unicode') native2unicode(hex2dec({'70' 'b9'}), 'unicode') 'z'
native2unicode(hex2dec({'57' '50'}), 'unicode') native2unicode(hex2dec({'68' '07'}), 'unicode')]];
model.result('pg8').feature('lngr1').set('resolution', 'normal');
model.result.export('data1').label([native2unicode(hex2dec({'4f' '4d'}), 'unicode') native2unicode(hex2dec({'79' 'fb'}), 'unicode') 'V']);
model.result.export('data1').set('looplevelinput', {'manualindices'});
model.result.export('data1').set('looplevelindices', [8]);
model.result.export('data1').set('expr', {'v'});
model.result.export('data1').set('unit', {'m'});
model.result.export('data1').set('descr', {[native2unicode(hex2dec({'4f' '4d'}), 'unicode') native2unicode(hex2dec({'79' 'fb'}), 'unicode')
native2unicode(hex2dec({'57' '3a'}), 'unicode') native2unicode(hex2dec({'ff' '0c'}), 'unicode') 'Y' native2unicode(hex2dec({'52' '06'}), 'unicode')
native2unicode(hex2dec({'91' 'cf'}), 'unicode')]}];
model.result.export('data1').set('const', {'solid.refpntx' '0'
[native2unicode(hex2dec({'52' '9b'}), 'unicode') native2unicode(hex2dec({'77' 'e9'}), 'unicode') native2unicode(hex2dec({'8b' 'a1'}), 'unicode')
native2unicode(hex2dec({'7b' '97'}), 'unicode') native2unicode(hex2dec({'53' 'c2'}), 'unicode') native2unicode(hex2dec({'80' '03'}), 'unicode')
native2unicode(hex2dec({'70' 'b9'}), 'unicode') 'x' native2unicode(hex2dec({'57' '50'}), 'unicode') native2unicode(hex2dec({'68' '07'}), 'unicode')];
'solid.refpnty' '0' [native2unicode(hex2dec({'52' '9b'}), 'unicode')
native2unicode(hex2dec({'77' 'e9'}), 'unicode') native2unicode(hex2dec({'8b' 'a1'}), 'unicode') native2unicode(hex2dec({'7b' '97'}), 'unicode')
native2unicode(hex2dec({'53' 'c2'}), 'unicode') native2unicode(hex2dec({'80' '03'}), 'unicode') native2unicode(hex2dec({'70' 'b9'}), 'unicode') 'y'
native2unicode(hex2dec({'57' '50'}), 'unicode') native2unicode(hex2dec({'68' '07'}), 'unicode')]; 'solid.refpntz' '0' [native2unicode(hex2dec({'52' '9b'}), 'unicode')
native2unicode(hex2dec({'77' 'e9'}), 'unicode') native2unicode(hex2dec({'8b' 'a1'}), 'unicode') native2unicode(hex2dec({'7b' '97'}), 'unicode')
native2unicode(hex2dec({'53' 'c2'}), 'unicode') native2unicode(hex2dec({'80' '03'}), 'unicode') native2unicode(hex2dec({'70' 'b9'}), 'unicode') 'z'
native2unicode(hex2dec({'57' '50'}), 'unicode') native2unicode(hex2dec({'68' '07'}), 'unicode')]}]);
model.result.export('data1').set('filename',
'C:\Users\Administrator\Downloads\v_ALM.txt');
model.result.export('data1').set('header', false);
```

```
model.result.export('data1').set('sort', true);
model.result.export('data2').label([native2unicode(hex2dec({'4f' '4d'})),
'unicode') native2unicode(hex2dec({'79' 'fb'}), 'unicode') 'U']);
model.result.export('data2').set('looplevelinput', {'manualindices'});
model.result.export('data2').set('looplevelindices', [8]);
model.result.export('data2').set('expr', {'u'});
model.result.export('data2').set('unit', {'m'});
model.result.export('data2').set('descr', {[native2unicode(hex2dec({'4f' '4d'}),
'unicode') native2unicode(hex2dec({'79' 'fb'}), 'unicode')
native2unicode(hex2dec({'57' '3a'}), 'unicode') native2unicode(hex2dec({'ff'
'0c'}), 'unicode') 'X ' native2unicode(hex2dec({'52' '06'}), 'unicode')
native2unicode(hex2dec({'91' 'cf'}), 'unicode')]});
model.result.export('data2').set('const', {'solid.refpntx' '0'
[native2unicode(hex2dec({'52' '9b'}), 'unicode') native2unicode(hex2dec({'77'
'e9'}), 'unicode') native2unicode(hex2dec({'8b' 'a1'}), 'unicode')
native2unicode(hex2dec({'7b' '97'}), 'unicode') native2unicode(hex2dec({'53'
'c2'}), 'unicode') native2unicode(hex2dec({'80' '03'}), 'unicode')
native2unicode(hex2dec({'70' 'b9'}), 'unicode') ' x ' native2unicode(hex2dec({'57'
'50'}), 'unicode') native2unicode(hex2dec({'68' '07'}), 'unicode') ];
'solid.refpnty' '0' [native2unicode(hex2dec({'52' '9b'}), 'unicode')
native2unicode(hex2dec({'77' 'e9'}), 'unicode') native2unicode(hex2dec({'8b'
'a1'}), 'unicode') native2unicode(hex2dec({'7b' '97'}), 'unicode')
native2unicode(hex2dec({'53' 'c2'}), 'unicode') native2unicode(hex2dec({'80'
'03'}), 'unicode') native2unicode(hex2dec({'70' 'b9'}), 'unicode') ' y '
native2unicode(hex2dec({'57' '50'}), 'unicode') native2unicode(hex2dec({'68'
'07'}), 'unicode')]; 'solid.refpntz' '0' [native2unicode(hex2dec({'52' '9b'}),
'unicode') native2unicode(hex2dec({'77' 'e9'}), 'unicode')
native2unicode(hex2dec({'8b' 'a1'}), 'unicode') native2unicode(hex2dec({'7b'
'97'}), 'unicode') native2unicode(hex2dec({'53' 'c2'}), 'unicode')
native2unicode(hex2dec({'80' '03'}), 'unicode') native2unicode(hex2dec({'70'
'b9'}), 'unicode') ' z ' native2unicode(hex2dec({'57' '50'}), 'unicode')
native2unicode(hex2dec({'68' '07'}), 'unicode')]});
model.result.export('data2').set('filename',
'C:\Users\Administrator\Downloads\u_ALM.txt');
model.result.export('data2').set('header', false);
model.result.export('data2').set('sort', true);
model.result.export('data3').label([native2unicode(hex2dec({'5e' '94'}),
'unicode') native2unicode(hex2dec({'52' '9b'}), 'unicode') 'sigma']]);
model.result.export('data3').set('looplevelinput', {'manualindices'});
model.result.export('data3').set('looplevelindices', [8]);
model.result.export('data3').set('expr', {'solid.sy'});
model.result.export('data3').set('unit', {'N/m^2'});
model.result.export('data3').set('descr', {[native2unicode(hex2dec({'5e' '94'}),
'unicode') native2unicode(hex2dec({'52' '9b'}), 'unicode')
native2unicode(hex2dec({'5f' '20'}), 'unicode') native2unicode(hex2dec({'91'
'cf'}), 'unicode') native2unicode(hex2dec({'ff' '0c'}), 'unicode') 'y '
native2unicode(hex2dec({'52' '06'}), 'unicode') native2unicode(hex2dec({'91'
'cf'}), 'unicode')]});
model.result.export('data3').set('const', {'solid.refpntx' '0'
[native2unicode(hex2dec({'52' '9b'}), 'unicode') native2unicode(hex2dec({'77'
'e9'}), 'unicode') native2unicode(hex2dec({'8b' 'a1'}), 'unicode')
native2unicode(hex2dec({'7b' '97'}), 'unicode') native2unicode(hex2dec({'53'
'c2'}), 'unicode') native2unicode(hex2dec({'80' '03'}), 'unicode')
native2unicode(hex2dec({'70' 'b9'}), 'unicode') ' x ' native2unicode(hex2dec({'57'
'50'}), 'unicode')]});
model.result.export('data3').set('header', false);
model.result.export('data3').set('sort', true);
```

```
'50'}), 'unicode') native2unicode(hex2dec({'68' '07'}), 'unicode') ];
'solid.refpnty' '0' [native2unicode(hex2dec({'52' '9b'}), 'unicode')
native2unicode(hex2dec({'77' 'e9'}), 'unicode') native2unicode(hex2dec({'8b'
'a1'}), 'unicode') native2unicode(hex2dec({'7b' '97'}), 'unicode')
native2unicode(hex2dec({'53' 'c2'}), 'unicode') native2unicode(hex2dec({'80'
'03'}), 'unicode') native2unicode(hex2dec({'70' 'b9'}), 'unicode') ' y '
native2unicode(hex2dec({'57' '50'}), 'unicode') native2unicode(hex2dec({'68'
'07'}), 'unicode')]; 'solid.refpntz' '0' [native2unicode(hex2dec({'52' '9b'}),
'unicode') native2unicode(hex2dec({'77' 'e9'}), 'unicode')
native2unicode(hex2dec({'8b' 'a1'}), 'unicode') native2unicode(hex2dec({'7b'
'97'}), 'unicode') native2unicode(hex2dec({'53' 'c2'}), 'unicode')
native2unicode(hex2dec({'80' '03'}), 'unicode') native2unicode(hex2dec({'70'
'b9'}), 'unicode') ' z ' native2unicode(hex2dec({'57' '50'}), 'unicode')
native2unicode(hex2dec({'68' '07'}), 'unicode') ]});
model.result.export('data3').set('filename',
'C:\Users\Administrator\Downloads\sig_ALM.txt');
model.result.export('data3').set('header', false);
model.result.export('data3').set('sort', true);
model.result.export('data4').label([native2unicode(hex2dec({'5e' '94'}),
'unicode') native2unicode(hex2dec({'52' '9b'}), 'unicode') 'tau']);
model.result.export('data4').set('looplevelinput', {'manualindices'});
model.result.export('data4').set('looplevelindices', [8]);
model.result.export('data4').set('expr', {'solid.sxy'});
model.result.export('data4').set('unit', {'N/m^2'});
model.result.export('data4').set('descr', {[native2unicode(hex2dec({'5e' '94'}),
'unicode') native2unicode(hex2dec({'52' '9b'}), 'unicode')
native2unicode(hex2dec({'5f' '20'}), 'unicode') native2unicode(hex2dec({'91'
'cf'}), 'unicode') native2unicode(hex2dec({'ff' '0c'}), 'unicode') 'xy '
native2unicode(hex2dec({'52' '06'}), 'unicode') native2unicode(hex2dec({'91'
'cf'}), 'unicode')]}));
model.result.export('data4').set('const', {'solid.refpntx' '0'
[native2unicode(hex2dec({'52' '9b'}), 'unicode') native2unicode(hex2dec({'77'
'e9'}), 'unicode') native2unicode(hex2dec({'8b' 'a1'}), 'unicode')
native2unicode(hex2dec({'7b' '97'}), 'unicode') native2unicode(hex2dec({'53'
'c2'}), 'unicode') native2unicode(hex2dec({'80' '03'}), 'unicode')
native2unicode(hex2dec({'70' 'b9'}), 'unicode') ' x ' native2unicode(hex2dec({'57'
'50'}), 'unicode') native2unicode(hex2dec({'68' '07'}), 'unicode')];
'solid.refpnty' '0' [native2unicode(hex2dec({'52' '9b'}), 'unicode')
native2unicode(hex2dec({'77' 'e9'}), 'unicode') native2unicode(hex2dec({'8b'
'a1'}), 'unicode') native2unicode(hex2dec({'7b' '97'}), 'unicode')
native2unicode(hex2dec({'53' 'c2'}), 'unicode') native2unicode(hex2dec({'80'
'03'}), 'unicode') native2unicode(hex2dec({'70' 'b9'}), 'unicode') ' y '
native2unicode(hex2dec({'57' '50'}), 'unicode') native2unicode(hex2dec({'68'
'07'}), 'unicode')]; 'solid.refpntz' '0' [native2unicode(hex2dec({'52' '9b'}),
'unicode') native2unicode(hex2dec({'77' 'e9'}), 'unicode')
native2unicode(hex2dec({'8b' 'a1'}), 'unicode') native2unicode(hex2dec({'7b'
'97'}), 'unicode') native2unicode(hex2dec({'53' 'c2'}), 'unicode')
native2unicode(hex2dec({'80' '03'}), 'unicode') native2unicode(hex2dec({'70'
'b9'}), 'unicode') ' z ' native2unicode(hex2dec({'57' '50'}), 'unicode')
native2unicode(hex2dec({'68' '07'}), 'unicode')]}));
model.result.export('data4').set('filename',
'C:\Users\Administrator\Downloads\tau_ALM.txt');
model.result.export('data4').set('header', false);
model.result.export('data4').set('sort', true);
```

```
out = model;
```